

Funktionelle Bildgebung  
der cerebralen Repräsentation  
des Schluckens

Aus der Abteilung für Funktionelle Bildgebung  
(Leiter: Univ.-Prof. Dr. med. Martin Lotze)  
des Instituts für Diagnostische Radiologie und Neuroradiologie  
(Direktor: Univ.-Prof. Dr. med. Norbert Hosten)  
der Universitätsmedizin der Ernst-Moritz-Arndt-Universität Greifswald



## Funktionelle Bildgebung der cerebralen Repräsentation des Schluckens

*Inaugural Dissertation zur  
Erlangung des akademischen Grades  
Doktor der Wissenschaft in der Medizin  
(Dr. rer. med.)  
der Universitätsmedizin der Ernst-Moritz-Arndt-Universität  
Greifswald  
2014*

Vorgelegt von PAUL GLAD MIHAI  
geb. am 27.06.1982  
in Sibiu, Rumänien

Dekan: Univ.-Prof. Dr. med. dent. Reiner Biffar,  
1. Gutachter: Prof. Dr. med. Martin Lotze,  
2. Gutachter: Prof. Dr. Christoph Braun,  
3. Gutachter: \_\_\_\_\_,  
Ort, Raum: Greifswald,  
Tag der Disputation: 10.06.2015.

Für meine Eltern  
Ohne sie wäre ich nicht hier

# *Zusammenfassung*

Ziel dieser Arbeit war es, cerebrale Hirnaktivitätsmuster assoziiert mit dem Schluckakt von jungen Gesunden, räumlich und zeitlich zu erfassen. Darüber hinaus wurde die Möglichkeit einer gemeinsamen neuronalen Struktur zwischen Kiefergelenkbewegungen (Okklusion) und Schluckakt untersucht. Im Anschluss befasste sich diese Studie mit der Änderung der kortikalen Schluckrepräsentation im Alter. Es wurden hierzu junge und alte, gesunde Versuchspersonen mit Hilfe der fMRT-Bildgebung während der Schluckaufgabe untersucht. Um die Spezifität des Schlucknetzwerkes zu testen wurden als Kontrollparadigma die Kiefergelenkbewegungen bei jungen Gesunden gemessen. Voruntersuchungen zeigten, dass sich eine Erhöhung des allgemeinen fMRT-Aktivierungsniveaus schon allein durch eine Erhöhung der Anstrengung zu erklären ist. Um diesen Faktor zu kontrollieren wurden während der fMRT-Untersuchung physiologische Parameter aufgezeichnet, die mit der Anstrengung korrelieren. Insgesamt wurden für die Okklusion und das Schlucken ein vergleichbares Repräsentationsmuster gefunden, jedoch waren mehr neuronale Ressourcen erforderlich um den Schluckakt durchzuführen. Die peripherphysiologische Messung zeigte, dass diese Mehraktivierung nicht auf eine verstärkte Anstrengung der Aufgabe zurückzuführen war. Erstmals wurde mittels fMRT eine Repräsentation im Hirnstamm für Schlucken und Okklusion nachgewiesen. Die Hirnstammaktivierung erfolgte in dem sensorischen Kern des Nervus trigeminus, sowie dem Nucleus tractus solitarii beim Schlucken und dem Nucleus trigemini bei der Okklusion. Um die zeitliche Abfolge des Schluckens in ihrer Repräsentation zu untersuchen, wurde eine zeitlich optimierte fMRT-Messung aufgenommen. Durch die zeitliche Analyse konnten wir nachweisen, dass eine aufeinanderfolgende Aktivierung stattfand, beginnend im prämotorischem Cortex mit Übergang zum supplementär-motorischem Areal, gefolgt vom primären sensomotorischen Cortex, der Insula und dem Cerebellum und letztlich der Aktivierung in der Pons. Zudem wurde mittels effektiver Konnektivitätsanalyse nachgewiesen, dass ein Modell mit zwei Eingängen, ein zum supplementär-motorischem Areal und der anderen zum primären motorisch-somatosensorischem Cortex, die wahrscheinlichste Erklärung zeitlich aufeinander folgender Aktivierungsprozesse darstellt. Zur Auswertung der Daten hinsichtlich der Änderung der Schluckrepräsentation im Alter wurden sowohl klassische als auch Bayes-statistische Verfahren verwendet. Die klassische Inferenz ist konservativer und die Bayes-Statistik spezifischer. Zudem wird mit letzterer das Problem der multiplen Vergleiche vermieden. Den einzigen Unterschied im Gruppenvergleich lieferte die Bayes-Statistik mit einer signifikanten Aktivierung im Frontalpol 1 der Brodmann Area 10. Während der Schluckaufgabe zeigten Senioren eine verlängerte Schluckdauer und eine erhöhte elektrodermale Aktivität (EDA). Zusätzlich zeigte die Korrelation von EDA und fMRT-Daten bei Senioren eine positive Assoziation in Bereichen der sensomotorischen Verarbeitung, Erregbarkeit und emotionalen Empfindung. Die Ergebnisse der Senioren weisen darauf hin, dass das hoch automatisierte Schlucknetzwerk seine Fähigkeiten im Alter konstant beibehält. Die erhöhte Aktivierung bei den älteren Versuchspersonen könnte möglicherweise mit der erhöhten Erregbarkeit und Aufmerksamkeitsanforderung zusammen hängen, die sich aus den EDA-Daten ableiten lässt.

# *Inhaltsverzeichnis*

<b>Abbildungsverzeichnis</b>	viii
<b>Tabellenverzeichnis</b>	viii
<b>Abkürzungen</b>	ix
<b>1 Einleitung</b>	1
<b>2 Material und Methoden</b>	5
2.1 Versuchspersonen . . . . .	5
2.2 Aufgabe . . . . .	6
2.3 Datenerfassung . . . . .	7
2.4 Statistische Auswertung der Daten . . . . .	9
<b>3 Ergebnisse</b>	16
3.1 Erster Teil . . . . .	16
3.2 Zweiter Teil . . . . .	19
3.3 Dritter Teil . . . . .	21
<b>4 Diskussion</b>	27
4.1 Erster Teil . . . . .	28
4.2 Zweiter Teil . . . . .	31
4.3 Dritter Teil . . . . .	33
4.4 Einschränkungen . . . . .	36
<b>Schlussfolgerungen</b>	40
<b>Appendices</b>	43
<b>A Tabellen</b>	44

§0.0

INHALTSVERZEICHNIS

vii

**Literaturverzeichnis**

**49**

# *Abbildungsverzeichnis*

2.1	Aufbau des Experiments . . . . .	7
2.2	(a) Der gemessene Bereich für hohe zeitliche Auflösung. (b) Die sechs hämodynamischen Antwortfunktionen . . . . .	8
2.3	DCM Modelle . . . . .	13
2.4	Posteriore Wahrscheinlichkeit . . . . .	15
3.1	Repräsentationskarten von Schlucken und Okklusion . . . . .	17
3.2	Hirnstammaktivität bei Schlucken und Okklusion . . . . .	18
3.3	Hautleitfähigkeit . . . . .	19
3.4	Zeitliche Abfolge beim Schlucken . . . . .	20
3.5	Wahrscheinlichkeiten der DCM Modelle . . . . .	22
3.6	Kortikale Aktivität beim Schlucken korreliert mit EDA . . . . .	26

# *Tabellenverzeichnis*

A.1	Repräsentationsmaxima beim Schlucken, Okklusion und Schlucken – Okklusion . . . . .	45
A.2	Repräsentationsmaxima beim Schlucken über 6 Zeitpunkte . .	46
A.3	Repräsentationsmaxima der Aktivierungsmaxima bei alten Gesunden korreliert mit EDA . . . . .	47

# *Abkürzungen*

**ACC** anteriorer cingulärer Cortex

**ARAS** aufsteigendes retikuläres Aktivierungssystem

**BMS** Bayesian Model Selection

**BOLD** Blood Oxygen Level Dependent

**BA** Brodmann Areal

**CMG** craniomandibuläres Gelenk

**DCM** Dynamic Causal Modeling

**EDA** elektrodermale Aktivität

**EPI** Echo-Planar-Imaging

**fMRT** funktionelle Magnetresonanztomographie

**Fp1** Frontalpol 1

**FWE** Family-Wise Error

**GLM** General Linear Model

**M1** primärer motorischer Cortex

**M1S1** primärer sensormotorischer Cortex

**MCC** medialer cingulärer Cortex

**MEG** Magnetoencephalographie

**MNI** Montreal Neurological Institute

§0.0

x

**NTS** Nucleus tractus solitarii

**PMC** prämotorischer Cortex

**PWK** Posteriore Wahrscheinlichkeitskarten

**ROI** Regions of Interest

**S1** primärer somatosensorischer Cortex

**S2** sekundär-somatosensorischer Cortex

**SMA** supplementär-motorische Areal

**SPM** Statistical Parametric Mapping

**ZMG** zentrale Mustergeneratoren

## KAPITEL EINS

# *Einleitung*

Neurogene Dysphagien sind ein häufiges (und potenziell gefährliches) Krankheitsbild, das im Rahmen verschiedenster neurologischer Erkrankungen auftreten kann. Dabei sind Schlaganfälle zu 80% für das Auftreten neurogener Dysphagien verantwortlich (68). Die Hälfte der Schlaganfallpatienten weist in der Akutphase eine Dysphagie auf und ein großer Teil davon stirbt bereits in den ersten vier Wochen. Deswegen ist es von äußerster medizinischer Relevanz die cerebrale Steuerung des Schluckens bei Gesunden wie auch bei Patienten nach der Restitution der Schluckfunktion zu verstehen. Diese Arbeit befasst sich mit der Differenzierung der Schluckphasen und deren Anforderung hinsichtlich der funktionellen Repräsentation bei jungen Gesunden<sup>1</sup> im Vergleich mit älteren Gesunden<sup>2</sup>. Außerdem wurde die neuronale Aktivität von Kiefergelenkbewegungen mit der Schluckrepräsentation verglichen, um potentielle gemeinsame neuronale Strukturen zu beschreiben. Das Ziel dieser Arbeit ist ebenso eine Grundlage für eine Untersuchung von restituierten Dysphagiepatienten zu schaffen. Sie ist somit der erste Schritt um eine Veränderung der Schluckareale nach einem Schlaganfall und restituierte Schluckfunktionen mit funktioneller Bildgebung zu erforschen.

Der Schluckakt besteht aus drei Phasen: der oralen, pharyngealen und

1. Durchschnittsalter 25 Jahre.
2. Durchschnittsalter 65 Jahre.

der ösophagealen Phase. Während der oralen Phase wird das Material durch Mischen mit Speichel, Kauen und Formung eines Boluses für die pharyngeale Phase vorbereitet (15). Hierzu gehören unter anderem Bewegungen des craniomandibulären Gelenks (CMG). Die pharyngeale und die ösophageale Phase laufen unwillkürlich ab. Für eine störfreie Schluckfunktion sind diese nicht auf die Aktion des Cortex angewiesen (15; 38; 58).

CMG-Bewegungen sind durch die Okklusion des Kiefers charakterisiert. Die Bewegungen des CMG werden durch rhythmische Muskelaktivitäten hervorgerufen, die von einem neuronalen Netzwerk beeinflusst werden, das sich im Hirnstamm befindet. Man bezeichnet es als zentrale Mustergeneratoren (ZMG) (engl. central pattern generators) (61). Die Gruppen der Neuronen, die dabei involviert sind, befinden sich in der Umgebung des trigeminalen Systems. Hierbei ist der trigeminale Nerv entscheidend für Bewegungen des CMG, zusammen mit dessen assoziierten sensorischen, motorischen und premotorischen Kernen (61).

Auf kortikaler und subkortikaler Ebene rufen okklusale Bewegungen Aktivitätsmuster in primären und sekundären motorischen Arealen, Thalamus und cerebralen Hemisphären, im frontoparietalen Netzwerk, bilateral in der Insel und im cingulären Cortex hervor (46). Generell scheinen die für die Okklusion zuständigen Areale deckungsgleich mit den Schluckarealen zu sein (41). Schon 1955 wurde eine „linguomandibuläre Homotropie“ postuliert, mit der Annahme einer funktionellen Überlappung von Schlucken und CMG Bewegungen (86). Außerdem suggeriert die direkte Stimulation des primären motorischen Cortex bei Tieren (88) und Menschen (22; 66) eine Überlappung der primären motorischen Repräsentationsareale.

Auch die funktionelle Repräsentation des Schluckens ist weitgehend erforscht und klinisch höchst relevant (30), da bei einer Schluckstörung mit einer unerkannten Aspiration die Mortalität aufgrund rezidivierender Pneumonien hoch ist (14). Für die corticale Repräsentation wurden folgende Areale beschrieben: bilateraler inferiorer prä- und postzentraler Gyrus (49; 82), bilaterale anteriore Insel (35; 36; 70), anteriorer cingulärer

Cortex (ACC) (82), bilateraler Temporallappen und das supplementär-motorische Areal (SMA) (31; 64). Operkuläre Areale sind zur linken Hemisphäre lateralisiert (52; 54). Subkortikal wurden das linke Cerebellum und der dorsale Hirnstamm beschrieben, zusammen mit den Basalganglien (Putamen und Pallidum (77)) und dem Thalamus (49). In Tierversuchen wurde, die dem Hirnstamm zugewiesene reflektive Rekrutierung des Schluckens beschrieben (16). Diese zentralen Mustergeneratoren sind im vierten Ventrikel im dorsalen Hirnstamm zu finden. Interessanterweise stimmen sie in ihrer Lokalisation mit denen überein, die beim Schlucken in einer Positron-Emissions-Tomographie-Studie aktiviert wurden (31).

Eine Lateralisierung wurde in der linken Hemisphäre bei der Planung des Schluckens und in der rechten Hemisphäre während der Ausführung der Aufgabe entdeckt (50). In einer zeitaufgelösten Magnetenzephalographie-Studie wurde eine Lateralisierung, die einer früheren Stufe (orale Phase) beim Schlucken entspricht, in der linken Hemisphäre beschrieben. Diese verschiebt sich allmählich während der späteren Stufen (pharyngeale und ösophageale Phase) nach rechts (78). Dennoch ist die räumliche Auflösung der Magnetenzephalographie begrenzt und die Identifizierung von Dipolen ist in der Tiefe nur näherungsweise zu ermitteln (42). So bleibt noch offen, wie die zeitliche Abfolge der neuronalen Aktivierung beim Schlucken zwischen den Hirnregionen in einem funktionellen Magnetresonanztomographie (fMRT) Experiment zusammenhängen.

Neben der zeitlichen Abfolge der Aktivierungen ist die Änderung der Schluckrepräsentation im Alter zu berücksichtigen, denn Schluckstörungen sind häufiger bei Senioren anzutreffen. Verglichen mit jungen Probanden zeigen Experimente mit Senioren einen verzögteren Beginn des Schluckaktes (11; 35; 72). Bisherige fMRT Studien zeigen uneinheitliche Ergebnisse über die neuronale Aktivität des Schluckens bei älteren Menschen (35; 50; 52; 79). Allerdings ist hier anzumerken, dass die besagten Studien eine geringe Anzahl an Probanden (9–11) und unterschiedliche statistische Auswertungsmethoden benutzt haben. Die vorgeschlagene

Probandenzahl für eine robuste fMRT-Gruppenstatistik liegt bei 20 — optimal wären 27 (80). Somit bestehen methodische Differenzen, die zu den unterschiedlichen Ergebnissen geführt haben könnten. Der gemeinsame Nenner dieser Studien ist der Vorschlag, dass ältere gesunde Menschen kompensatorische Mechanismen in der Ausübung des Schluckaktes brauchen.

Die Arbeit der zugrunde liegenden fMRT Studie ist in drei Teile gegliedert. Der erste Teil befasst sich mit der Untersuchung der neuronalen Aktivität beim Schlucken und bei der Okklusion, wobei in dieser Studie eine höhere räumliche Auflösung angestrebt wurde. Der zweite Teil behandelt den zeitlichen Verlauf der Gehirnaktivität und die effektiven Konnektivität beim Schlucken. Dies wurde mit einer höheren zeitlichen Auflösung untersucht. Im dritten Teil geht es um den Unterschied in kortikaler Aktivität während des Schluckakts zwischen jungen und alten gesunden Probanden.

Die Ergebnisse dieser Studien wurden in drei wissenschaftlichen Zeitschriften veröffentlicht (56; 57; 87). Die Kopien der Publikationen sind dieser Arbeit beigefügt. An entsprechenden Stellen wird auf diese verwiesen.

## KAPITEL ZWEI

# *Material und Methoden*

Die hier beschriebenen Protokolle wurden von der Ethikkommission der Medizinischen Fakultät der Universität Greifswald als ethisch unbedenklich bewertet.

## **2.1 Versuchspersonen**

Eine Einverständniserklärung wurde von jeder Versuchsperson unterzeichnet. Bei keinem der Versuchspersonen lagen sensorisch-motorische, Schluck- oder craniomandibuläre Beschwerden vor.

Für den Vergleich von Schluck- und Okklusionsrepräsentation nahmen 21 neurologisch gesunde Versuchspersonen (Durchschnittsalter:  $24,8 \pm 3,2$  Jahre [Mittelwert  $\pm$  Standardabweichung], zwischen 20-33 Jahre, 16 Frauen) an der Studie gegen eine finanzielle Aufwandsentschädigung teil. Die zeitliche Analyse und Konnektivität umfasste Daten von 16 neurologisch gesunden Versuchspersonen (Durchschnittsalter:  $24,9 \pm 3,5$  Jahre, zwischen 20-33 Jahre, 11 Frauen). 24 junge (Durchschnittsalter:  $24 \pm 3,1$  Jahre, zwischen 20-33 Jahre, 16 Frauen) und 27 alte gesunde Versuchspersonen (Durchschnittsalter:  $64,8 \pm 6,5$  Jahre, zwischen 50-75 Jahre, 22 Frauen) bilden die Gruppen für die Untersuchung der Änderung der Schluckrepräsentation im Alter. Alle Versuchspersonen erhielten eine finanzielle Aufwandsentschädigung.

## 2.2 Aufgabe

Die Versuchspersonen wurden in eine Schluck- und eine Kieferbewegungsaufgabe eingewiesen. Für die Schluckaufgabe sollten sie alle 10 s, 2 ml Wasser schlucken, welches mittels einem MR-tauglichen Kontrastmittelapplikationsgerät (Spectris Solaris; Medrad, Warrendale, PA) durch einen dünnen Schlauch in die Mundhöhle verabreicht wurde. Es wurde Wasser verwendet, weil damit das Schlucken leichter ist als mit Speichel, jedoch nicht so leicht wie mit dickeren Flüssigkeiten (35). Außerdem ist die Viskosität von Wasser über Temperaturschwankungen im Zimmertemperaturbereich vernachlässigbar, was eine Reproduzierbarkeit des Experiments erleichtert. Der Schlauch wurde mittig zwischen den Lippen von den Versuchspersonen gehalten. Die Wasserdarbietung wurde zeitlich mit einem Farbwechsel (von blau [Ruhe] zu grün [Schlucken]) getriggert, welches in den Scanner projiziert wurde. Die Anweisung lautete, direkt nach vollständigem Ankommen des Wassers zu schlucken, und Schlucken in den Ruhepausen zu unterlassen.

Um die genaue Zeit des Schluckles aufzunehmen, wurde die Bewegung des Kehlkopfes mit einem Luftpolster aufgezeichnet. Der Kehlkopf übte einen Druck auf das Kissen aus, welches am Hals befestigt war. Die Veränderung des Luftdruckes wurde durch einen Druckdetektor in ein elektrisches Signal umgewandelt, welches von einem elektrooptischen Aufnahmegerät (Vario-b; Becker Meditec, Karlsruhe, Deutschland) gespeichert wurde. Hiermit konnte auch kontrolliert werden, ob die Versuchspersonen zwischendurch tatsächlich schluckten.

Für die Bewegung des Kiefergelenks mussten die Versuchspersonen innerhalb eines Zeitraums von 2 s drei Okklusionsbewegungen (sogenannte Taps) durchführen. Diese sollten alle 10 s bei dem oben beschriebenen Farbwechsel stattfinden, mit einer Gesamtzahl von 20 Wiederholungen pro Durchlauf. Ein weicher Gummischlauch wurde zwischen dem oberen und unteren Kiefer wie ein Zügel etwa in der Tiefe des ersten oder zweiten Prämolaren (Abb. 2.1, unten) platziert. Mit Hilfe des Schlauchs wurden okklusale Stärke und Frequenz durch einen Druck-

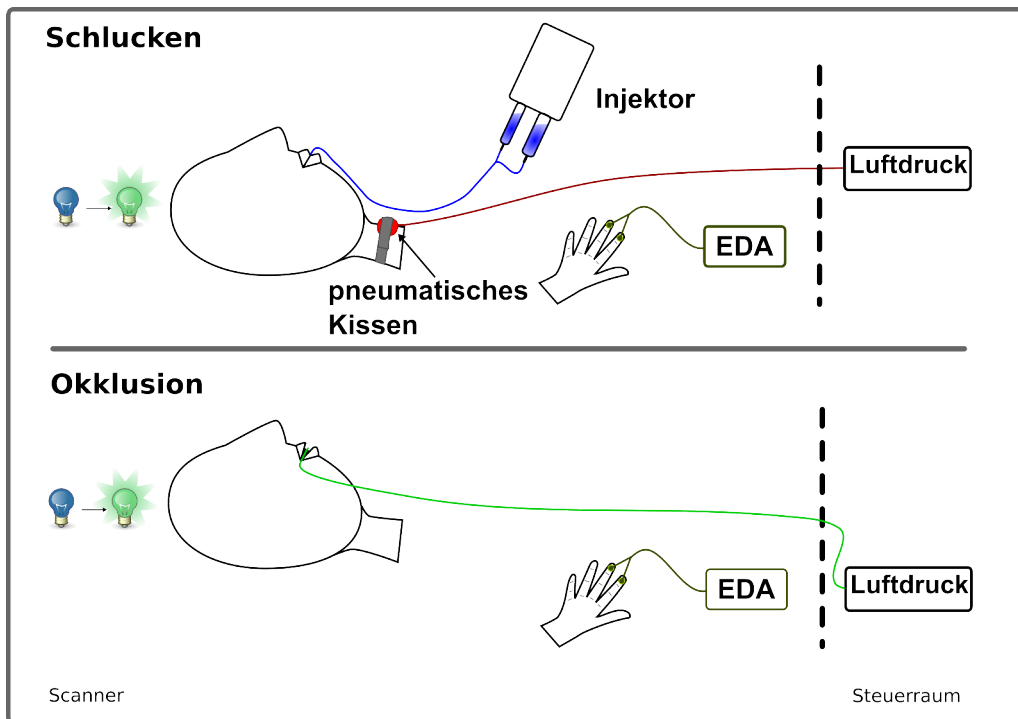


Abbildung 2.1: Aufbau des Experiments für Schlucken (oben) und Okklusion (unten).

detektor gemessen, der mit einem elektrooptischen Biosignal-Recorder (Vario-b, Becker Meditec) verbunden war. Um die Erregung während der Aufgaben zu kontrollieren, wurde gleichzeitig die Hautleitfähigkeit gemessen. Die dafür benutzten Elektroden wurden auf der Höhe des Phalanx distalis an den Zeige- und Mittelfinger der rechten Hand geklebt. Abbildung 2.1 skizziert den Aufbau des Experiments.

## 2.3 Datenerfassung

### fMRT Grundlagen

Anfang der 1990er Jahre wurde festgestellt, dass Hirnaktivität im Menschen zu lokalen Signalerhöhungen im MRT führte, welches für die funktionelle Hirnkartierung genutzt werden kann. Dieser Effekt wurde unter dem Namen Blood Oxygenation Level Dependent Effekt, oder kurz

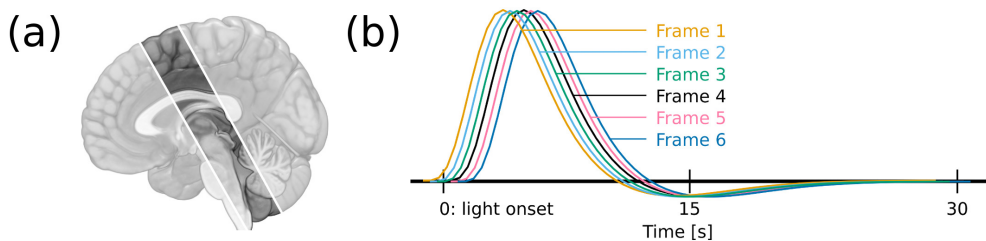


Abbildung 2.2: (a) Die schematische Darstellung des aufgenommenen Volumens in saggitaler Richtung für eine hohe zeitliche Auflösung. (b) Die sechs hämodynamischen Antwortfunktionen, zeigen schematisch, wie die zeitliche Analyse beim Schlucken durchgeführt wurde. Der Zeitpunkt 0 bezieht sich auf den Farbwechsel bzw. die Wasserverabreichung.

BOLD-Effekt bekannt (9). Dieser basiert auf biophysischen und physiologischen Prozessen. Zum einen erzeugt Desoxyhämoglobin, sauerstoffarmes Blut, Magnetfeldgradienten in und um Blutgefäße, welche das MR Signal minimieren. Zum anderen reduziert Gehirnaktivität die Konzentration von Desoxyhämoglobin, welches zu einem schwachen Anstieg des MR Signals führt (9). Diese Intensitätsunterschiede lassen somit indirekt auf neuronale Aktivitätsunterschiede schließen.

## fMRT Messung

MRT Daten wurden mit einem 3 T Scanner und einer 32-Kanal Kopfspule erfasst. Es wurden drei funktionelle, eine anatomische und eine kinematographische Sequenz für jede Versuchsperson aufgenommen.

Um für den zweiten Teil der Studie eine hohe zeitliche mit gleichbleibender räumlicher Auflösung zu gewährleisten, mussten die Anzahl der Schichten im Messvolumen des Gehirns reduziert werden. Deswegen wurden nur sieben Schichten gemessen was zu einer Repetitionszeit von 514 ms führte. Diese umfassten PMC, SMA, M1, S1, S2, Thalamus, Insel, Striatum, ventral das Cerebellum und den Hirnstamm, wie in Abb. 2.2(a) abgebildet.

Um eine Synchronisation der unterschiedlichen Erfassungsmethoden zu gewährleisten, wurden vom MRT Trigger ausgesendet, die als Referenz benutzt und gleichzeitig mit der Kehlkopf-, Okklusionsbewegung

und Hautleitfähigkeit synchronisiert wurden.

Für eine ausführliche Beschreibung der Sequenzen, sowie der Vorverarbeitung der Daten und der Auswertung der Hautleitfähigkeit sei an dieser Stelle auf die Methoden der beigefügten Publikation verwiesen.

## 2.4 Statistische Auswertung der Daten

### Klassisch-frequentistische Datenauswertung

Die statistische Auswertung der fMRI Daten wurde mit dem Programm Statistical Parametric Mapping (SPM) Version 8 durchgeführt. Hierbei wird eine *t*-Statistik gegen die Null-Hypothese (d.h. es gibt keinen statistisch signifikanten Effekt) unabhängig für jedes einzelne Voxel<sup>3</sup> berechnet. Um eine große Anzahl falsch positiver Voxel zu vermeiden, die wegen der noch größeren Anzahl der getesteten Voxel auftreten kann, wird mittels *Random Field Theory* eine sogenannte Family-Wise Error (FWE) Korrektur durchgeführt<sup>4</sup>. Diese besitzt eine Irrtumswahrscheinlichkeit von 5%. Hier werden die Daten geglättet und über die Größe der Glättung, statt des einzelnen Voxels, korrigiert. Eine ausführliche Beschreibung dieser Methode findet sich unter (6).

### Erster Teil: Schlucken und Okklusion

Individuelle statistische Karten (auch Kontraste genannt) wurden für Schluckaktivierung (Schlucken), Kiefergelenkbewegungen (Okklusion) und für den Vergleich der beiden Aktivierungen (Schlucken – Okklusion, Okklusion – Schlucken) berechnet. Die letzten beiden Differenzkontraste (Schlucken – Okklusion, Okklusion – Schlucken) testen die Gesamtdifferenz zwischen den zwei Aufgaben, um gezielte Regionen und

3. Ein Voxel ist eine 3-dimensionale Bildeinheit.

4. Um dieses sogenannte Problem der multiplen Vergleiche zu vermeiden, sollte man eine Bonferroni-Korrektur durchführen. Allerdings ist diese Korrektur zu konservativ (6) und deswegen ist eine FWE-Korrektur zu bevorzugen.

Aktivitätsstärken zwischen den Aufgaben zu erfassen. Um die Varianz zwischen den Versuchspersonen zu berücksichtigen, wird eine Random-Effects-Analyse als Gruppenstatistik berechnet. Das Signifikanzniveau aller Kontraste wurde mit  $p < 0.05$  FWE-korrigiert.

Zur anatomischen Zuordnung der Aktivierungen wurde die Anatomy Toolbox (20) verwendet, die die Jülicher cytoarchitektonischen Wahrscheinlichkeitskarten nutzt (1; 90). Distanzen zwischen den Repräsentationsmaxima wurden euklidisch berechnet.

Die Auswertung der elektrodermalen Aktivität (EDA)-Daten erfolgte mit dem Ledalab Toolkit (3) in Matlab. Die mittleren „Trough-to-Peak-Amplituden“ von Schlucken und Okklusion wurden mit einem gepaarten  $t$ -Test verglichen.

## Zweiter Teil: Zeitliche Analyse und Konnektivität

### Statistische Karten über die Zeit

Statistische Karten (engl. statistical parametric maps [SPM]) wurden für die Schluckaktivierung an sechs verschiedenen Zeitpunkten in Schritten von 1.5 s ( $-4.5$  s bis 3.0 s) berechnet. Der Zeitpunkt bei null Sekunden entspricht dem Farbwechsel bzw. der Verabreichungszeit des Wassers (Abb. 2.2[b]). Diese Schritte wurden empirisch gewählt, um signifikante Veränderungen zwischen den Intervallen zu erfassen. Kleinere Schritte führten zu kleineren Veränderungen von einem Bild zum nächsten.

Eine Random-Effects-Gruppenanalyse wurde für jeden Zeitpunkt berechnet. Aktivitätsmaxima wurden mittels anatomischer Masken, auch als Regions of Interest (ROI) bekannt, aus der Anatomy Toolbox für SMA, prämotorischer Cortex (PMC) und primärer sensomotorischer Cortex (M1S1) ausgesucht. Karten fürs Cerebellum (Larsell IV-VI), Insel und Pons wurden dem WFU PickAtlas (51) entnommen.

### Varianzanalyse mit Messwiederholungen

Beta-Werte<sup>5</sup> wurden mittels einer 6 mm Sphäre um den höchsten aktivierte Voxel in jedes ROI ausgesucht. Diese wurden dann in einer Varianzanalyse mit Messwiederholungen benutzt um folgende Faktoren zu untersuchen:

- Region (PMC, SMA, M1S1, Insel, Cerebellum),
- Seite (rechts, links),
- Zeit (Zeitfenster 1, 2, 3, 4, 5, 6).

Basierend auf unseren Hypothesen und Ergebnissen aus vorherigen Studien, wurden signifikante Effekte in der Varianzanalyse von einem post-hoc *t*-test gefolgt:

1. Lateralisationseinfluss über die Zeit in drei Zeitfenstern: 1, 2 und 6 (drei Vergleiche pro Region;  $p_{corr} = 0.016$ );
2. Zeiteinfluss für jede Region (gemittelt für jede Seite; 6 Vergleiche;  $p_{corr} = 0.008$ );
3. Onseteinfluss zwischen Regionen (gemittelt für jede Seite; 5 Vergleiche;  $p_{corr} = 0.010$ ).

### Dynamic Causal Modelling

Zur Untersuchung effektiven Konnektivität wurde Dynamic Causal Modeling (DCM) (24) für SPM8 benutzt. Die effektive Konnektivität bezeichnet den Einfluss eines neuronalen Systems auf ein anderes. Dabei geht es darum Rückschlüsse über die Kopplung zwischen Hirnregionen und wie diese Kopplung durch experimentelle Zusammenhänge beeinflusst wird, treffen zu können.

5. Die Beta-Werte sind die Parameter der Matrix des experimentellen Designs. Sie definieren den Beitrag jeder Komponente (in diesem Fall die Schluckzeiten) der Design-Matrix und werden geschätzt, sodass der Fehler minimiert wird. Sie werden auch zur Kontrastberechnung benutzt.

Die Ziele der DCM-Analyse waren zunächst die Rolle des Inputs (eine äußere Störung, die experimentell herbeigeführt wird) zu erforschen, da es sowohl einen visuellen (Farbwechsel) als auch einen somatosensorischen (Wasser dringt in die Mundhöhle ein) „Onset<sup>6</sup>“ zur Planung und Ausführung des Schluckakts gab. Basierend auf diese „Onsets“ wollten wir zudem Informationen über die Richtungsabhängigkeit während der motorischen Planung, Durchführung und Vermittlung beim Schlucken bekommen. Die Modelle wurden einfach gehalten und waren auf drei Regionen fokussiert: 1. die SMA, welches die Planung und Durchführung von komplexen motorischen Bewegungen wie Schlucken verarbeitet wird (31; 63); 2. M1S1, der eine wichtige Rolle bei der Muskelkontrolle und sensorischer Rückkopplung während des Schluckens spielt (49) und 3. die Insel, die Verbindungen zum primären Motorcortex und der supplementär-motorischen Area besitzt und eine wichtige Rolle bei der Mediation vom oropharyngealem Schlucken spielt. Der primäre motorische Cortex (M1) und der primäre somatosensorische Cortex (S1) wurden wegen der geringen räumlichen Auflösung zusammengelegt. Linke und rechte Gehirnhälften wurden getrennt analysiert, mit Ausnahme der SMA wegen ihrer zentralen Lage und der zumeist bilateralen Repräsentation in diesem Areal.

Die Seed Regionen für die DCM wurden durch eine Kombination von funktionellen und den oben genannten anatomischen Karten erzeugt. Eine repräsentative Zeitreihe von den Voxeldaten als erste Eigenvariate in allen überschwelligen Voxeln ( $p < 0.05$  FWE korrigiert) wurde von den zeitlich hoch aufgelösten Echo-Planar-Imaging (EPI)-Aufnahmen für alle Versuchspersonen extrahiert.

### Modellauswahl und -vergleich

Die sechs aufgestellten DCM Modelle sind in Abb. 2.3 dargestellt. Im Modell (a) tritt der Stimulus in die SMA ein, welches direktonal zum M1S1

6. Als Onset bezeichnet man den Beginn der Stimulation.

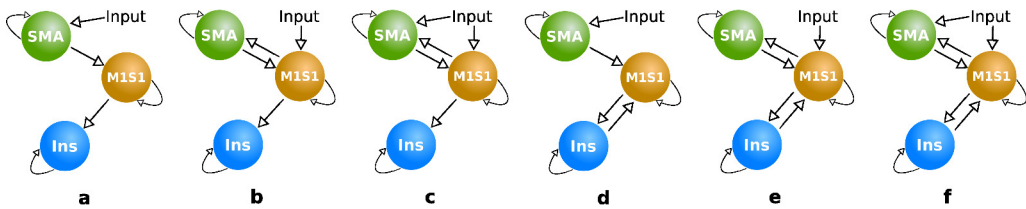


Abbildung 2.3: Die sechs DCM Modelle die hier untersucht wurden. Sie unterscheiden sich in den Verbindungen und Inputs.

verbunden ist. Hier könnte der Farbwechsel durch den visuellen Kortex die Vorbereitung des Schluckes beeinflussen. Im Modell (b) tritt der Stimulus hingegen bei M1S1 ein. Hier könnte das in den Mund eintretende Wasser S1 stimulieren, das ein Signal an die SMA weiterleitet, um den Schluck vorzubereiten, der dann durch den M1 ausgeführt wird. Um diese Kommunikation zu gewährleisten, wurde die Verbindung zwischen SMA und M1S1 in beiden Richtungen angegeben. Modell (c) basiert auf Modell (b) hat aber zwei Stimuluseingänge, den visuellen zur SMA und den somatosensorischen zum M1S1. Alle Modelle haben eine gerichtete Verbindung zur posterioren Insel. Modelle (d) bis (f) ähneln denen von (a) bis (c) mit der Ausnahme, dass die Verbindung zwischen M1S1 und Insel bidirektional verläuft. Alle Modelle wurden geschätzt und über die Gruppe mittels Bayesian Model Selection (BMS) (75) verglichen.

### Dritter Teil: Veränderung der kortikalen Schluckrepräsentation im Alter

Zwei statistische Ansätze wurden hier angewendet. Beide basieren auf das General Linear Model (GLM), welches in SPM8 implementiert ist. Der erste Ansatz ist der klassisch-frequentistische. Dieser ist konservativer weil die Korrektur für die multiplen Vergleiche sehr streng ist (25) und dadurch die Sensitivität der Inferenz verringert wird. Der zweite Ansatz, die viel spezifischere Bayes-Statistik, hat zudem nicht das Problem multiple Vergleiche durchzuführen (25).

### Klassisch-frequentistische Inferenz

Statistische parametrische Karten wurden für die Schluckaktivierung bei jungen und alten Gesunden separat berechnet. Die Hautleitfähigkeit wurde als Kovariate in eine Regressionsanalyse für jung und alt separat berechnet. Außerdem wurde die durchschnittliche Dauer des Schlucks als Kovariate mit berechnet.

### Bayes Statistik

Die klassisch-frequentistische Inferenz weist ein paar Unzulänglichkeiten auf. Zum einen spiegelt der  $p$ -Wert nicht das Vorhandensein des Effekts wider, sondern die Wahrscheinlichkeit der Erscheinung des Features wenn der Effekt fehlt (23). Zusätzlich kann die alternative Hypothese nie verworfen werden, weil die Wahrscheinlichkeit eines Null-Effekts null ist. Wenn genug Scans oder Versuchspersonen gemessen werden, besteht die Möglichkeit eines Auftreten des Effekts für jedes Voxel. Außerdem steigt die Schwelle mit dem einbezogenen Volumen, d.h. kleinere Volumen zeigen signifikantere Effekte. Daher ändert sich der  $p$ -Wert, auch wenn die Wahrscheinlichkeit eines aktiven Voxels unverändert bleibt (23).

Es macht also mehr Sinn, die Wahrscheinlichkeit des Effekts mit den gegebenen Daten zu finden, anstatt die Wahrscheinlichkeit der Daten zu suchen, wenn kein Effekt vorhanden ist. Die Bayes Statistik benutzt genau diesen Ansatz mit dem Ergebnis einer posterioren Wahrscheinlichkeit. Diese wird mittels der Anfangswahrscheinlichkeit oder A-priori-Wahrscheinlichkeit [ $P(A)$ ] und der Likelihood [ $P(B|A)$ ] mit Hilfe von dem Satz von Bayes berechnet (44):

$$P(A|B) = \frac{P(A) \cdot P(B|A)}{\sum_A P(A) \cdot P(B|A)}.$$

Posteriore Wahrscheinlichkeitskarten wurden für die gleichen Bedingungen berechnet, wie in Abschnitt 2.4 beschrieben, unter Berücksichtigung der Baysschen Inferenz. Um den Effekt über die Gruppe zu berechnen, wählt man die Varianz über die Voxel als Anfangswahrscheinlichkeit,

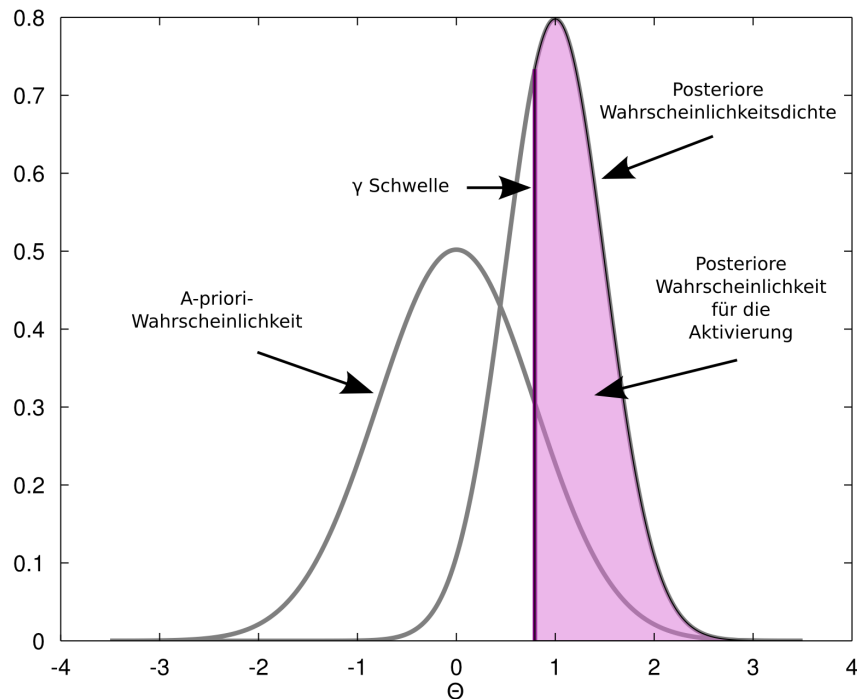


Abbildung 2.4: Die Fläche unter der posterioren Wahrscheinlichkeitsdichte wird für jedes Voxel berechnet, um eine Bayessche Aussage zu treffen. Die Schwelle  $\gamma$  bezeichnet die Varianz über die Voxel gegeben durch die A-priori-Standardabweichung, das sogenannte „Grundrauschen“. Die posteriore Wahrscheinlichkeit einer Aktivierung ist durch die Fläche unter der posterioren Wahrscheinlichkeitsdichte und der  $\gamma$ -Grenze gegeben.

keit (26). Die A-priori-Standardabweichung kann als neuronales „Grundrauschen“ betrachtet werden und entspricht einem Aktivierungslevel, welches das ganze Gehirn umfasst (19). Das Ergebnis ist das Vertrauen, dass der Effekt eine höhere Wahrscheinlichkeit als das „Grundrauschen“, also als die A-priori-Standardabweichung hat (25; 26). Diese Schwelle wird mit dem Buchstaben  $\gamma$  bezeichnet. Ein visuelles Beispiel der A-priori- und posterioren Wahrscheinlichkeit ist in Abb. 2.4 dargestellt.

## KAPITEL DREI

# *Ergebnisse*

### **3.1 Erster Teil: Schlucken und Okklusion**

#### **Schlucken**

Die Schluckdauer vom visuellen Reiz zur Kehlkopfbewegung betrug  $2,6 \pm 0,4$  s (Mittelwert  $\pm$  Standardabweichung) und beinhaltet die Zeit der Wasserverabreichung (1 s), was darauf hinweist, dass die Versuchspersonen sofort nach vollständiger Ankunft des Wasservolumens reagiert haben.

Für die Schluckaufgabe (Abb. 3.1, Tabelle A.1 links) wurden Repräsentationsareale bilateral im M1S1, sekundär-somatosensorischer Cortex (S2), PMC, SMA, medialen Gyrus cinguli, Pars opercularis, Insel, Thalamus, Kleinhirnrinde, Vermis cerebelli, Pallidum und Pons identifiziert. Eine Übersicht gibt Abb. 3.1. In Tabelle A.1 links sind die Aktivierungsmaxima und deren Koordinaten dargestellt.

#### **Okklusion**

Die drei Taps bei der Okklusionsbewegung hatten eine Dauer von  $1,5 \pm 0,2$  s. Hier wurden die gleichen Repräsentationsareale wie beim Schlucken gefunden, ausgenommen von der SMA, dem linken Thalamus, dem rechten Kleinhirn, dem Vermis cerebelli und der linken Pons (Abb. 3.1 und 3.2, Tabelle A.1, mitte).

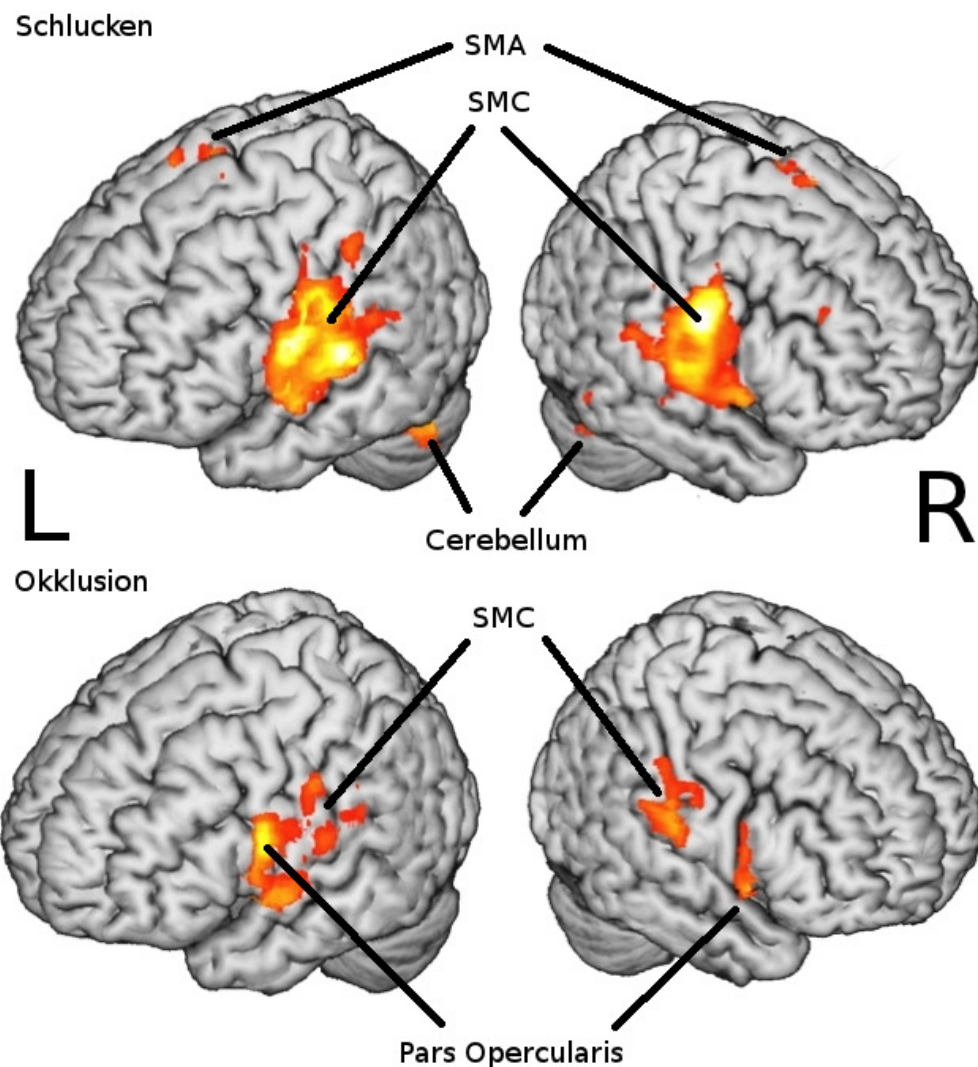


Abbildung 3.1: Repräsentationskarten projiziert auf das segmentierte Montreal Neurological Institute (MNI)-Referenzgehirn. Oben: Schlucken; unten: Okklusion. Hier gezeigte kortikale Aktivität wurde im primär somatosensorischem und motorischem Kortex (M1S1), im sekundär-somatosensorischem Kortex (S2), der Pars opercularis des inferioren frontalen Gyrus (BA 44) und in den cerebellären Hemisphären für beide Aufgaben, und im supplementär-motorischem Areal (SMA) für das Schlucken gefunden.

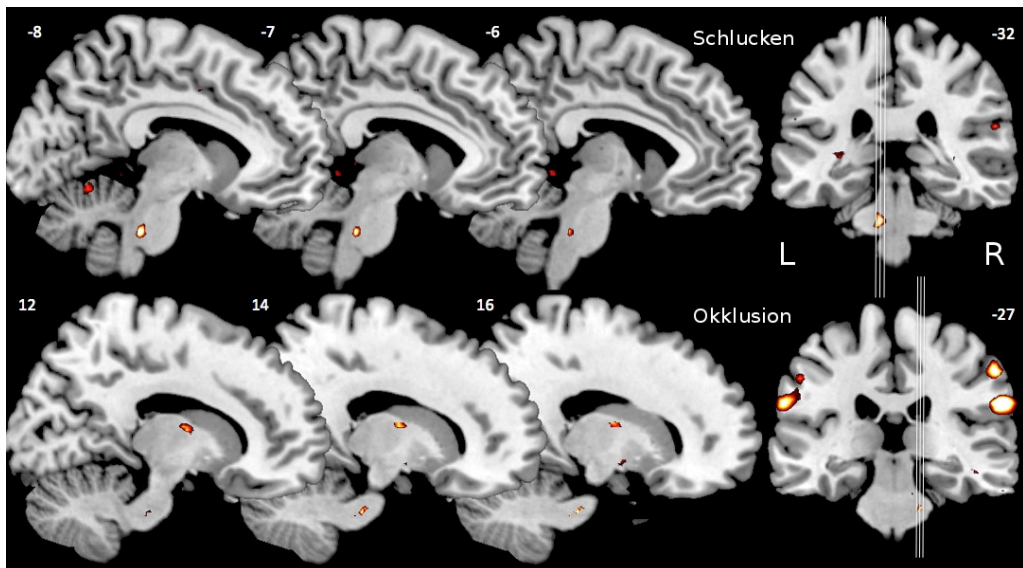


Abbildung 3.2: Hirnstammaktivität während Schlucken und Okklusion dargestellt für 3 sagittale Schnitte. Die Schnittposition wird rechts in der koronaren Ebene gezeigt ( $y$ -MNI Koordinate ist oben rechts zu finden). Die  $x$ -MNI Koordinate der sagittalen Schnitte befindet sich oben links. Oben: Hirnstammaktivität für Schlucken zeigt den sensorischen Kern des Nervus trigeminus. Die Aktivierung des Nucleus des Tractus solitarius ist hier nicht gezeigt. Unten: Hirnstammaktivität für Okklusion zeigt Aktivität im Nervus trigeminus.

Die Repräsentationsmaxima in M1 zwischen Schlucken und Okklusion liegen nebeneinander: Links war die euklidische Distanz 4.5 mm und rechts 4.9 mm. Eine nähere Analyse im Hirnstamm zeigte Aktivierung im sensorischen Kern des Nervus trigeminus und im Nucleus tractus solitarii (NTS) für das Schlucken. Bei der Okklusion zeigte sich die Aktivierung etwas lateraler im Nervus trigeminus (Abb. 3.2).

### Schlucken im Vergleich mit Okklusion

Der Kontrast Schlucken minus Okklusion zeigte signifikante Aktivierung in fast allen Bereichen, die im Haupteffekt beim Schlucken gefunden wurden, außer im Vermis cerebelli, im rechten Pallidum und in der Medulla (Tabelle A.1, rechts). Der umgekehrte Kontrast (Okklusion minus Schlucken) zeigte keine signifikanten Voxel, was die Aussage unterstreicht, dass beim Schlucken mehr zerebrale und cerebelläre Ressourcen

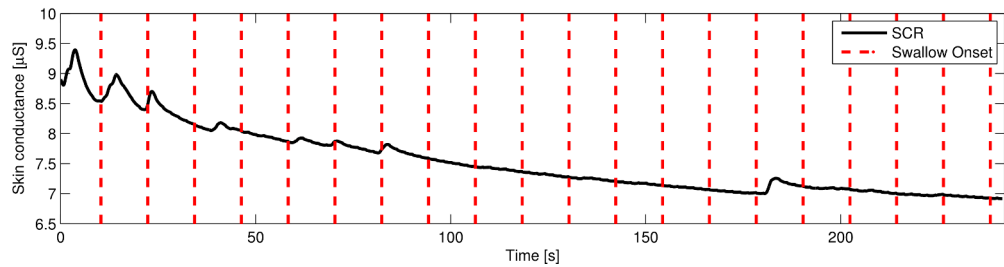


Abbildung 3.3: Hautleitfähigkeit einer Versuchsperson beim Schluckexperiment. Die vertikalen Linien zeigen die Zeit der Wasserverabreichung an. Die hohen Werte am Anfang deuten auf eine Schreckreaktion zu Beginn des Scannens und die Ungewöhnlichkeit der Stimulation (visuell und somatosensorisch) hin, welches mit der Zeit und mit der Gewöhnung an die Umgebung absinkt.

als beim Kauen notwendig sind.

## Hautleitfähigkeit

Die gepaarten *t*-Test Ergebnisse der Hautleitfähigkeitsuntersuchung zwischen Schlucken und Okklusion wiesen keine Unterschiede auf. Die Daten zeigten am Anfang eine dramatische Änderung des tonischen Signals gefolgt von ein paar phasischen Peaks die mit dem Lichtonset korrelierten und anschließend während des Durchlaufs verschwanden (Abb. 3.3).

## 3.2 Zweiter Teil: Zeitliche Analyse und Konnektivität

### Statistische Karten über die Zeit

Die Entwicklung der Blood Oxygen Level Dependent (BOLD)-Aktivität über die Zeit, ermittelt durch die GLM-Analyse ist in Abb. 3.4 dargestellt. Im ersten Zeitrahmen wurde kortikale Aktivität in der linken posterioren SMA, dem PMC in der somatotopen Höhe der Lippe und Zunge und im subkortikalen bilateralen Thalamus gefunden. Zum zweiten Zeitpunkt wurde die bilaterale anteriore und posteriore SMA und der PMC, der primäre Motorkortex und bilateraler Thalamus aktiviert. Im dritten Zeit-

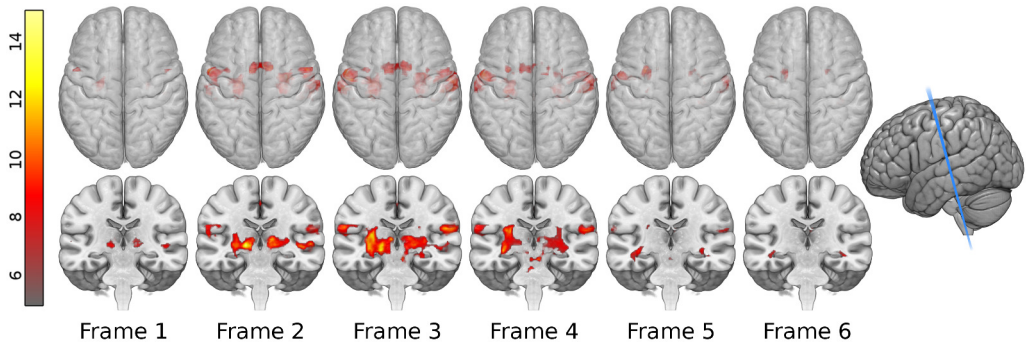


Abbildung 3.4: Statistische parametrische Karten für sechs HRF, die in der GLM Analyse benutzt wurden. Die obere Reihe zeigt die leicht durchsichtigen Gehirne in axialer Richtung. Die untere Reihe zeigt einen leicht gekippten coronaren Schnitt, wie ganz rechts gezeigt wird. Der Farbbalken zeigt die t-Wertkodierung von grau (niedrig) bis leuchtend gelb (hoch).

fenster war die Aktivierung am stärksten für alle bisher beschriebenen Bereiche. Zusätzlich zeigten sich Aktivierungen im bilateralen S1 und S2 sowie bilateral in der Insel. Kaum Unterschied konnte man im nächsten Zeitfenster (Frame 4, Farbwechsel/Wasserverabreichung) erkennen, mit Ausnahme der Hirnstammaktivität. Das fünfte Zeitfenster zeigte eine Restaktivierung in der linken SMA und M1/S1. Das letzte Zeitfenster (Frame 6) zeigte keine signifikanten Aktivierungen. Die durch die anatomischen Karten aufgezeichneten Aktivierungsmaxima sind in Tabelle A.2 im Appendix A (S. 44) für alle Zeitfenster zusammengetragen.

Für die Zeitpunkte der oralen und pharyngealen Phasen wurden keine signifikanten (FWE korrigiert,  $p < 0.05$ ) Aktivierungen gefunden.

## Varianzanalyse mit Messwiederholungen

Die Varianzanalyse mit Messwiederholungen hatte einen signifikanten Haupteffekt für *Region*, *Zeit* und eine signifikante Interaktion zwischen *Region*  $\times$  *Zeit* und *Region*  $\times$  *Seite*  $\times$  *Zeit*. Post-hoc *t*-Tests zeigten einen signifikanten Lateralisierungseffekt über die *Zeit* für M1S1 angefangen mit einer Linkslateralisierung im Zeitfenster 2 welche abschließend nach rechts im Zeitfenster 6 gerückt war. Eine Lateralisierung in der Insel wurde für das Zeitfenster 3 beobachtet. In anderen Bereichen war jedoch kei-

ne signifikante Lateralisierung vorhanden. Da der Effekt der Seite nicht als Hauptfaktor signifikant war, wurden alle Aktivierungsgrößen pro Region und Zeit für beide Hemisphären gemittelt. Beim Test über die Zeit war ein Anstieg im PMC und M1S1 vom ersten zum dritten Zeitfenster zu beobachten, gefolgt von einem Plateau (M1S1 und PMC zwischen Zeitfenster 3 und 4), der schließlich in einer signifikanten Abnahme endete (Zeitfenster 4 bis 5). In der SMA kam der Anstieg etwas früher und kehrte sich schon im dritten zum vierten Zeitfenster um. Es gab keine relevanten Änderungen über die Zeit in den Kleinhirnhemisphären.

## **Dynamic Causal Modeling**

Die Analyse durch die Random Effects Bayesian Model Selection hat gezeigt, dass Modell (c) (Abb. 3.5) für beide Hemisphären alle anderen Modelle übertroffen hat. Hier ging der Input zur SMA und zum M1S1, wobei beide Areale bidirektional verbunden waren und M1S1 gerichtet zur Insel verbunden war. Die Erwartungswahrscheinlichkeiten waren 0,30 für die linke Hemisphäre und 0,29 für die rechte Hemisphäre. Die Überschreitungswahrscheinlichkeit<sup>7</sup> (engl. exceedance probability) war 0,49 links und 0,46 rechts.

### **3.3 Dritter Teil: Veränderung der kortikalen Schluckrepräsentation im Alter**

#### **Verhaltensdaten – Schlucklatenz**

Die älteren Probanden wiesen eine etwas verlängerte Schluckzeit auf, verglichen mit den jungen Probanden ( $t(39) = 4.69, p < 0.001$ ). Im Durchschnitt betrug die Schluckzeit bei den älteren  $3.42 \pm 0.53$  s verglichen mit  $2.60 \pm 0.40$  s bei den jungen Gesunden. Beide Werte enthalten

7. Die Wahrscheinlichkeit, dass ein Modell wahrscheinlicher ist als alle anderen untersuchten Modelle.

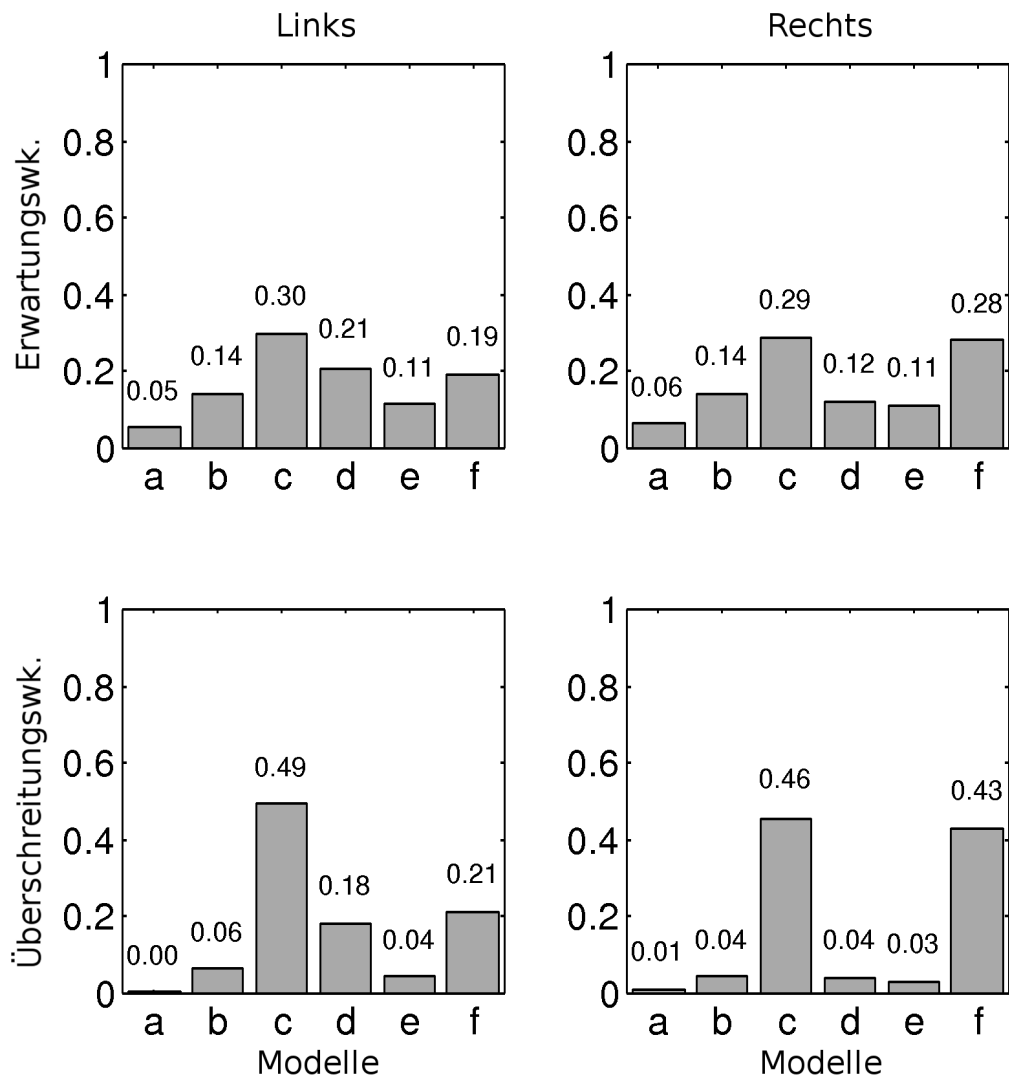


Abbildung 3.5: Erwartungs- und Überschreitungswahrscheinlichkeit der sechs getesteten DCM Modelle. Die linke Spalte zeigt die Ergebnisse für die linke Hemisphäre und die rechte Spalte für die rechte Hemisphäre.

eine Sekunde Verzögerung, die für die Verabreichung des Wassers notwendig ist.

### **Hautleitfähigkeit**

Die Hautleitfähigkeitswerte waren bei den Senioren größer als bei den jungen Gesunden (gemittelt:  $0.148 \pm 0.126 \mu\text{S}$  vs.  $0.073 \pm 0.068 \mu\text{S}$ ;  $t(47) = 2.46, p < 0.05$ .)

### **Korrelationsanalyse von elektrodermaler Aktivität, Ausführung und Alter**

Wegen der großen Altersspanne bei den älteren Probanden (zwischen 55–75 Jahre) wurde eine lineare Korrelation zwischen Alter und EDA, Alter und Schluckzeit sowie EDA und Schluckzeit berechnet. Es gab keine relevante Assoziation für Alter und EDA bei den alten Probanden ( $r^2 = 0.09$ , n.s.). Nicht-signifikante Korrelationen gab es bei Alter und Schluckzeit ( $r^2 = 0.02$ , n.s.) und EDA und Schluckzeit ( $r^2 = 0.0002$ , n.s.) für die Daten der Senioren.

Die Testung für EDA und Schluckzeit über die ganze Gruppe (jung und alt) ergab keine signifikante Korrelation ( $r^2 = 0.015$ , n.s.).

### **Statistische parametrische Karten – klassische Inferenz**

Die schluckbedingte Gehirnaktivität bei den alten Probanden wurde im bilateralen M1S1, S2, PMC, der SMA, Broca Areal und Broca Analogon, der Pars opercularis, in der Insel, im Thalamus, dem Nucleus caudatus, Pallidum, Putamen, Pons im Gebiet des Nervus trigeminus und NTS, bilateral in den cerebellären Hemisphären I-VIIa und im Vermis, dem bilateralen Hippocampus, der rechten Amygdala, dem ACC, visuellen Cortex, Lobus parietalis inferior, intraparietalen Sulcus, mittleren und inferioren Gyrus temporalis und auditorischem Kortex gefunden.

Die Gehirnaktivität der jungen Gesunden wurde im Abschnitt 3.1 beschrieben. Die Haupteffekte sind mit denen im hier beschriebenen Ab-

schnitt vergleichbar mit zusätzlicher Aktivität im linken medialem cingulärem Cortex (MCC) und rechtem posterioren cingulären Cortex.

Der Vergleich der Repräsentationskarten zwischen den beiden Gruppen ergab keine relevanten Unterschiede (FWE,  $p < 0.05$ ). Das selbe gilt auch für einen unkorrigierten Test ( $p < 0.001$ ) sowie für eine Begrenzung des Testvolumens (engl. small volume correction). Diese zusätzlichen Tests und deren Ergebnisse unterstreichen die Interpretation eines fehlenden Unterschieds in den Aktivierungsmuster zwischen Jung und Alt.

### **Posteriore Wahrscheinlichkeitskarten – Bayes Statistik**

Die Bayes-Statistik bei den alten Gesunden zeigte zusätzlich zu den oben genannten aktivierten Arealen Aktivität im ACC und bilateral in den cerebellären Hemisphären I-IX. Bei den jungen Gesunden wurde zusätzlich im Cerebellum (VII und IX) Aktivität gefunden. Der Vergleich zwischen den Gruppen mit einem *t*-Test bei zwei Stichproben lieferte eine erhöhte bilaterale Aktivierung bei der älteren Gruppe in Brodmann Areal (BA) 10 welches dem Frontalpol 1 (Fp1) entspricht (5). Bei den jungen Gesunden zeigte sich keine statistisch signifikante Aktivität.

### **Korrelationsanalyse – klassische Inferenz**

Die Korrelationsanalyse der BOLD-Antwort mit dem Alter bei jungen und alten Gesunden zeigte keine signifikanten Ergebnisse. Das gleiche Ergebnis wurde gefunden, wenn man die BOLD-Antwort und die EDA bei den jungen Gesunden korreliert. Die Korrelation von BOLD-Antwort und Schluckzeit ergab keine signifikante Assoziation bei Jung und Alt. Allerdings zeigte eine Korrelationsanalyse der BOLD-Antwort mit EDA bei den alten Probanden aktivierte Voxel in der linken SMA, im linken superioren Temporallappen und rechtem Broca Analogon (BA 45). Die Ergebnisse sind in der Tabelle A.3 zu finden.

## Korrelationsanalyse – Bayes Statistik

Es gab keine signifikanten Korrelationen zwischen BOLD-Antwort und Alter sowie BOLD-Antwort und Schluckzeit bei Jung oder Alt. Die Korrelation von BOLD-Antwort und EDA bei den jungen Probanden war nicht signifikant. Allerdings zeigte sich eine signifikante Korrelation zwischen BOLD-Antwort und EDA bei den alten Probanden im bilateralen M1S1, linken S2, bilateralem SMA, ACC, und MCC, linken BA 44 und BA 45, linken Hippocampus, der linken Insel und dorsolateraler Pons in der Umgebung des aufsteigenden retikulären Aktivierungssystems (ARAS). Diese sind in Tabelle A.3 aufgelistet und in Abb 3.6 zu sehen.

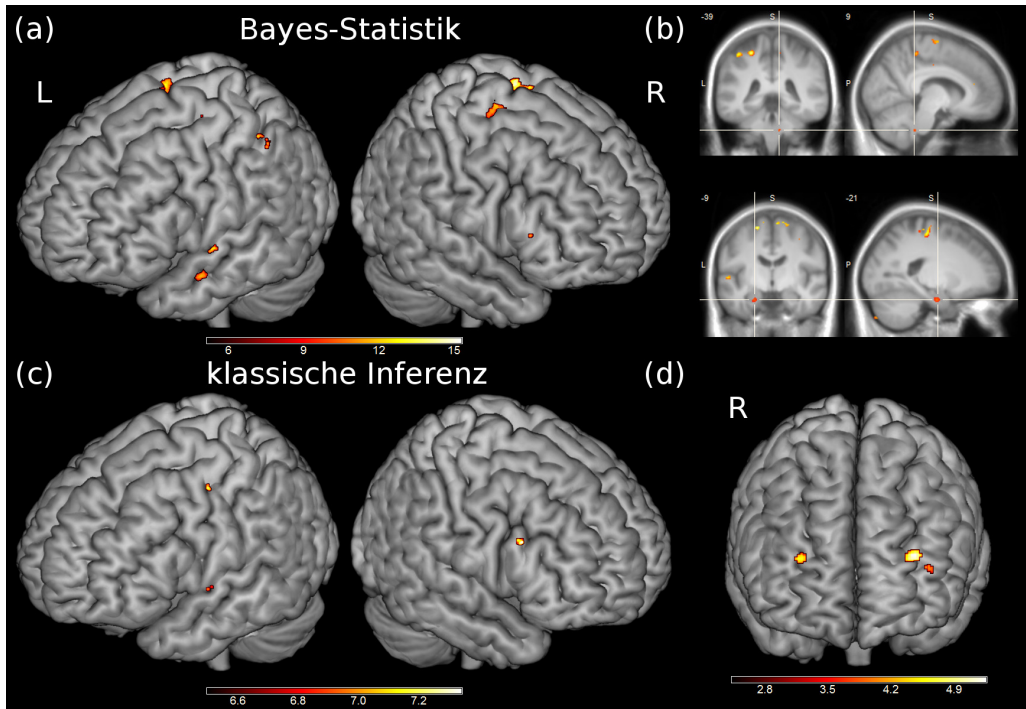


Abbildung 3.6: BOLD-Antwort beim Schlucken korreliert positiv mit der Hautleitfähigkeit. (a) Posteriore Wahrscheinlichkeitskarten (PWK) mit Bayes-Statistik berechnet ( $P > 95\%$ ) projiziert auf ein 3D-Gehirn. Dargestellte Aktivierungen sind im primär motorischem Kortex (M1), primär somatosensorischem Cortex (S1), sekundär somatosensorischem Cortex, bilateraler supplementär-motorischer Area (SMA) und im linken Brodmann Areal (BA) 44 und BA 45 zu finden. (b) Die gleiche PWK wie in (a) überlagert auf ein gemitteltes normalisiertes T1 Bild von 51 Probanden (coronal: links, saggital: rechts). Das Bild oben zeigt die Aktivierung in der Pons welches dem aufsteigendem retikulärem Aktivierungssystems (ARAS) entspricht. Das untere Bild zeigt die Aktivierung im Hippocampus. (c) Statistische parametrische Karten welche mittels klassischer Inferenz berechnet wurden (FWE-korrigiert,  $p < 0.05$ ). Aktivierungen sind in der linken SMA, dem rechten Broca Analogon (BA 45) und linkem superiorem temporalem Gyrus zu finden. (d) PWK für den Kontrast alt vs. jung der mit einer 95% Wahrscheinlichkeit zeigt, dass die Aktivierung im bilateralem BA 10 größer ist als die a-priori Standardabweichung.

## KAPITEL VIER

# *Diskussion*

Ziel der zugrunde liegenden Untersuchung war es, zum einen den Unterschied in zerebraler Aktivität zwischen Schlucken und Okklusion mittels fMRT zu untersuchen, wobei der Fokus auf Hirnstammprozesse gelegt wurde. Zum anderen wollten wir die zeitliche Abfolge und effektive Konnektivität beim Schlucken untersuchen. Zudem sollten Unterschiede in der Hirnaktivität während des Schluckens zwischen jungen und alten Gesunden herausgearbeitet werden. Hautleitfähigkeitsmessungen dienten zur Kontrolle der Anstrengung beim Ausführen der Aufgaben. Die Aktivierung beim Schlucken unterschied sich von derjenigen während der Okklusion in erster Linie in der Stärke und in der Ausbreitung. Im zweiten Teil wurden funktionelle Bilder mit hoher zeitlicher Auflösung aufgenommen und eine GLM Analyse über sechs Zeitpunkte berechnet. Die zeitliche Analyse zeigte eine sukzessive Gehirnaktivität angefangen beim PMC, der SMA und bilateralen Thalamus, gefolgt vom M1S1, der posterioreren Insel und dem Cerebellum. Das Ende der Sequenz war gekennzeichnet durch eine Aktivierung in der Pons. Die Varianzanalyse mit Messwiederholungen zeigte eine anfänglich linkshemisphärisch lateralisierte Aktivierung, welche sich mit der Zeit zur rechten Hemisphäre verschob. Das Resultat der DCM Analyse ergab als wahrscheinlichstes Modell eine bidirektionale Verbindung zwischen SMA und M1S1, mit einer einseitigen Verbindung von M1S1 zur posterioren Insel. Der dritte Teil beschäftigte sich mit der Veränderung der Gehirnaktivität im Alter beim

Schlucken. Eine Differenz der kortikalen Schluckrepräsentation von alten minus jungen Gesunden wurde nur in BA 10 mit Hilfe der Bayes Statistik gefunden. Senioren zeigten zudem eine verlängerte Schluckzeit und höhere Hautleitfähigkeit. Die Gehirnaktivität war bei manchen Senioren positiv mit der Hautleitfähigkeit assoziiert, was auf eine höhere Aufmerksamkeitsanforderung hindeutet.

## 4.1 Erster Teil: Schlucken und Okklusion

In Bezug auf die beteiligten Bereiche wurde ein gemeinsames Repräsentationsmuster für beide Aufgaben in den bilateralen primären und sekundären sensomotorischen Bereichen, den Kleinhirnhemisphären, dem Pallidum, dem Thalamus und der Insel gefunden. Die funktionelle Repräsentation im Gyrus praecentralis zeigte Maxima beim Schlucken die inferior-anterior zu den Aktivierungen der Okklusion lagen. Eine völlig neue Erkenntnis ist die Aktivierung im Mittelhirn und der rechten Pons, die für beide Aufgaben beobachtet wurde.

Hirnstammaktivierung für Schlucken wurde im sensorischen Kern des Nervus trigeminus und dem NTS gefunden. Basierend auf Experimenten mit Schafen wird eine Gruppe von Neuronen auf der Ebene des sensorischen Trigeminuskerns als sensorische Weiterleitungsneuronen klassifiziert. Diese geben sensorische Informationen von Mund-Rachen-Rezeptoren zu den höheren Nervenzentren weiter und sind nicht Teil des ZMG-Netzwerkes des Schluckens (39). Mit Hilfe von Mikroelektrodenableitungen bei Schafen, Ratten, Hunde, Katzen und Affen konnte man den NTS in der dorsalen Schluckgruppe als Teil der Schluckneuronen im Hirnstamm lokalisieren (38).

Das Hirnstamm-Schlucknetzwerk umfasst den NTS und den Nucleus ambiguus, mit der Formatio reticularis, die synaptisch mit den Schädelmotoneuronenpool bilateral verbunden sind. Unter normaler Funktion empfängt das Hirnstamm-Schlucknetzwerk Informationen von der Hirnrinde (21). Der NTS enthält wahrscheinlich die sensorischen Neuronen sowie die Muster-Erzeugungsschaltung der pharyngealen und öso-

phagealen Phasen des Schluckens (45). Vor kurzem wurde vorgeschlagen, dass Wasser eine unabhängige Geschmacksart ist. Somatosensorische Antworten auf Wasser durch wassergerichtete Neuronen innerhalb des NTS könnten Teil des neuronalen Netzwerkes sein, welches die Reflexe zur Nahrungsaufnahme produzieren, wie z.B. Schlucken (73).

Okklusale Hirnstammaktivitäten wurden lateral im Kerngebiet des Nervus trigeminus lokalisiert (61). Der okklusale ZMG besteht hauptsächlich aus Neuronen des Trigeminussystems (45), während der Schluck-ZMG die Motorkerne der Hirnnerven V, VII, und XII und den Nucleus ambiguus rekrutiert (16).

Einige neuere Studien haben gezeigt, dass Interneuronen, die in dorsalen oder ventralen Regionen des Schlucknetzwerks zu finden sind auch während unterschiedlicher motorischer Verhaltensweisen wie Schlucken, Atmung, Kauen und Stimmgebung feuern. Die gemeinsamen Motoneuronen könnten deshalb durch gemeinsame Pools von Interneuronen ausgelöst werden. Diese Ergebnisse zeigen, dass bei Säugetieren die Neuronen für Mustererzeugung zu unterschiedlichen ZMGs gehören (38).

Die Hirnstamm-Aktivierung für beide Aufgaben kommt wahrscheinlich durch die größere Feldstärke von 3 Tesla zustande. Dadurch wird das Signal-zu-Rausch und Kontrast-zu-Rausch Verhältnis erhöht, was zu einer insgesamt größeren Empfindlichkeit führt (43). Die kleinen Aktivierungsstellen im Hirnstamm könnten auch von höherer räumlicher Auflösung und geringerer räumlicher Glättung (2) profitiert haben.

Der Grad der Aktivierung zwischen Schlucken und Okklusion unterscheidet sich stark. Schlucken ist eine sehr aufwendige motorische Funktion, die eine Koordinierung von 25 Muskelpaaren im Mund, Rachen, Kehlkopf und der Speiseröhre benötigt (10; 16; 40; 59). Außerdem liefert der somatosensorische Reiz eine Rückkopplung für die richtige Kontrolle des Bolus. Die Gehirnaktivität beim Schlucken zeigte somit eine kumulative Aktivierung von verschiedenen sensorischen und motorischen biomechanischen Ereignissen.

Im Gegensatz dazu ist Okklusion die Bewegung des craniomandi-

bulären Gelenks, welches überwiegend mit vier Muskelpaaren durchgeführt wird. Es ist daher nicht verwunderlich, dass wir sowohl eine höhere BOLD-Antwort im Grosshirn und Kleinhirn sowie ein größeres Aktivierungsvolumen (9400 gegenüber 2119 Voxeln) für die Schluckaufgabe verglichen mit der Okklusionsaufgabe gefunden haben. Allerdings wurde ein Anstieg der Anstrengung mit Hilfe der EDA-Messungen nicht verifiziert. Stattdessen zeigten diese eine Habituation über die Zeit, was auf eine anfängliche Stress-Reaktion hindeutet, die mit der Zeit und dessen Gewöhnung abnimmt (91).

Aktivierte Areale, die bei beiden Aufgaben gefunden wurden, waren eventuell nicht Aufgaben-spezifisch. In einer „Go, No-Go“ Studie während einer freiwilligen Schluckaufgabe (82) wurde die zinguläre Cortex-Aktivierung der Verarbeitung vom experimentellen Kontext einschließlich der Cues zugeschrieben. In diesem Experiment könnte der Farbwechsel für beide Aufgaben und die Wasserverabreichung beim Schlucken als ein Cue bezeichnet werden.

Außerdem, könnte die Aktivierung der rechten Insel bei der Koordination der Aufgabendurchführung helfen (18). Der Intensitätsunterschied im Aktivierungsmuster ( $t = 14.26$  bei Okklusion und  $t = 10.25$  beim Schlucken,  $p < 0.05$  FWE-korrigiert) könnte mit der erhöhten Aufmerksamkeit bei der Durchführung von genau drei Okklusionsbewegungen pro visuellem Trigger verbunden sein.

Experimente mit intrakortikaler Mikrostimulation des perizentralen/perisylvischen Cortex haben bei wachen Affen Schluckbewegungen zusammen mit rhythmischen Kieferbewegungen hervorgerufen (34; 53; 88). Die Autoren schlagen daher vor, dass bestimmte kortikale Areale Schluck- und Kieferbewegungen integrieren. Ein weiterer erwähnenswerter Punkt ist, dass Okklusion den Schluckakt begleitet (64). Wenn sich beispielsweise der Kiefer nach rechts bewegt, so folgt ihm die Zunge, was bedeutet, dass sie sich in der Bewegung gegenseitig beeinflussen. Diese gleichzeitige und kongruente Bewegung der Zunge und des Kiefers beim Kauen wurde von Wild (86) als linguomandibuläre Homotropie beschrieben.

Insgesamt deuten die erhobenen Daten darauf hin, dass die zerebrale Repräsentation von Okklusion und Schlucken sich räumlich stark überlappen. Jedoch unterscheiden sie sich überwiegend in der Anzahl der beteiligten neuronalen Ressourcen.

## 4.2 Zweiter Teil: Zeitliche Analyse und Konnektivität

Unter Verwendung des allgemeinen linearen Modells wurden statistische  $t$ -Karten für sechs Zeitpunkte für den gesamten Schluckakt einschließlich der oralen und pharyngealen Phase aufgestellt. Die Ergebnisse zeigten eine Zunahme der Aktivierung über die Zeit angefangen mit dem PMC und der SMA, gefolgt von M1S1, Insula und Kleinhirn. Aktivierungen im PMC und der SMA traten kurz vor der Bewegungsausführung auf und waren die ersten Areale, die beim Schlucken aktivierten. Subkortikale Aktivierung im Thalamus könnte auf die somatonsensorische Rückkopplung des Wasserdrucks zurückgeführt werden, welcher die Zunge stimuliert bevor der Schluckakt ausgelöst ist.

Die tatsächliche Ausführung der Bewegung und der damit einhergehenden somatosensorischen Verarbeitung beim Schlucken wurde in der Aktivierung von M1S1, Insula und des Kleinhirns ausgedrückt. Zunge und Lippen führen die koordinierte Bewegung durch und werden dabei durch die sensorische Rückkopplung unterstützt, um das Wasser in Richtung des (Mund-)Rachenraums zu drücken. Die Aktivierung der Pons könnte ein Hinweis auf die pharyngeale Phase des Schluckens sein, in dem das Wasser in den Rachen gelangt, um in die Speiseröhre weitergeführt zu werden. Diese Aktivierung entspricht derjenigen aus dem ersten Teil dieser Arbeit, in welcher der sensorische Kern des Nervus trigeminus und des Nucleus des Tractus solitarii beim Schlucken aktiviert wurden.

Die Varianzanalyse mit Messwiederholungen zeigte eine Lateralisierung in der Zeit in M1S1, welche langsam von der linken zur rechten Hemisphäre (Anfang: Zeitpunkt 1, Ende: Zeitpunkt 6) überging.

Frühere Phasen, einschließlich der Vorbereitungsphase, waren nach links lateralisiert, spätere Phasen waren nach rechts lateralisiert. Unsere Ergebnisse stehen daher im Einklang mit den Erkenntnissen der Magnetoenzephalographie (MEG)-Studie von Teismann et al. (78), bei der für die ersten 600 ms eine linkshemisphärische Aktivierung stattfand, gefolgt von einer bi-hemisphärischen Aktivierung in den nächsten 200 ms und welche mit einer rechtshemisphärischen Aktivierung während der letzten 200 ms endete.

Die Insel zeigte eine signifikante Lateralisierung nur im 3. Zeitfenster. Dies könnte mit einem frühen Anstieg und fruhem Abklingen zusammenhängen, da wir in der Interaktion *Region* × *Zeit* nur eine vergleichsweise geringe Aktivierung feststellen konnten. Die SMA-Aktivierung begann früher und endete früher entsprechend seiner Funktionen zur Vorbereitung des Schluckvorgangs. Dies erklärt aber nicht, warum die PMC-Aktivierung der M1S1-Aktivierung folgt, mit einem relevanten Anstieg an früheren Zeitpunkten (Zeitfenster 1-3), einem Plateau (Zeitfenster 3-4) und einer signifikanten Abnahme in den letzten beiden Zeitfenstern. Die M1S1-Aktivierung ist ein Spiegelbild der sensorisch-motorischen Interaktion beim Schlucken. Die sensorischen Aspekte der Wassereinspritzung zusammen mit dem Schluckvorgang führen zu einer starken Aktivierung dieser Bereiche über die Zeit.

Die Ergebnisse der DCM-Analyse zeigten, dass das Modell (c) aus Abb. 2.3 das wahrscheinlichste ist. Hier agiert der Input auf der SMA und dem M1S1. Beide sind bidirektional verbunden, während M1S1 zur Insel durch eine gerichtete Verbindung kommuniziert. Das SMA empfängt wahrscheinlich den Input durch den visuellen Cortex. Aufgrund der Notwendigkeit einer hohen zeitlichen Auflösung wurde die Anzahl der Schichten reduziert, wodurch der visuelle Cortex nicht aufgenommen werden konnte. Insofern konnte ein Modell welches diesen kortikalen Bereich einbezieht nicht getestet werden. Der Input zum M1S1 hängt mit dem somatosensorischen Reiz des eingespritzten Wassers zusammen. Die Annahme, dass sowohl der visuelle als auch der somatosensorische Reiz eine Rolle spielen, wird durch die beidseitige Verbin-

dung zwischen SMA und M1S1 widergespiegelt. Der somatosensorische Cortex gibt die Information der Wassereinspritzung an die SMA weiter, um die Bewegung vorzubereiten. Kurz bevor dies geschieht, wird die Versuchsperson durch das Lichtsignal darauf aufmerksam gemacht, dass das Wasser bald in die Mundhöhle eintrifft. Die Integration dieser beiden Signale führt dann zum Schluckvorgang, der vom M1 durchgeführt wird.

### **4.3 Dritter Teil: Veränderung der kortikalen Schluckrepräsentation im Alter**

Um potentielle Unterschiede in der Gehirnaktivität beim Schlucken zwischen jungen und alten Probanden zu untersuchen, wurden zwei unterschiedliche statistische Verfahren angewendet. Zusätzlich wurde die Durchführung der Aufgabe und EDA gemessen. Der klassisch-frequentistische Ansatz zeigte keinen Unterschied in der Gehirnaktivität beim Schlucken zwischen den Gruppen. Die Bayes-Statistik war sensitiver und identifizierte eine bilaterale Aktivierung in Fp1 als Teil von BA 10 beim Kontrast alt > jung. Die Gruppe junger Probanden zeigte keine Assoziation zwischen BOLD-Antwort und EDA oder BOLD-Antwort und Schluckzeit. Bei den alten Gesunden war die Schluckzeit verlängert, jedoch wies diese keine Assoziation mit der BOLD-Antwort auf. Dieses Ergebnis deutet darauf hin, dass obwohl sich die Ausführung der Aufgabe zeitlich verlängert, die kortikale Repräsentation konstant bleibt. Die Erregung während der Aufgabe schien ein relevanter Faktor bei der Rekrutierung von kortikalen Arealen zu sein, die sowohl mit Planung und Integration von somatosensorischen Aufgaben wie auch mit emotionaler Verarbeitung bei manchen Senioren assoziiert war.

Die Aktivierung bei Jungen und Alten entsprechen denen aus vorherigen Studien die sich mit funktioneller Bildgebung des Schluckaktes befassen (21; 31; 35; 47; 50; 52; 57; 62; 79). Zusätzlich haben wir Aktivierungen in der Pons beobachten können, welche den Gebieten des Nervus trigeminus und NTS entsprechen könnten. Diese Befunde wurden auch

im ersten Teil dieser Arbeit beschrieben.

Die alten Probanden zeigten eine verlängerte Schluckzeit. Eine verzögerte pharyngeale Aktivität in älteren Probanden wurde in früheren Studien beschrieben(11; 72; 83) und wurde mit altersbedingter Abnahme der Muskelfasern assoziiert (7). Gleichzeitig beeinflusst die verzögerte pharyngeale Phase die Repräsentation des Schluckens auf der kortikalen Ebene nicht. Es gab keinen Unterschied im Schlucknetzwerk zwischen der alten und jungen Gruppe, was dem Ergebnis von Malandraki und Kollegen (48) entspricht. Dieses Ergebnis bestätigte sich auch mit einem unkorrigierten, liberalerem Ansatz.

Allerdings war die Bayes-Statistik sensitiver. Wir fanden kortikale Aktivierung im BA 10, insbesondere in Fp1, im Vergleich alt gegen jung. Der Anstieg in kortikaler Aktivität scheint bei den alten Probanden aufgabenunabhängig zu sein (32; 37; 55; 71; 84). Als Teil des präfrontalen Cortex ist BA10 mit Aufmerksamkeit und Arbeitsgedächtnisabfragen verbunden (28). Fp1 könnte eine wichtige Basis für organisiertes Verhalten, Handlungsplanung und das Leiten mehrerer Ziele basierend auf episodischem und Kurzzeitgedächtnis bilden (5). Ältere Probanden benötigen demnach mehr Aufmerksamkeit bei der Schluckaufgabe, was auch für andere motorischen Aufgaben gezeigt wurde (32; 37).

Die EDA-Werte waren in dieser Studie bei den alten Probanden erhöht. Dies könnte ein Hinweis auf eine gesteigerte Erregung sein und möglicherweise eine höhere Aufmerksamkeit während des Schluckens darstellen. Eine lineare Assoziation zwischen der Intensität von negativen emotionalen Stimuli und EDA wurde unlängst nachgewiesen (27). In unserer Studie könnte eine höhere EDA mit mehr negativen emotionalen Erfahrungen während des Schluckvorgangs zusammen hängen. Manche Senioren haben tatsächlich in diesem Experiment Äußerungen über die Angst vor dem Verschlucken im Liegen gemacht, die jungen Probanden hingegen nicht. Es ist verständlich, dass manche ältere Versuchspersonen sich unwohl fühlten in einer liegenden Position zu schlucken, wenn man bedenkt, dass laryngeale Penetration beim Schlucken öfter bei alten Gesunden als bei jungen Gesunden stattfindet (8). Wenn man die Unter-

schiede in den Schluckzeiten, motorischer Planung und Aufmerksamkeit wie oben besprochen interpretiert, darf man einer längeren Schluckzeit und höheren Aktivität in der motorischen Planung nicht zu viel Wichtigkeit schenken. Angstgefühle und höhere Aufgabenanforderungen könnten die primären Ursachen der Gruppendifferenz darstellen.

Die EDA-Werte bei den alten Versuchspersonen waren zwar höher, ergaben aber keine signifikante Assoziation mit dem Alter. Allerdings war die kortikale Aktivität beim Schlucken innerhalb der Senioren-Versuchsgruppe positiv mit der EDA assoziiert, was zu einer individuellen aber nicht einer altersbedingten Interpretation der kortikalen Überaktivierung führt. Zum einen könnte die Assoziation der prämotorischen und somatosensorischen Areale mit einer höheren EDA eine zusätzliche Verstärkung der kortikalen Areale die für Planung, Vorbereitung und Ausführung der komplexen Schluckbewegung darstellen (33; 69). Beispielsweise beschreiben andere Studien einen erhöhten BOLD-Effekt in motorischen Arealen mit einer herausfordernden Aufgabe (60; 85). Zum anderen könnte sich die zusätzliche Aktivierung in der Pons, Insel, ACC, MCC und Hippocampus auch auf eine höhere Erregung und höhere Aufmerksamkeit beziehen. Dies hängt wahrscheinlich mit einer gefühl anstrengenderen Aufgabe und emotionalen Verarbeitung zusammen, verglichen mit anderen Senioren ohne erhöhte EDA-Werte. Eine Aktivierung im Pons wurde zudem als wichtig für die Erzeugung des EDA-Stimulus beschrieben (69). In der vorliegenden Studie wurde die Aktivierung in der Pons dem aufsteigendem retikulärem Aktivierungssystem zugeordnet, welches wichtig für die generelle Erregbarkeit ist (17). Auch der ACC wurde als ein integratives Areal für kognitive Prozesse und autonome Erregbarkeit beschrieben, angezeigt durch eine höhere EDA, was mit einer kognitiven Leistung in Aufmerksamkeitsaufgaben assoziiert ist (13; 67). Die Aktivierung der Insel zusammen mit dem dorsalen ACC wurde als charakteristisch für viszerale Erregung dargestellt, kombiniert mit Aufmerksamkeit, Wahrnehmung und Erkenntnis von Emotionen (12; 13) wie z.B. Angst (65). Unter Berücksichtigung all dieser Befunde, d.h. der Rekrutierung von ACC, MCC, Insel und Hippocampus,

könnte man implizieren, dass die alten Versuchspersonen mit höheren EDA-Werten mehr erregte Aufmerksamkeit mit einer emotionalen Bewertung der Aufgabe aufweisen, weil sie es als fordernder und schwerer empfanden die Aufgabe auszuüben, zu integrieren und zu koordinieren.

## 4.4 Einschränkungen

### Erster Teil: Schlucken und Okklusion

Bei Experimenten, in denen Bewegung des Kopfes möglich ist, vor allem wenn diese mit der Aufgabe synchronisiert sind, können falsch-positive Effekte nicht ausgeschlossen werden. Auch wenn diese Bewegungen außerhalb des Bildfeldes sind, kann es zu einer Signalintensität von der gleichen oder sogar erhöhten Größenordnung des BOLD-Signals im nahegelegenen Gewebe kommen (89). Um bewegungskorrelierte Aktivität zu reduzieren, wurden die Bewegungsparameter als Regressoren im statistischen Modell einbezogen. Tatsächlich sind ereigniskorrelierte Versuche wie der hier beschriebene, weniger von Bewegungsartefakten beeinflusst (74) und weil die Aufgabe kurz ist, kann die Bewegung von der BOLD-Antwort getrennt werden (4).

Hirnstammnervenzellen, insbesondere im Nucleus ambiguus sind so organisiert, dass sie nacheinander feuern, um somit eine sequentielle Anregung der Speiseröhrenmuskulatur, die zur Peristaltik führt, zu erzeugen (81). Solche Bewegungen haben eine Laufzeit von 10 oder mehr Sekunden (29). Diese lang anhaltende Erregung könnte eine Reihe von BOLD-Reaktionen induzieren, die sich mit denen vom vorherigen Schluckakt überlappen könnten. Allerdings zeigte eine Analyse in der Zeit mittels der hämodynamischen Antwortfunktion, wie in SPM8 modelliert, eine Hirnstammaktivierung nur bei der eigentlichen Aufgabe und nicht dazwischen. Diese zeitlich begrenzte BOLD-Antwort könnte mit der Tatsache zusammenhängen, dass ein überdimensionalisierte Transport an sauerstoffreichem Blut (9) alle Zellen mit genug Sauerstoff beliefert, um die Peristaltik auszuführen.

## Zweiter Teil: Zeitliche Analyse und Konnektivität

Für die GLM Analyse wurden keine signifikanten Ergebnisse während der oralen und pharyngealen Zeitpunkte gefunden. Eine erfahrene Schlucktherapeutin hat jedoch mit der Hilfe der kinematographischen Bilder die Zeitpunkte der beiden Phasen für jede Versuchsperson differenziert. Die temporalen Zeitpunkte der kinematographischen und funktionellen Daten wurden mittels des pneumatischen Kissens zugeordnet, das die Kehlkopfbewegung aufnimmt. Die Ergebnisse zeigten keine überschwelligen Voxel für beide Phasen. Allerdings gab es ein klares Indiz für eine fortlaufende Progression beim Schlucken, welche diese zwei Phasen beinhaltet, wenn man die Aktivierung über die Zeit beobachtet. Durchschnittszeiten von der kinematographischen Sequenz wurden für die funktionelle Berechnung benutzt und es gibt keine Garantie, dass die Versuchspersonen während der funktionellen Messung ähnlich geschluckt haben. Die Filmsequenz hatte eine zeitliche Auflösung von 305 ms (ca. 3,3 Bilder pro Sekunde), die vergleichbar ist mit der gepulsten Videofluoroskopie die in der Niedrigdosisdiagnostik (3,75 Bilder pro Sekunde) benutzt wird (76). Andererseits könnte das modellierte BOLD-Signal nicht gut genug zwischen der Aktivierung zum Zeitpunkt Null (Lichtwechsel, Zeit der Wasserverabreichung) und der berechneten oralen Phase des Schluckens differenziert haben. Aufgrund der Natur der BOLD-Antwort und wie diese in SPM modelliert ist, stellt die Zeitinformation, die durch die GLM Analyse extrahiert wird, einen begrenzten Einblick dar und kann verwirrend sein. Die Aktivierung beginnt bei  $-4,5$  s bevor der Farbwechsel stattfindet, und somit vor Wassereinspritzung, was kein getreues Spiegelbild der tatsächlichen Ereignisse ist. Statt dessen ist es ein Ergebnis des HRF Modells und dessen Anpassung an das BOLD Signal. Der nützliche Informationsinhalt ist hier nicht die absolute Zeiteinteilung sondern die relative Entwicklung der sequentiellen kortikalen und subkortikalen Aktivierung bezogen auf die Aufgabe.

Um den visuellen vom sensorischen Input tatsächlich zu differenzieren, sollte der visuelle Cortex auch in die Messung und in die DCM Ana-

lyse einbezogen werden. Eine hohe zeitliche Auflösung auf Kosten der räumlichen Abdeckung war jedoch eine Priorität in diesem Experiment. Bei höheren Feldstärken und schnelleren Sequenzen kann auch die räumliche Abdeckung in Zukunft möglich sein. Zusätzlich wurden der PMC, die Basalganglien, das Kleinhirn und die Pons ausgelassen, um die Komplexität der Modelle zu reduzieren. Der Hauptfokus der Studie war die sequentielle Aktivierung beim Schlucken über die Zeit. DCM ist ein Mittel um herauszufinden, an welcher Stelle der Input im Modell eintrifft und wie die Richtungsabhängigkeit der Verbindungen zwischen den Regionen zusammen hängt. Diese Ergebnisse helfen bei der Interpretation der GLM Analyse. Allerdings könnten komplexere Modelle, die über drei Regionen hinausgehen, in einer DCM-spezifischen Analyse von Schlucken in Zukunft hilfreich sein.

### **Dritter Teil: Veränderung der kortikalen Schluckrepräsentation im Alter**

Die alten Versuchspersonen die bei dieser Studie mitgemacht haben, zeigten eine hohe soziale und sportliche Aktivität. Es könnte sein, dass diese Studie deswegen einen sogenannten healthy-bias-Effekt aufweist. In zukünftigen Studien ist es ratsam den Status der körperlichen Aktivitäten für jede Versuchsperson einzubeziehen, um die Ergebnisse besser interpretieren zu können. Zudem kann es sein, dass die Durchführung der Aufgabe bei diesen Versuchspersonen besser ist als für Personen, die wegen anderer Krankheiten oder Behinderungen nicht in der Studie eingeschlossen wurden. Eine heterogener Auswahl der Versuchspersonen sollte für eine zukünftige Studie getroffen werden. Wie schon oben beschrieben äußerten sich manche ältere Versuchspersonen über Nervosität oder Anstrengung bei der Aufgabendurchführung. Ein objektiver Fragebogen oder visuelle Analogskalen über die empfundene Aufmerksamkeitsleistung und Emotion neben der EDA-Messung sollte einbezogen werden, um besser die neuronale Repräsentation der Erregbarkeit hervorzuheben und die emotionale Empfindung beim Schlucken im Alter

zu differenzieren.

## *Schlussfolgerungen*

Ziel der vorliegenden Untersuchung war es, die neuronale Aktivität beim Schlucken mittels fMRT zu untersuchen. Die erste Fragestellung befasste sich mit dem Unterschied der corticalen und subcorticalen Repräsentation von Schlucken und Okklusion mit dem Fokus auf automatisierte Prozesse im Hirnstamm. Ferner wurde die zeitliche Abfolge und die effektive Konnektivität beim Schlucken erarbeitet. Im Anschluss befasst sich diese Studie mit der Veränderung der neuronalen Schluckrepräsentation im Alter.

Zerebrale Repräsentationsareale zwischen Schlucken und Okklusion zeigten eine erhebliche Überschneidung, allerdings war das Niveau der Aktivierung zwischen den Bedingungen wesentlich unterschiedlich. Dieses Ergebnis gibt den Anlass zur Annahme, dass sich die zerebrale Darstellung beider Aspekte der Nahrungsaufnahme qualitativ weit überlappen, sich jedoch unterscheiden in Bezug auf die Anzahl der neuronalen Ressourcen die dabei involviert sind. Allerdings ist diese Erhöhung nicht mit der peripher-physiologisch-gemessenen Anstrengung (Hautleitfähigkeit) assoziiert. Hirnstammaktivität beim Menschen mittels fMRT für Schlucken und Okklusion unterstützen vorherige Tierstudien und bieten einen neuen Einblick in die subkortikale Verarbeitung dieser Aufgaben. Hier wurde beim Schlucken der sensorische Kern des Nervus trigeminus zusammen mit dem Nucleus Tractus solitarii aktiviert, während Okklusion den Nervus trigeminus aktivierte.

Im zweiten Teil zeigen die Ergebnisse des allgemeinen Linearmodell eine fortlaufende Aktivierung beim Schlucken von 2 ml Wasser angefangen beim PMC und SMA, gefolgt von M1S1, Insel und Kleinhirn,

und abschließend der Hirnstammaktivierung. Dieser Verlauf spiegelt die Vorbereitungs- und Durchführungsphasen des Schluckaktes wider, inklusive der unfreiwilligen pharyngealen Phase. Die Varianzanalyse mit Messwiederholungen ergab eine signifikante Aktivierung über die Zeit in M1S1, angefangen in der linken Gehirnhälfte mit Übergang zur rechten. Im DCM Modellvergleich hatte die größte Wahrscheinlichkeit ein Modell bestehend aus SMA, M1S1 und Insel mit zwei unterschiedlichen Inputs: zur SMA und zum M1S1. Zwischen SMA und M1S1 lag eine bidirektionale Verbindung, während M1S1 mit einer einfachen Verbindung zur Insel verknüpft war.

Der dritte Teil befasste sich mit der Änderung im Alter der kortikalen Aktivität beim Schlucken. Die Ergebnisse zeigen eine verlängerte Schluckzeit und eine signifikant höhere Hautleitfähigkeit in alten Gesunden verglichen mit jungen Gesunden. Der Bayessche Ansatz brachte eine höhere Aktivierung im bilateralen Frontalpol 1 im BA10 in der älteren Gruppe hervor. Dies kann als eine erhöhte aufgabenspezifische Aufmerksamkeit interpretiert werden. Zudem zeigt es die Validität der Bayes-Statistik verglichen mit der klassisch-frequentistischen Inferenz. Senioren mit erhöhten Hautleitfähigkeitswerten zeigten cortikale und sub-cortikale Aktivität in Bereichen, die mit sensomotorischer Leistung, Erregung und Emotion assoziiert waren. Senioren die eine höhere Erregung beim Schluckakt zeigten, brauchten mehr Aufmerksamkeit für die Durchführung der Aufgabe, waren emotional involvierter im Schluckprozess und zeigten deswegen eine höhere neuronale Aktivität in den beschriebenen Arealen.

Es bleiben noch viele Fragen offen bezüglich der gesunden Schluckrepräsentation, sowohl räumlich wie auch zeitlich. Der nächste sinnvolle Schritt ist jedoch die Untersuchung der neuronalen Vernetzung des Schlucksystems nach restituiertem neurogener Dysphagie. Dieses Krankheitsbild bedeutet nicht nur ein Verlust an Lebensqualität, sondern in den schwierigen (und recht häufigen) Fällen auch den Tod. So kann man, z.B. folgende Fragen stellen und versuchen zu beantworten. Gibt es ein spezifisches Muster der Neuanordnung des Schlucknetzwerkes? Was ist der

Unterschied in der Restitution von einer sub-corticalen verglichen mit einer corticalen Schädigung? Wo genau liegt die Läsion und warum verursacht sie eine Schluckstörung?

# **Appendices**

## APPENDIX A

### *Tabellen*

Tabelle A.1: SPM Koordinaten (MNI, x,y,z), t-Werte und Anzahl der aktivierten Voxel pro Region (k) für Schlucken, Okklusion und Schlucken – Okklusion, FWE-korrigiert,  $p < 0.05$ . L: links, R: rechts. BA: Brodmann Area; ant: anterior; post: posterior; MI: primärer motor Kortex; S1: primärer somatosensorischer Kortex; S2: sekundär-somatosensorischer Kortex; PMC: prämotorischer Kortex; SMA: supplementär-motorisches Areal, MGC: medialer Gyrus cinguli; CerHem: cerebelläre Hemisphere Larsell IV–VII; T: t-Wert; x,y,z: Koordinaten, k: Anzahl aktivierter Voxel.

makroanatomische Lage	Schlucken						Okklusion						Schlucken – Okklusion						
	k	T	x	y	z	k	T	x	y	z	k	T	x	y	z	k	T	x	y
L M1 (BA 4)	161	14.12	-52	-8	30	34	6.07	-54	-8	74	145	10.29	-50	-6	30				
R M1 (BA 4)	141	16.87	56	-6	32	95	7.03	58	-8	36	125	10.27	46	-8	38				
L S1 (BA 1,2,3)	523	15.55	-52	-8	26	91	9.03	-58	-16	42	238	11.67	-52	-6	24				
R S1	506	19.02	58	-6	30	123	8.15	54	-14	28	309	10.42	54	-10	30				
L S2	2219	15.14	-66	-16	14	367	9.53	-50	6	10	302	11.51	-52	-8	22				
R S2	1574	12.12	56	-6	24	340	10.10	58	-20	24	262	10.12	54	-12	26				
L PMC (BA 6 lateral)	108	14.18	-60	2	20	79	11.13	-58	6	28	19	8.57	-56	0	22				
R PMC	227	17.97	58	-4	30	2	7.17	60	-6	34	74	9.21	54	0	36				
SMA ant (BA 6 medial)	52	9.78	0	0	52	-	-	-	-	-	-	-	22	8.26	0	2	66		
SMA post	77	10.20	2	-4	68	-	-	-	-	-	-	8	7.76	0	0	66			
L Pars opercularis (BA 44)	221	13.32	-60	4	18	273	12.33	-58	6	22	316	9.19	-42	16	30				
R Pars opercularis	219	10.46	60	12	2	2	10.57	54	12	-2	80	8.21	56	10	32				
MCC	186	9.66	10	16	36	222	8.49	4	16	30	40	8.90	-14	16	42				
L Insula(BA 15)	422	11.56	-48	2	4	273	11.08	-38	8	10	1	7.36	-32	-24	18				
R Insula	437	10.25	42	0	2	435	14.26	40	6	2	29	8.53	34	-14	10				
L Thalamus	259	9.25	-4	-10	10	-	-	-	-	-	2	8.40	-24	-32	8				
R Thalamus	376	8.91	6	-20	8	5	7.68	4	-20	8	157	9.51	8	-22	14				
L CerHem	539	9.85	-8	-60	-10	3	7.24	-42	-56	-26	335	14.87	-18	-52	-18				
R CerHem	459	11.30	6	-52	-10	-	-	-	-	-	132	9.32	20	-56	-16				
Cerebellar vermis	182	10.39	-6	-60	-10	-	-	-	-	-	-	-	-	-	-				
L Pallidum	90	8.65	-24	-10	-2	2	7.42	-18	-2	-6	24	8.64	-18	-4	-4				
R Pallidum	36	8.21	22	-2	-6	3	7.22	20	-4	-6	-	-	-	-	-				
L Pons	220	11.83	-10	-30	-34	-	-	-	-	-	2	8.39	-18	-34	-30				
R Pons	208	10.80	8	-26	-34	4	9.05	16	-26	-34	6	7.78	2	-24	-24				
Midbrain	398	12.31	6	-28	-8	1	6.93	2	-14	-18	5	8.23	4	-24	-22				

Tabelle 2: 2. Koordinaten der Aktivierungsspitzen in der GLM Analyse für alle sechs Zeitfenster SPM-Koordinaten (Montreal Neurological Institute, x, y und z Werte) der Aktivierungsspitzen für sechs unterschiedliche HRFs die der GLM Analyse benutzt wurden. Alle Werte sind FWE-korrektiert mit  $p < 0.05$ . L: links, R: rechts, PMc: premotorischer Kortex, SMA: supplementär-motorisches Areal, M1: primär cerebellär, L: linkes Cerebellum, R: rechtes Cerebellum.

Tabelle A.3: Koordinaten der Aktivierungsmaxima bei alten Gesunden korreliert mit EDA. Oben sind SPM Koordinaten – klassische Inferenz (Montreal Neurological Institute,  $x, y, z$  [mm]),  $k$ : Anzahl der Voxel,  $T$ :  $t$ -Wert angegeben. Unten sind PPM Koordinaten – Bayes-Statistik mit  $P$ -Werten angegeben. L: links, R: rechts, SMA: supplementär-motorisches Areal, M1: primär motorisches Areal, S1: pri-märe somatosensorisches Areal, S2: sekundär somatosenso-risches Areal, ACC: anterior cingulärer Cortex, MCC: me-dial cingulärer Kortex.

SPM (frequentistische Inferenz)	$k$	$T$	$x$	$y$	$z$
L SMA (BA 6)	5	7.2	-42	-10	53
L Gyrus temporalis superior	7	6.94	-53	-5	-1
R Brocas analogon (BA45 pars triangularis)	10	7.34	45	16	27
PWK (Bayes-Statistik)	$k$	$P$	$x$	$y$	$z$
L M1 (BA 4)	228	13.94	-17	-28	63
		13.21	-26	-34	56
		13.05	-20	-24	57
	10	11.93	-35	-34	56
	9	10.87	-35	-25	53
R M1 (BA 4)	1	11.75	20	-27	69
	11	11.59	9	-36	56
	6	11.58	24	-24	53
	3	11.4	33	-33	57
	1	10.58	20	-25	56
	1	10.33	23	-33	62
	6	10.28	37	-15	51
	5	10.26	2	-30	62
L S1 (BA 1,2,3)	209	14.95	-26	-37	56
		14.42	-41	-37	54
	16	11.37	-33	-33	44
	5	10.31	-38	-25	53
R S1 (BA 1,2,3)	8	11.3	33	-33	59
	5	11.01	11	-37	56
	11	10.99	23	-33	60
L S2	8	12.81	-51	-4	0

Fortsetzung auf nächster Seite

PWK (Bayes-Statistik)	k	P	x	y	z
L+R SMA	23	15.25	18	-25	72
	56	14.84	-8	-18	72
		12.62	-11	-10	71
	25	14.22	-18	-9	63
	237	14.05	15	-12	71
		13.23	5	-10	69
		11.26	25	-13	68
	70	13.99	24	-22	56
	85	13.3	-20	-22	59
	6	12.97	-14	-27	62
	3	12.24	-21	-27	62
	11	12.02	-6	-25	56
	20	11.72	36	-12	50
	12	11.27	-6	-15	62
	4	10.43	31	-19	54
	1	9.51	-24	-24	51
L Broca pars opercularis (BA 44/45)	9	12.57	-48	9	23
	3	10.63	-47	23	11
ACC	4	11.35	11	36	17
MCC	7	11.4	9	-37	54
	4	10.4	8	8	41
L Hippocampus	121	14.27	-53	-3	-1
	48	11.97	-51	-19	5
	56	11.68	-53	0	-16
	10	11.02	-50	-25	9
	1	9.75	-24	-10	-27
	1	9.74	-62	3	-13
L Insula	2	10.81	-50	-3	0
Pons	8	10.21	9	-37	-40

# *Literaturverzeichnis*

*Anstelle eines Index wird jeder Eintrag durch eine in Klammern gesetzte Liste der Seiten angegeben.*

- [1] K Amunts, A Schleicher, and K Zilles. Cytoarchitecture of the cerebral cortex - more than localization. *NeuroImage*, 37:1061–5, 2007. [10]
- [2] Tonio Ball, Thomas P K Breckel, Isabella Mutschler, Ad Aertsen, Andreas Schulze-Bonhage, Jürgen Hennig, and Oliver Speck. Variability of fMRI-response patterns at different spatial observation scales. *Human brain mapping*, 1171(January 2011):1155–1171, March 2011. [29]
- [3] Mathias Benedek and Christian Kaernbach. A continuous measure of phasic electrodermal activity. *Journal of neuroscience methods*, 190(1):80–91, June 2010. [10]
- [4] R M Birn, P a Bandettini, R W Cox, and R Shaker. Event-related fMRI of tasks involving brief motion. *Human brain mapping*, 7(2):106–14, January 1999. [36]
- [5] S Bludau, S B Eickhoff, H Mohlberg, S Caspers, a R Laird, P T Fox, a Schleicher, K Zilles, and K Amunts. Cytoarchitecture, probability maps and functions of the human frontal pole. *NeuroImage*, 93 Pt 2:260–75, June 2014. [24, 34]
- [6] M Brett, W Penny, and S Kiebel. Parametric procedures. In Karl J Friston, John T Ashburner, S J Kiebel, Thomas E Nichols, and Will D Penny, editors, *Statistical Parametric Mapping*, chapter 17, pages 223–231. Academic Press, first edition, 2007. [9]
- [7] S V Brooks and J A Faulkner. Skeletal muscle weakness in old age: underlying mechanisms. *Med Sci Sports Exerc*, 26:432–439, 1994. [34]
- [8] Susan G Butler, Andrew Stuart, Xiaoyan Leng, Erika Wilhelm, Catherine Rees, Jeff Williamson, and Stephen B Kritchevsky. The relationship of aspiration status with tongue and handgrip strength in healthy older adults.

- The Journals of Gerontology Series A: Biological Sciences and Medical Sciences*, 66(4):452–8, 2011. [34]
- [9] RB Buxton. *Introduction to functional magnetic resonance imaging: principles and techniques*. Cambridge University Press, Cambridge, 2002. [8, 36]
- [10] C F Code, J R Brobeck, and W Heidel. *Handbook of physiology: Alimentary canal*. American Physiological Society, 1968. [29]
- [11] IJ Cook, M D Weltman, K Wallace, D W Shaw, E McKay, R C Smart, and S P Butler. Influence of aging on oral-pharyngeal bolus transit and clearance during swallowing: scintigraphic study. *The American journal of physiology*, 266:G972–G977, 1994. [3, 34]
- [12] A D Bud Craig. How do you feel–now? The anterior insula and human awareness. *Nature reviews Neuroscience*, 10:59–70, 2009. [35]
- [13] Hugo D. Critchley. Neural mechanisms of autonomic, affective, and cognitive integration. In *Journal of Comparative Neurology*, volume 493, pages 154–166, 2005. [35]
- [14] S K Daniels, K Brailey, D H Priestly, L R Herrington, L A Weisberg, and A L Foundas. Aspiration in patients with acute stroke. *Archives of physical medicine and rehabilitation*, 79:14–19, 1998. [2]
- [15] WJ Dodds. The physiology of swallowing. *Dysphagia*, 178:171–178, 1989. [2]
- [16] RW Doty and JF Bosma. An electromyographic analysis of reflex deglutition. *Journal of Neurophysiology*, 19(1):44–60, 1956. [3, 29]
- [17] Leon Dnil and ML Pascu. Contributions to the Understanding of the Neural Bases of the Consciousness. In Terry Lichtor, editor, *Contributions to the Understanding of the Neural Bases of the Consciousness, Clinical Management and Evolving Novel Therapeutic Strategies for Patients with Brain Tumors*. 2013. [35]
- [18] Mark a Eckert, Vinod Menon, Adam Walczak, Jayne Ahlstrom, Stewart Denslow, Amy Horwitz, and Judy R Dubno. At the heart of the ventral attention system: the right anterior insula. *Human brain mapping*, 30(8):2530–41, August 2009. [30]
- [19] S B Eickhoff, C Grefkes, G R Fink, and K Zilles. Functional lateralization of face, hand, and trunk representation in anatomically defined human somatosensory areas. *Cerebral cortex (New York, N.Y. : 1991)*, 18(12):2820–30, December 2008. [15]

- [20] Simon B Eickhoff, Klaas E Stephan, Hartmut Mohlberg, Christian Grefkes, Gereon R Fink, Katrin Amunts, and Karl Zilles. A new SPM toolbox for combining probabilistic cytoarchitectonic maps and functional imaging data. *NeuroImage*, 25(4):1325–35, May 2005. [10]
- [21] Cumhur Ertekin and Ibrahim Aydogdu. Neurophysiology of swallowing. *Clinical Neurophysiology*, 114(12):2226–2244, December 2003. [28, 33]
- [22] O Foerster. The motor cortex in man in the light of Hughlings Jackson's doctrines. *Brain*, 89, 1936. [2]
- [23] Karl J Friston, John T Ashburner, Sefan J Kiebel, Thomas E Nichols, and William D Penny, editors. *Statistical Parametric Mapping: The Analysis of Functional Brain Images*. Academic Press, London, first edit edition, 2007. [14]
- [24] K.J. Friston, L. Harrison, and W. Penny. Dynamic causal modelling. *NeuroImage*, 19(4):1273–1302, August 2003. [11]
- [25] K.J. Friston and W. Penny. Posterior probability maps and SPMs. *NeuroImage*, 19(3):1240–1249, July 2003. [13, 15]
- [26] KJ Friston and WD Penny. Chapter 47 - Classical and Bayesian inference. In Richard S.J. Frackowiak, Karl J. Friston, Christopher D. Frith, Raymond J. Dolan, Cathy J. Price, Semir Zeki, John T. Ashburner, and William D. Penny, editors, *Human brain function*, chapter 47, pages 911–968. Academic Press, Oxford, 2nd edition, 2003. [15]
- [27] P. Fusar-Poli, P. Landi, and C. O'Connor. Neurophysiological response to emotional faces with increasing intensity of fear: A skin conductance response study. *Journal of Clinical Neuroscience*, 16:981–982, 2009. [34]
- [28] Sam J Gilbert, Stephanie Spengler, Jon S Simons, J Douglas Steele, Stephen M Lawrie, Christopher D Frith, and Paul W Burgess. Functional specialization within rostral prefrontal cortex (area 10): a meta-analysis. *Journal of cognitive neuroscience*, 18:932–948, 2006. [34]
- [29] RK Goyal and BW Cobb. Motility of the pharynx, esophagus, and esophageal sphincters. In Leonard R. Johnson, editor, *Physiology of the gastrointestinal tract*, chapter 11, pages 359–391. Raven Press, New York, 1981. [36]
- [30] S Hamdy, Q Aziz, J C Rothwell, R Crone, D Hughes, R C Tallis, and D G Thompson. Explaining oropharyngeal dysphagia after unilateral hemispheric stroke. *Lancet*, 350(9079):686–92, September 1997. [2]

- [31] S Hamdy, J C Rothwell, D J Brooks, D Bailey, Q Aziz, and D G Thompson. Identification of the cerebral loci processing human swallowing with H<sub>2</sub>(15)O PET activation. *Journal of neurophysiology*, 81(4):1917–26, April 1999. [3, 12, 33]
- [32] Sofie Heuninckx, Nicole Wenderoth, Filiep Debaere, Ronald Peeters, and Stephan P Swinnen. Neural basis of aging: the penetration of cognition into action control. *The Journal of neuroscience : the official journal of the Society for Neuroscience*, 25:6787–6796, 2005. [34]
- [33] Fleur M Howells, Dan J Stein, and Vivienne a Russell. Perceived mental effort correlates with changes in tonic arousal during attentional tasks. *Behavioral and brain functions : BBF*, 6:39, January 2010. [35]
- [34] CS Huang, H Hiraba, GM Murray, and BJ Sessel. Topographical distribution and functional properties of cortically induced rhythmical jaw movements in the monkey (*Macaca fascicularis*). *Journal of Neurophysiology*, 6(3), 1989. [30]
- [35] Ianessa a Humbert, Michelle E Fitzgerald, Donald G McLaren, Sterling Johnson, Eva Porcaro, Kris Kosmatka, Jacqueline Hind, and Joanne Robbins. Neurophysiology of swallowing: effects of age and bolus type. *NeuroImage*, 44(3):982–91, February 2009. [2, 3, 6, 33]
- [36] Ianessa a Humbert and JoAnne Robbins. Normal swallowing and functional magnetic resonance imaging: a systematic review. *Dysphagia*, 22(3):266–75, July 2007. [2]
- [37] S Hutchinson. Age-Related Differences in Movement Representation. *NeuroImage*, 17(4):1720–1728, December 2002. [34]
- [38] André Jean. Brain stem control of swallowing: neuronal network and cellular mechanisms. *Physiological reviews*, 81(2):929–69, April 2001. [2, 28, 29]
- [39] André Jean, A Car, and C Roman. Comparison of activity in pontine versus medullary neurones during swallowing. *Experimental brain research. Experimentelle Hirnforschung. Expérimentation cérébrale*, 22(2):211–20, January 1975. [28]
- [40] Bronwyn Jones, editor. *Normal and abnormal swallowing: imaging in diagnosis and therapy*. Springer, Berlin, 1991. [29]
- [41] M Kern, R Birn, S Jaradeh, A Jesmanowicz, R Cox, J Hyde, and R Shaker. Swallow-related cerebral cortical activity maps are not specific to deglutition. *American journal of physiology. Gastrointestinal and liver physiology*, 280(4):G531–8, April 2001. [2]

- [42] Stephen B Klein and B Michael Thorne. *Biological psychology*. Macmillan, 2006. [3]
- [43] G Krüger, A Kastrup, and G H Glover. Neuroimaging at 1.5 T and 3.0 T: comparison of oxygenation-sensitive magnetic resonance imaging. *Magnetic resonance in medicine*, 45(4):595–604, April 2001. [29]
- [44] John Kruschke. *Doing Bayesian data analysis: a tutorial introduction with R*. Academic Press, Burlington, MA, USA, 1 edition, 2010. [14]
- [45] Ivan M Lang. Brain stem control of the phases of swallowing. *Dysphagia*, 24(3):333–48, September 2009. [29]
- [46] Martin Lotze, Christian Lucas, Martin Domin, and Bernd Kordass. The cerebral representation of temporomandibular joint occlusion and its alternation by occlusal splints. *Human brain mapping*, 33(12):2984–93, November 2011. [2]
- [47] Georgia A Malandraki, Sterling Johnson, and Joanne Robbins. Functional MRI of swallowing: from neurophysiology to neuroplasticity. *October*, 33 Suppl 1(October):S14–20, 2011. [33]
- [48] Georgia a Malandraki, Adrienne L Perlman, Dimitrios C Karampinos, and Bradley P Sutton. Reduced somatosensory activations in swallowing with age. *Human brain mapping*, 32(5):730–43, May 2011. [34]
- [49] Georgia a Malandraki, Bradley P Sutton, Adrienne L Perlman, Dimitrios C Karampinos, and Charles Conway. Neural activation of swallowing and swallowing-related tasks in healthy young adults: an attempt to separate the components of deglutition. *Human brain mapping*, 30(10):3209–26, October 2009. [2, 3, 12]
- [50] GeorgiaA. Malandraki, BradleyP. Sutton, AdrienneL. Perlman, and DimitriosC. Karampinos. Age-Related Differences in Laterality of Cortical Activations in Swallowing. *Dysphagia*, 25(3):238–249, 2010. [3, 33]
- [51] Joseph a. Maldjian, Paul J. Laurienti, Robert a. Kraft, and Jonathan H. Burdette. An automated method for neuroanatomic and cytoarchitectonic atlas-based interrogation of fMRI data sets. *NeuroImage*, 19(3):1233–1239, July 2003. [10]
- [52] Ruth Martin, Amy Barr, Bradley MacIntosh, Rebecca Smith, Todd Stevens, Donald Taves, Joseph Gati, Ravi Menon, and Vladimir Hachinski. Cerebral cortical processing of swallowing in older adults. *Experimental brain research. Experimentelle Hirnforschung. Expérimentation cérébrale*, 176(1):12–22, January 2007. [3, 33]

- [53] Ruth E. Martin, Pentti Kemppainen, Dongyuan Yao Yuji Masuda, Gregory M. Murray, and Barry J Sessle. Features of cortically evoked swallowing in the awake primate (*Macaca fascicularis*). *Journal of Neurophysiology*, 82(3):1529–1541, 1999. [30]
- [54] Ruth E Martin, Bradley J MacIntosh, Rebecca C Smith, Amy M Barr, Todd K Stevens, Joseph S Gati, and Ravi S Menon. Cerebral areas processing swallowing and tongue movement are overlapping but distinct: a functional magnetic resonance imaging study. *Journal of neurophysiology*, 92(4):2428–43, October 2004. [3]
- [55] V.S. Mattay, F. Fera, a. Tessitore, a.R. Hariri, S. Das, J.H. Callicott, and D.R. Weinberger. Neurophysiological correlates of age-related changes in human motor function. *Neurology*, 58(4):630–635, February 2002. [34]
- [56] Paul Glad Mihai, Mareile Otto, Thomas Platz, Simon B Eickhoff, and Martin Lotze. Sequential evolution of cortical activity and effective connectivity of swallowing using fMRI. *Human brain mapping*, 2014. [4]
- [57] Paul Glad Mihai, Oliver von Bohlen Und Halbach, and Martin Lotze. Differentiation of cerebral representation of occlusion and swallowing with fMRI. *American journal of physiology. Gastrointestinal and liver physiology*, 304(10):847–54, March 2013. [4, 33]
- [58] AJ Miller. Neurophysiological basis of swallowing. *Dysphagia*, 100:91–100, 1986. [2]
- [59] Arthur J Miller. The neurobiology of swallowing and dysphagia. *Developmental disabilities research reviews*, 14(2):77–86, January 2008. [29]
- [60] G Mochizuki, T Hoque, R Mraz, B J Macintosh, S J Graham, S E Black, W R Staines, and W E McIlroy. Challenging the brain: Exploring the link between effort and cortical activation. *Brain research*, 1301:9–19, December 2009. [35]
- [61] Philippe Morquette, Raphaël Lavoie, Mitch-David Fhima, Xavier Lamoureaux, Dorly Verdier, and Arlette Kolta. Generation of the masticatory central pattern and its modulation by sensory feedback. *Progress in neurobiology*, 96(3):340–55, March 2012. [2, 29]
- [62] K M Mosier, W C Liu, J a Maldjian, R Shah, and B Modi. Lateralization of cortical function in swallowing: a functional MR imaging study. *AJNR. American journal of neuroradiology*, 20(8):1520–6, September 1999. [33]
- [63] Kristine Mosier and Irina Bereznaya. Parallel cortical networks for voluntary control of swallowing in humans. *Experimental Brain Research*, 140(3):280–289, October 2001. [12]

- [64] JHN Pameijer, Irving Glickman, and FW Roeber. Intraoral occlusal telemetry. Part II. Registration of tooth contacts in chewing and swallowing. *The Journal of Prosthetic Dentistry*, 19(2):151–159, 1968. [3, 30]
- [65] MP Paulus and MB Stein. An insular view of anxiety. *Biological psychiatry*, 60:383–387, 2006. [35]
- [66] B Y Wilder Penfield. Somatic motor and sensory representation in the cerebral cortex of man as studied by electrical stimulation. *Brain*, 1937. [2]
- [67] K Luan Phan, Tor Wager, Stephan F Taylor, and Israel Liberzon. Functional neuroanatomy of emotion: a meta-analysis of emotion activation studies in PET and fMRI. *NeuroImage*, 16(2):331–48, June 2002. [35]
- [68] Mario Prosiegel. Neurologie von Schluckstörungen. In Mario Prosiegel, editor, *Praxisleitfaden Dysphagie*, pages 9–46. Verlag Hygieneplan, Bad Homburg, 2002. [1]
- [69] A Raine, G P Reynolds, and C Sheard. Neuroanatomical correlates of skin conductance orienting in normal humans: a magnetic resonance imaging study. *Psychophysiology*, 28:548–558, 1991. [35]
- [70] Axel Riecker, Regina Gastl, Peter Kühnlein, Jan Kassubek, and Mario Prosiegel. Dysphagia due to unilateral infarction in the vascular territory of the anterior insula. *Dysphagia*, 24(1):114–8, March 2009. [2]
- [71] Axel Riecker, Klaus Gröschel, Hermann Ackermann, Claudia Steinbrink, Otto Witte, and Andreas Kastrup. Functional significance of age-related differences in motor activation patterns. *NeuroImage*, 32(3):1345–54, September 2006. [34]
- [72] J Robbins, J W Hamilton, G L Lof, and G B Kempster. Oropharyngeal swallowing in normal adults of different ages. *Gastroenterology*, 103:823–829, 1992. [3, 34]
- [73] Andrew M Rosen, Andre T Roussin, and Patricia M Di Lorenzo. Water as an independent taste modality. *Frontiers in neuroscience*, 4(October):175, January 2010. [29]
- [74] David a Soltysik and James S Hyde. Strategies for block-design fMRI experiments during task-related motion of structures of the oral cavity. *NeuroImage*, 29(4):1260–71, March 2006. [36]
- [75] Klaas Enno Stephan, Will D Penny, Jean Daunizeau, Rosalyn J Moran, and Karl J Friston. Bayesian model selection for group studies. *NeuroImage*, 46(4):1004–17, July 2009. [13]

- [76] Dick Stueve. Management of pediatric radiation dose using Philips fluoroscopy systems DoseWise: perfect image, perfect sense. *Pediatric radiology*, 36 Suppl 2:216–20, September 2006. [37]
- [77] Mikio Suzuki, Yuko Asada, Jin Ito, Kouji Hayashi, Hiroshi Inoue, and Hiroya Kitano. Activation of cerebellum and basal ganglia on volitional swallowing detected by functional magnetic resonance imaging. *Dysphagia*, 18(2):71–7, January 2003. [3]
- [78] Inga K Teismann, Rainer Dziewas, Olaf Steinstraeter, and Christo Pantev. Time-dependent hemispheric shift of the cortical control of volitional swallowing. *Human brain mapping*, 30(1):92–100, January 2009. [3, 32]
- [79] Inga K Teismann, Olaf Steinstraeter, Wolfram Schwindt, E Bernd Ringelstein, Christo Pantev, and Rainer Dziewas. Age-related changes in cortical swallowing processing. *Neurobiology of aging*, 31(6):1044–50, June 2010. [3, 33]
- [80] Bertrand Thirion, Philippe Pinel, Sébastien Mériaux, Alexis Roche, Stanislas Dehaene, and Jean-Baptiste Poline. Analysis of a large fMRI cohort: Statistical and methodological issues for group analyses. *NeuroImage*, 35(1):105–20, March 2007. [4]
- [81] L Tieffenbach and C Roman. The role of extrinsic vagal innervation in the motility of the smooth-muscled portion of the esophagus: electromyographic study in the cat and the baboon. *J Physiol (Paris)*, 64(3):193–226, 1972. [36]
- [82] Jillian a Toogood, Amy M Barr, Todd K Stevens, Joseph S Gati, Ravi S Menon, and Ruth E Martin. Discrete functional contributions of cerebral cortical foci in voluntary swallowing: a functional magnetic resonance imaging (fMRI) "Go, No-Go" study. *Experimental brain research. Experimentelle Hirnforschung. Expérimentation cérébrale*, 161(1):81–90, February 2005. [2, 3, 30]
- [83] J F Tracy, J.A. Logemann, P J Kahrilas, P Jacob, M Kobara, and C Krugler. Preliminary observations on the effects of age on oropharyngeal deglutition. *Dysphagia*, 4:90–94, 1989. [34]
- [84] NS Ward and RSJ Frackowiak. Agerelated changes in the neural correlates of motor performance. *Brain*, 126(0 4):873–888, 2003. [34]
- [85] Bruce E. Wexler, Robert K. Fulbright, Cheryl M. Lacadie, Pawel Skudlarski, Max B. Kelz, R. Todd Constable, and John C. Gore. An fMRI study of the human cortical motor system response to increasing functional demands. *Magnetic Resonance Imaging*, 15:385–396, 1997. [35]

- [86] W. Wild. *Funktionelle prothetik*. B. Schwabe, Basel, Switzerland, 1950. [2, 30]
- [87] Anne-Sophie Windel, Paul Glad Mihai, and Martin Lotze. Functional representation of swallowing: Arousal but not age codes for an increase of representation in seniors. 2014. [4]
- [88] Dongyuan Yao, Kensuke Yamamura, Noriyuki Narita, Ruth E Martin, Gregory M Murray, and Barry J Sessle. Neuronal activity patterns in primate primary motor cortex related to trained or semiautomatic jaw and tongue movements. *Journal of neurophysiology*, 87(5):2531–41, May 2002. [2, 30]
- [89] F Z Yetkin, V M Haughton, R W Cox, J Hyde, R M Birn, E C Wong, and R Prost. Effect of motion outside the field of view on functional MR. *AJNR. American journal of neuroradiology*, 17(6):1005–9, 1996. [36]
- [90] Karl Zilles and Katrin Amunts. Centenary of Brodmann's map—conception and fate. *Nature reviews. Neuroscience*, 11:139–145, 2010. [10]
- [91] H J Zwaga. Psychophysiological reactions to mental tasks: effort or stress? *Ergonomics*, 16(1):61–7, January 1973. [30]

# *Danksagung*

Meinen besonderen Dank richte ich an Herrn Professor Martin Lotze, ohne dessen kompetente und durchgehende Unterstützung die Erstellung dieser Arbeit nicht möglich gewesen wäre. Seine Betreuungskunst und Hilfsbereitschaft waren insbesondere in schwierigen Phasen sehr ermutigend.

In diesem Zusammenhang danke ich ebenso Herrn Professor Norbert Hosten, der mir die Möglichkeit eröffnete, mich während meiner Promotion am Institut für Diagnostische Radiologie und Neuroradiologie intensiv mit vielfältigen wissenschaftlichen Fragestellungen auseinandersetzen zu können.

Herrn Professor Oliver von Bohlen und Halbach danke ich insbesondere für die Unterstützung im Bereich subkortikale Neuroanatomie.

Herrn Professor Simon Eickhoff gab mir viele wichtige Anregungen und sehr hilfreiche Hinweise bezüglich der effektiven Konnektivität.

Herrn Professor Thomas Platz und Frau Mareile Otto danke ich für Ihre Unterstützung bei der zeitlichen Analyse der fMRT Daten.

Frau Anne-Sophie Windel danke ich für die wunderbare und sehr erfolgreiche Zusammenarbeit bei der Untersuchung der Senioren.

Darüber hinaus danke ich allen Mitarbeitern der Arbeitsgruppe Funktionelle Bildgebung am Institut für Diagnostische Radiologie und Neuroradiologie der Universitätsmedizin Greifswald, die mich ausdauernd mit Ideen und Anregungen, fachlichen Hinweisen und Diskussionen bei dieser Arbeit unterstützt haben (Dr. Martin Domin, Dr. Jörg Pfannmöller, Marie Ladda, Dr. Nicola Neumann, Dr. Matthias Grothe, Dr. Julia Wendt [Institut für Psychologie]).

Mein Dank geht auch an die vielen mutigen Probanden, die es auf sich genommen haben, in der MRT-Röhre liegend Wasser zu schlucken. Ohne ihren unermüdlichen Einsatz, der die entscheidenden Daten für meine Forschung lieferte, wäre diese Arbeit nicht möglich gewesen.

Zu guter Letzt danke ich all denen von Herzen, die in meinem persönlichen Umfeld für mich da waren und mich ermutigt und bekräftigt haben, meine Forschung durchzuführen; ihr wisst wer ihr seid ☺.

## *Eidesstattliche Erklärung*

Hiermit erkläre ich, dass ich die vorliegende Dissertation selbstständig verfasst und keine anderen als die angegebenen Hilfsmittel benutzt habe.

Die Dissertation ist bisher keiner anderen Fakultät, keiner anderen wissenschaftlichen Einrichtung vorgelegt worden.

Ich erkläre, dass ich bisher kein Promotionsverfahren erfolglos beendet habe und dass eine Aberkennung eines bereits erworbenen Doktorgrades nicht vorliegt.

---

DATUM

---

UNTERSCHRIFT

## Differentiation of cerebral representation of occlusion and swallowing with fMRI

Paul G. Mihai,<sup>1</sup> Oliver von Bohlen und Halbach,<sup>2</sup> and Martin Lotze<sup>1</sup>

<sup>1</sup>Functional Imaging Unit, Department for Diagnostic Radiology and Neuroradiology and <sup>2</sup>Institute of Anatomy and Cell Biology, University of Greifswald, Germany

Submitted 27 November 2012; accepted in final form 11 March 2013

**Mihai PG, von Bohlen und Halbach O, Lotze M.** Differentiation of cerebral representation of occlusion and swallowing with fMRI. *Am J Physiol Gastrointest Liver Physiol* 304: G847–G854, 2013. First published March 14, 2013; doi:10.1152/ajpgi.00456.2012.—Early work on representational specificity and recent findings on temporomandibular joint (TMJ) movement representation raise doubts that a specific swallow representation does exist. Additionally, during cortical stimulation TMJ movements and swallowing show a high overlap of representational areas in the primary motor cortex. It has thus been hypothesized that they overall might share the same neural structures. To differentiate these two movements, we performed a functional MRI (fMRI) study that enabled a direct comparison of functional representation of both actions in the same subject group. Effort during these tasks was controlled by skin conductance response. When balancing effort, we found a comparable neural representation pattern for both tasks but increased resources necessary to perform swallowing in direct comparison between tasks. For the first time, with the usage of fMRI, we demonstrated a representation in the brainstem for swallowing and occlusion. Increased activation for swallowing was observed in bilateral sensorimotor cortex, bilateral premotor and supplementary motor cortex, motor cingulate, thalamus, cerebellar hemispheres, left pallidum, bilateral pons, and midbrain. Peaks of activation in primary motor cortex between both conditions were about 5 mm adjacent. Brainstem activation was found corresponding to the sensory nucleus of the trigeminal nerve, the solitary nucleus for swallowing, and the trigeminal nucleus for occlusion. Our data suggest that cerebral representation of occlusion and swallowing are spatially widely overlapping, differing predominantly with respect to the quantity of neural resources involved. Both brainstem and primary motor representation differ in location with respect to somatotopy and contribution of cranial nerve nuclei.

swallowing; temporomandibular joint movements; occlusion; brainstem; functional magnetic resonance imaging; skin conductance response

TEMPOROMANDIBULAR JOINT (TMJ) movements and swallowing are both complex motor behaviors that are part of movement patterns necessary for food intake. TMJ movements are characterized by occlusion of the jaw to form masticatory actions to break down food for easier swallowing. They are usually of interest for investigation of neurophysiological or pathological representation of the jaw, for instance, to define the cerebral representation pattern associated with dysgnathia (36). Rhythmic muscle activity leading to TMJ movements are determined by a neuronal network known as central pattern generators (CPG) located in the brainstem (44). The ensemble of neurons involved is located in the vicinity of the trigeminal system,

with the trigeminal nerve being the most important for TMJ movements together with its associated sensory, motor, and premotor nuclei (44).

When investigating occlusal movements in a blocked design, we found a representational map of primary and secondary motor areas, thalamus and cerebellar hemispheres, a frontoparietal network, bilateral insula, and cingulate cortex (37). Comparable to swallowing, a left hemispheric lateralization of bilateral occlusion of opercular areas to the dominant left hemisphere was reported (17, 37). Overall, representational sites described during occlusion seem to be widely congruent to those described during swallowing (30). Several decades ago, a “linguomandibular homotropy” was postulated, hypothesizing a functional overlap of swallowing and TMJ movements (61). Additionally, with respect to the primary motor cortex, direct cortical stimulation in man (16, 50) and animal (63) suggests an overlap of primary motor representational areas.

The functional representation of swallowing is widely investigated and clinically highly relevant (22). With respect to its cortical representation, the following representational sites have been described: bilateral inferior pre- and postcentral gyri (39, 59), bilateral anterior insula (25, 26, 51), anterior cingulate cortex (59), bilateral temporal pole, and the supplementary motor area (SMA) (23, 45). Opercular areas are lateralized to the left dominant hemisphere (40, 41). A time-shifted lateralization corresponding to the oral phase in the dominant hemisphere and the pharyngeal phase in the nondominant hemisphere is seen in an magnetoencephalography experiment (57). With respect to subcortical representational sites, the left cerebellum and dorsal brainstem have been reported, along with the basal ganglia (putamen and pallidum, Ref. 56) and the thalamus (39). Interestingly, the CPGs inferior to the fourth ventricle in the dorsal brainstem, which have been described to be crucially involved in reflective recruitment of swallowing in animal studies (10), were also observed to be activated during swallowing in a positron emission tomography study (23).

The common representational sights presented above led to the hypothesis that the activated regions of both tasks are overlapping. Furthermore, swallowing produces a greater cortical and subcortical activation compared with TMJ movements because the extent of movements involved in swallowing is more complex with respect to the interaction of muscles involved and movement patterns performed. The objective of our research was to qualitatively and quantitatively distinguish the cerebral activation of swallowing and occlusion using functional MRI (fMRI) with a special focus on automated processes in the brainstem.

Swallowing is composed of a coordinated sequence of motor activities with the help of sensory information to bring the

Address for reprint requests and other correspondence: M. Lotze, Functional Imaging Unit, Ctr. for Diagnostic Radiology and Neuroradiology, Univ. of Greifswald, Walther-Rathenau-Str. 46, D-17475 Greifswald, Germany (e-mail: martin.lotze@uni-greifswald.de).

bolus from the mouth to the esophagus. In contrast, occlusion consists of movement of the TMJ mainly involving four muscle pairs. The difference in complexity and coordination may lead to an increased effort during swallowing, especially in a supine position. Indeed, it has been described that the amplitude of skin conductance responses (SCR) is positively associated with effort (43). To control for possible differences in effort, we simultaneously measured SCR during fMRI scanning. We thus expect the SCR responses of swallowing in a supine position to be significantly higher than those during occlusion, in turn mirroring the blood oxygen level-dependent (BOLD) signal between conditions because swallowing is more exertive, requiring a more complex sensorimotor coordination.

#### MATERIALS AND METHODS

All procedures were approved by the Ethics Committee of the University of Greifswald (registration number BB 101/08).

**Subjects.** Twenty-one neurologically healthy volunteers [average age:  $24.8 \pm 3.2$  yr (means  $\pm$  SD); range: 20–33 yr, 16 female] participated in the study in return for monetary compensation. Informed, written consent was obtained before each study. All subjects reported no history of sensorimotor, swallowing, or crano-mandibular pain conditions.

**Tasks.** Two functional, event-related imaging runs (duration 4 min, 20 s) were recorded during a single experimental session together with a structural T1-weighted high-resolution whole head data set. Subjects were instructed immediately before each task.

For the swallowing task, every 10 s, 2 ml (injection velocity: 2 ml/s) of room-temperature water was delivered through a soft rubber tube (diameter: 1.5 mm) 20 times using a MR-safe contrast agent injector (Spectris Solaris; Medrad, Warrendale, PA) (Fig. 1, top). Water was used because it does not provide a high degree of swallowing difficulty compared with saliva and is not as easy to swallow as a thicker fluid (25). The tube was held between the subject's lips at midline. Water was delivered on a cued color change (blue to green) projected into the scanner as an ambient light. Subjects were instructed to swallow right after complete arrival of water. To

control for swallowing timing, the movement of the pharynx was recorded with a pneumatic cushion. The pharynx exerts a pressure on the cushion attached to the neck. The cushion is thus squeezed, and the change in air pressure is transformed by a pressure detector into an electrical signal measured by an electro-optical biosignal recorder (Varioport-b; Becker Meditec, Karlsruhe, Germany). The pressure indicates the time of pharyngeal swallowing action. Subjects were instructed to swallow only when the full water volume arrived in the mouth and to avoid swallowing in between water delivery. As a result, reflexive swallowing was avoided and was verified by the pneumatic cushion signal, which recorded every swallow. If subjects suppressed the thought to swallow and waited for the next water delivery, the reflexive swallow became a volitional one.

For the TMJ movement task, subjects were instructed to perform three jaw-tapping movements within a 2-s period every 10 s on a cued color change as described above. A total of 20 repetitions per run was performed. A soft rubber tube was held between the upper and lower jaw like a bridle bit at the depth of the first or second premolars (Fig. 1, bottom). With the help of this tube, occlusal strength and frequency were measured through a pressure detector connected to an electro-optical biosignal recorder (Varioport-b, Becker Meditec). To reduce experimental complexity and to apply the same procedure in a patient population, sham stimuli were avoided.

**Data acquisition.** MRI data were collected using a 3 T MRI scanner (Siemens Verio, Erlangen, Germany) equipped with a 32-channel head coil. For each scanning session, field homogeneity was optimized by a shimming sequence, and a gradient echo sequence (34 phase and magnitude images, TR 488 ms, TE<sub>1</sub> 4.92 ms, TE<sub>2</sub> 7.38 ms,  $\alpha = 60^\circ$ ) was acquired to calculate a field map aiming at correcting geometric distortions in the echo planar images. Echo planar images were measured during the two runs using the same field of view (FoV) as in the gradient echo sequence (TR 2 s, TE 22 ms, FoV 192 mm, slice spacing 2.5 mm, matrix 96  $\times$  96,  $\alpha = 90^\circ$ , voxel size 2  $\times$  2  $\times$  2 mm<sup>3</sup>). The imaging volume was limited to one that encompasses brain areas involved in sensorimotor processing, cerebellum, and brainstem to obtain the highest possible resolution in the direction of the somatotopy. A total of 34 slices was acquired for each one of the 125 volumes recorded during one run. Additionally, a T1-weighted anatomical image was acquired (MPRage, TR 1690 ms, TE 2.52 ms,  $\alpha = 90^\circ$ , matrix 256  $\times$  256, voxel size 1  $\times$  1  $\times$  1 mm<sup>3</sup>).

SCRs were measured during both trials from the distal phalanges of the index and middle fingers of the dominant hand using Ag/AgCl electrodes. Data were recorded using the BrainAmp MR system (Brain Products, Munich, Germany) with a gradient of 25 mV/ $\mu$ s, sampled at 5,000 Hz, and low-pass filtered with a cutoff frequency of 250 Hz. Units of skin conductance were recorded in microseconds.

Color changes were triggered with fMRI scans, and each color change sent a marker that was simultaneously recorded by the cushion pressure recorded as well as the SCR recorder. This ensured synchronization across multiple modalities without introduction of time lags. Pharyngeal movement recorded with the pressure cushion was analyzed with the cinematographic magnetic resonance sequence. The time of cushion compression coincided with the time of elevated pharynx. This instant was taken to be the end of the oral phase and beginning of the pharyngeal phase.

**Data processing.** Preprocessing and statistical analysis was performed with Statistical Parametric Mapping 8 (SPM8; Wellcome Department of Imaging Neuroscience, London, UK) running on MATLAB (MathWorks, Natick, MA). Unwarping of geometrically distorted echo planar images was performed in the phase-encoding direction with the help of a calculated field map. These images were then motion corrected and realigned to a mean image for each subject. Echo planar images were coregistered to the T1-weighted anatomical image. The structural T1 image was segmented into gray matter, white matter, and cerebro-spinal fluid maps. This segmentation was the basis for spatial normalization to the Montreal Neurological Institute (MNI) template. All echo planar images were smoothed with 6  $\times$  6  $\times$

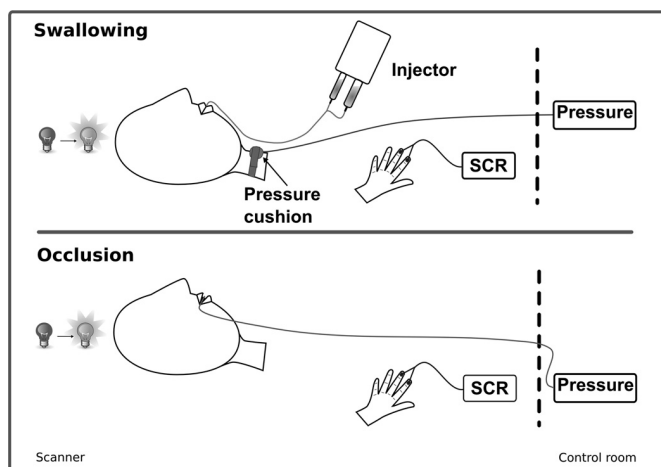


Fig. 1. Functional MRI (fMRI) setup for swallowing and occlusion conditions. Swallowing: water was delivered through a tube connected to an MR-compatible contrast agent injector as soon as the ambient light turned from blue to green. A pressure cushion monitored swallowing activity. Occlusion: on color change from blue to green, subjects produced 3 consecutive jaw movements while pressure from a soft rubber tube in the mouth helped to record occlusal strength and frequency. For both paradigms, skin conductance responses (SCR) were recorded.

6 mm<sup>3</sup> full-width half-maximum Gaussian kernel filter to increase signal to noise ratio. Low-frequency components were filtered with a cutoff of 128 s.

Using BrainAmp Analyzer 2.0 (Brain Products), skin conductance data were artifact corrected, downsampled to 100 Hz, low-pass filtered with a cutoff frequency of 40 Hz, and exported to a MATLAB-compatible file. SCR was analyzed using the Ledalab toolkit (4) in MATLAB through a deconvolution approach. The signal was separated into tonic and phasic activity, followed by a trough-to-peak analysis on the latter, as described in Ref. 4. The mean SCR trough-to-peak amplitudes from the swallow and occlusion conditions were subjected to a paired *t*-test.

**Statistical analysis.** Event intervals between each trial were modeled with a boxcar function convolved with a canonical hemodynamic response function. The six movement parameters from the motion correction were used as regressors to account for coordinated movement artifacts. Individual statistical maps using the Student's *t*-test were calculated for contrasts of interest: activation elicited by swallowing (swallowing), activation elicited by TMJ movements (occlusion), and comparison of activation (swallowing minus occlusion, occlusion minus swallowing). Statistical maps display location and intensity of activation of cortical and subcortical areas that are involved in swallowing or occlusion. The latter two differential contrasts test the overall difference between the two conditions to identify specific regions and activation strength between tasks. Contrast images for each were used in the group statistics calculated as a random-effects analysis at the second level, which takes the variance between subjects into account. The significance level for all contrasts was set to  $P < 0.05$  family-wise error rate corrected for the whole brain volume.

Anatomical maps were defined using the Anatomy Toolbox (13) to describe location, intensity, and activated voxels in anatomical regions (Table 1). To assess distances in three dimensions between highest activated voxels in the primary motor cortex between swal-

lowing and occlusion, Euclidean distances were calculated using the Pythagorean formula.

## RESULTS

Swallowing latency from the visual cue to larynx movement was on average  $2.6 \pm 0.4$  s (mean  $\pm$  SD). This latency includes the water delivery time (1 s) and shows that subjects responded immediately after full arrival of the water volume. For the swallowing condition (Fig. 2A, Table 1, left), representational sites were found bilaterally in the primary motor and somatosensory cortex (MS1), secondary somatosensory cortex (S2), premotor cortex (PMC), SMA, medial cingulate cortex (MCC), pars opercularis, insula, thalamus, cerebellar hemisphere, cerebellar vermis, pallidum, and pons.

For the occlusion condition, evaluation of performance data showed that the three taps had an average length of  $1.5 \pm 0.2$  s. The same representational sites as during swallowing were found except for the SMA, left thalamus, right cerebellar hemisphere, cerebellar vermis, and left pons (Figs. 2 and 3, Table 1, middle).

When focusing on the somatotopic representation in the primary motor cortex, representational maxima during swallowing and occlusion were adjacent: for the left hemisphere the Euclidean distance between swallowing and occlusion was 4.5 mm and 4.9 mm for the right hemisphere. A closer analysis of the location of swallowing in the brainstem revealed activation in the principal sensory nucleus of the trigeminal nerve (MNI coordinates left: -10, -30, -34; coordinates right: 8, -26, -34; Fig. 3). Additionally, activation of the solitary nucleus (MNI coordinates right: 4, -36, -44) was found more caudal. The localization of the brainstem activation for the occlusion

Table 1. Coordinates of highest activation

Area (Brodmann's Area)	Swallowing					Occlusion					Swallow Minus Occlusion				
	k	T	x	y	z	K	T	x	y	z	k	T	x	y	z
L M1 (BA 4)	161	14.12	-52	-8	30	74	6.07	-54	-8	34	145	10.29	-50	-6	30
R M1 (BA 4)	141	16.87	56	-6	32	95	7.03	58	-8	36	125	10.27	46	-8	38
L S1 (BA 1,2,3)	523	15.55	-52	-8	26	91	9.03	-58	-16	42	238	11.67	-52	-6	24
R S1	506	19.02	58	-6	30	123	8.15	54	-14	28	309	10.42	54	-10	30
L S2	2219	15.14	-66	-16	14	367	9.53	-50	6	10	302	11.51	-52	-8	22
R S2	1574	12.12	56	-6	24	340	10.10	58	-20	24	262	10.12	54	-12	26
L PMC (BA 6 lateral)	108	14.18	-60	2	20	79	11.13	-58	6	28	19	8.57	-56	0	22
R PMC	227	17.97	58	-4	30	2	7.17	60	-6	34	74	9.21	54	0	36
SMA ant (BA 6 medial)	52	9.78	0	0	52	—	—	—	—	—	22	8.26	0	2	66
SMA post	77	10.20	2	-4	68	—	—	—	—	—	8	7.76	0	0	66
L Pars opercularis (BA 44)	221	13.32	-60	4	18	273	12.33	-58	6	22	316	9.19	-42	16	30
R Pars opercularis (BA 44)	219	10.46	60	12	2	2	10.57	54	12	-2	80	8.21	56	10	32
MCC	186	9.66	10	16	36	222	8.49	4	16	30	40	8.90	-14	16	42
L Insula (BA 15)	422	11.56	-48	2	4	273	11.08	-38	8	10	1	7.36	-32	-24	18
R Insula	437	10.25	42	0	2	435	14.26	40	6	2	29	8.53	34	-14	10
L Thalamus	259	9.25	-4	-10	10	—	—	—	—	—	2	8.40	-24	-32	8
R Thalamus	376	8.91	6	-20	8	5	7.68	4	-20	8	157	9.51	8	-22	14
L CerHem	539	9.85	-8	-60	-10	3	7.24	-42	-56	-26	335	14.87	-18	-52	-18
R CerHem	459	11.30	6	-52	-10	—	—	—	—	—	132	9.32	20	-56	-16
Cerebellar vermis	182	10.39	-6	-60	-10	—	—	—	—	—	—	—	—	—	—
L Pallidum	90	8.65	-24	-10	-2	2	7.42	-18	-2	-6	24	8.64	-18	-4	-4
R Pallidum	36	8.21	22	-2	-6	3	7.22	20	-4	-6	—	—	—	—	—
L Pons	220	11.83	-10	-30	-34	—	—	—	—	—	2	8.39	-18	-34	-30
R Pons	208	10.80	8	-26	-34	4	9.05	16	-26	-34	6	7.78	2	-24	-24
Midbrain	398	12.31	6	-28	-8	1	6.93	2	-14	-18	5	8.23	4	-24	-22

Statistical parametric mapping coordinates (Montreal Neurological Institute, *x*, *y*, *z*), *t*-values (T), and number of activated voxels per mask (k) of the highest activated voxel for the conditions swallowing, occlusion, and swallowing minus occlusion. All results are plotted for  $P < 0.05$ , family-wise error corrected. BA, Brodmann's Area; L, left; R, right; ant, anterior; post, posterior; M1, primary motor cortex; S1, primary somatosensory cortex; S2, secondary somatosensory cortex; PMC, premotor cortex; SMA, supplementary motor area; MCC, medial cingulate cortex; CerHem, cerebellar hemisphere Larsell IV-VII.

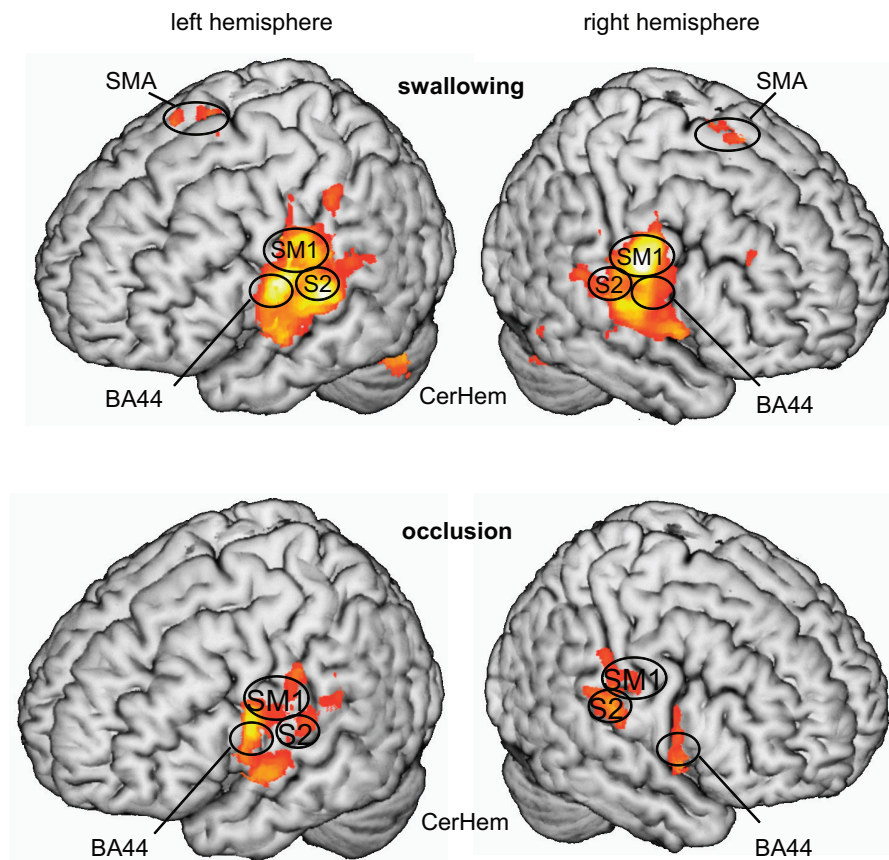


Fig. 2. Overview of the representational maps projected on the segmented Montreal Neurological Institute (MNI)-reference brain. *Top:* swallowing; *bottom:* occlusion. Cortical activation depicted here was found in the sensorimotor cortex (SM1), the secondary somatosensory cortex (S2), pars opercularis of the inferior frontal gyrus (BA 44), and the cerebellar hemispheres (CerHem) bilaterally for both tasks and the supplementary motor area (SMA) only for swallowing.

condition was located more laterally in the trigeminal nerve and its nuclei (MNI coordinates: 16, -26, -34; Fig. 3).

The contrast swallowing minus occlusion showed significant activation in almost all areas reported for the main effect of swallowing except in the cerebellar vermis, right pallidum, and medulla (Table 1, *right*). The reverse contrast (occlusion minus swallowing) showed no significant voxels, underlining the increased cerebral and cerebellar resources necessary for the processing of swallowing.

SCR mean amplitude and standard deviation of trough-to-peak amplitudes across subjects were  $0.079 \pm 0.066 \mu\text{s}$  for swallowing and  $0.076 \pm 0.056 \mu\text{s}$  for occlusion. The paired *t*-test results of SCR data between conditions revealed no differences [swallowing minus occlusion:  $t(20) = 0.32$ , n.s.]. The data showed a drastic tonic change at the start of each scan accompanied by a few phasic peaks that were correlated with the onset light changes at the beginning, which subsequently diminished throughout the run (Fig. 4).

## DISCUSSION

The objective of this experiment was to determine the difference in cerebral activation of swallowing compared with occlusion using fMRI. Furthermore, we controlled for possible differences of task effort using SCR measurements. Whereas previous fMRI studies have focused on the cortical areas involved in deglutition and occlusion, our study was aimed at subcortical processing networks, specifically at automated processes in the brainstem.

With respect to the areas involved, we found a common representational pattern of both tasks in the bilateral primary and secondary sensorimotor areas, the cerebellar hemispheres, the pallidum, the thalamus, and the insula. Functional representation in the precentral gyrus was represented as expected with representation maxima of swallowing inferior-anterior to those of occlusion. A completely new finding is a representation in the midbrain and the right pons, which was observed for both tasks, although different in location.

Brainstem activation for deglutition was found to correspond to the principal sensory nucleus of the trigeminal nerve and the nucleus tractus solitarius (NTS). Based on experiments done in sheep, a group of neurons at the level of the principal sensory trigeminal nucleus is classified as sensory relay neurons. These provide sensory information from the oropharyngeal receptors to the higher nervous centers and are not part of the swallowing CPG network (27). Microelectrode recordings performed on sheep, rat, dog, cat, and monkey place the NTS in the dorsal swallowing group as part of the brainstem swallowing neurons (1, 7, 9, 15, 28, 31, 35, 38, 46, 60). In humans, the cervical esophagus is composed of striated muscles that are innervated by the lower motor neurons. Peristalsis in this segment is due to sequential activation of the motor neurons in the nucleus ambiguus (19).

The brain stem swallowing network includes the NTS and nucleus ambiguus, with the reticular formation linking synaptically to cranial motoneuron pools bilaterally. Under normal function, the brain stem swallowing network receives descend-

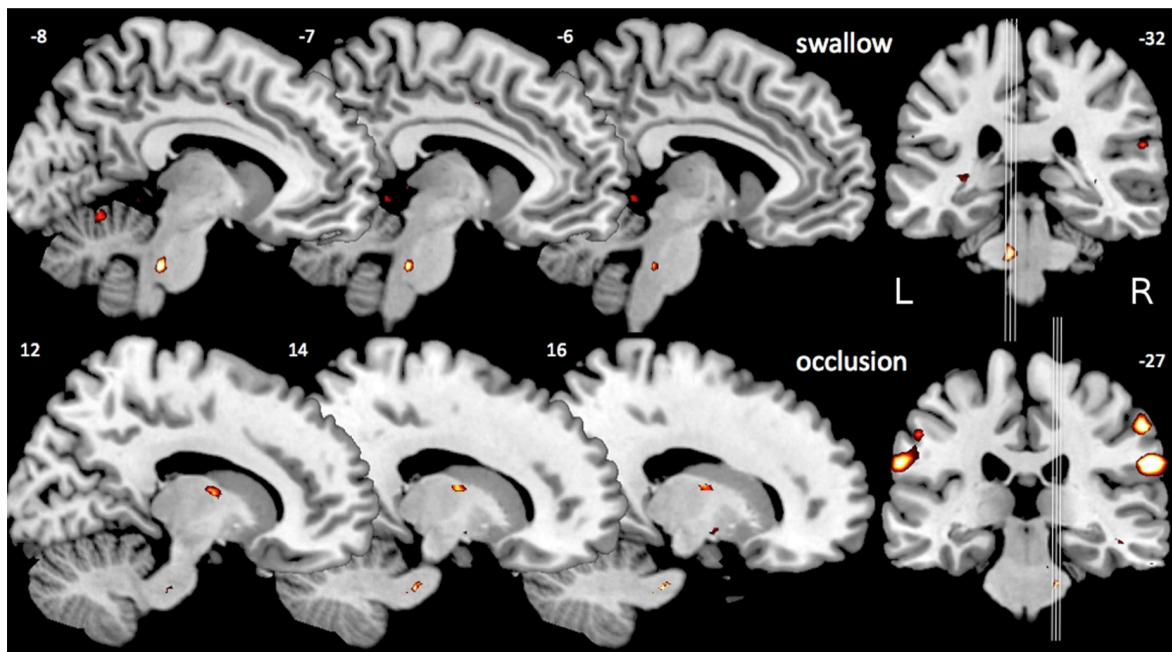


Fig. 3. Brainstem activation during both tasks shown for 3 sagittal slices. Slice position indicated on the coronal slice ( $y$ -MNI coordinate is indicated on the top right corner) on the right of the images. The  $x$ -MNI coordinate of the sagittal slice is provided on the left top corner. Top: brainstem activation for the swallow task showing the principal sensory nucleus of the trigeminal nerve. The activation of the solitary nucleus is not depicted here. Bottom: brainstem activation for the occlusion task showing activation in the trigeminal nerve.

ing inputs from the cerebral cortex (14). The NTS probably contains the second-order sensory neurons as well as the pattern-generating circuitry of both the pharyngeal and esophageal phases of swallowing (34). It recently has been proposed that water may constitute an independent taste modality and that somatosensory responses to water by water-dedicated neurons within the NTS may be part of neural circuits extending from the caudal NTS that produce ingestive reflexes such as swallowing (53).

Occlusional brainstem responses were localized more lateral in the trigeminal nerve (CN V) known to be most important for chewing (44). The Euclidian distance between the two activation maxima (swallowing and occlusion) on the right side was 8 mm. The occlusal CPG is primarily composed of neurons in the region of the trigeminal system (CN V) (44), whereas the swallowing CPG recruits the V, VII, XII motor nuclei, and the nucleus ambiguus (10).

Some recent results have indicated that interneurons localized in the dorsal or ventral regions of the swallowing network also fire during several motor behaviors, such as swallowing, respiration, mastication, and vocalization. The common mo-

toneurons might therefore be triggered by common pools of interneurons. These results indicate that, in mammals, the neurons liable to be involved in pattern generation can belong to different CPGs (2, 7, 18, 32, 35, 47, 48, 62).

Brainstem activation for both tasks is most likely caused by the greater field strength of 3 Tesla, which increases the signal-to-noise ratio and contrasts to noise ratio, leading to an overall greater sensitivity (33). The small activation sites seen in the brainstem might also profit from high spatial resolution and low spatial smoothing used here (3).

The level of activation between both conditions differed substantially. Swallowing is a highly elaborate motor function requiring a coordination of a bilateral sequence of activation and inhibition among more than 25 pairs of muscles in the mouth, pharynx, larynx, and esophagus (8, 10, 29, 42). The sensory input provides feedback for proper bolus control. The contrast thus showed a cumulative activation of different sensory and motor biomechanical events, involving obligate muscles such as the geniohyoid, palatopharyngeus, and thyrohyoid muscles, the pharyngeal constrictors, muscles of the tongue and upper cervical esophagus (8, 11), and facultative ones such as tongue

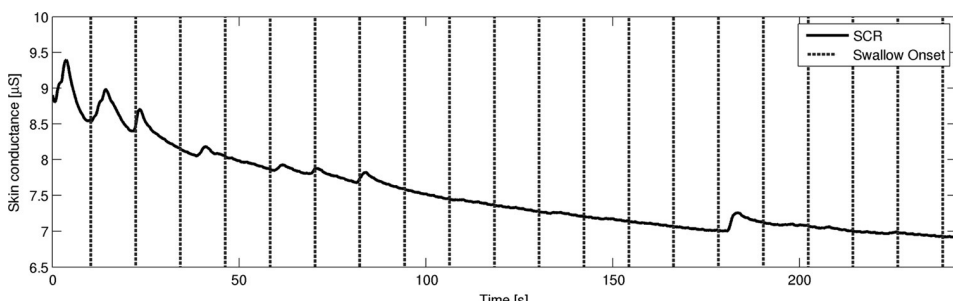


Fig. 4. SCR curve of a single subject during swallowing. The vertical lines indicate water delivery immediately followed by a swallow. The high values at the beginning are associated with a novelty response subsequently subsiding, as the measurement progresses and the subject adjusts to scanner noise and task.

muscles, facial muscles, and lip muscles (11). In contrast, occlusion is movement of one joint (TMJ) predominantly involving four muscle pairs. It comes as no surprise to see both a higher cerebral and cerebellar BOLD magnitude as well as a larger activated volume (9,400 voxels vs. 2,119 voxels) during the swallowing task as opposed to the occlusion task. However, an increase of effort was not verified by simultaneously conducted SCR measurements. Instead they depicted habituation responses over time, pointing to a novelty stress response to scanner noise rather than increased effort (65).

A significant lateralized response, as described by others for occlusion (17, 37) and for swallowing (57) was absent in our study for both tasks.

Areas found to be involved in both actions may not necessarily be task specific. In a "Go, No-Go" study of voluntary swallowing (59), cingulate cortex activation was attributed to processing of experimental context including task cues. Here, a change in color of the light used as a task cue for both swallowing and occlusion, as well as the injection of the water into the mouth, could cause the medial cingulate cortex to be activated. Furthermore, right insular activation found in both tasks may aid in the coordination of task performance (12). The difference in intensity ( $t = 14.26$  for occlusion and  $t = 10.25$  for swallowing,  $P < 0.05$  family-wise error corrected) might be associated with heightened attention necessary for the counting of three occlusal movements right after the light changed color.

The simultaneous and congruent movement of tongue and jaw during mastication, e.g., when the jaw moves to the right so does the tongue, meaning they influence movements of each other, was described by Wild (61) as linguomandibular homotopy. Furthermore, experiments using intracortical micro-stimulation of the pericentral/perisylvian cortex (face-MS1, BA6 immediately lateral to face-M1) in awake monkeys evoked pharyngeal swallowing together with rhythmic jaw movements (24, 39a, 63). The authors thus suggest that certain cortical sites may integrate swallowing with TMJ movements. Functional MRI measurements during lip pursing, jaw clenching, and tongue rolling compared with swallowing of saliva show a high degree of similarity, suggesting a common processing network not specific to swallowing (30). These similarities encompass the regions of activity, the volume of activated voxels, and increases of signal intensity. A further point worth mentioning is that occlusion accompanies swallowing (49).

**Limitations.** Although we carefully optimized the setting in the scanner, applied realignment procedures, and used realign parameters as additional regressor, false-positive effects induced by motion, especially when synchronized with the task, cannot be excluded completely. Even if this motion is outside the FoV, an increase in signal intensity of the same order or above the percent signal change of the BOLD signal is induced in nearby tissue (64). Susceptibility artifacts in the static magnetic field caused by transition between different tissue types were made more uniform using a shimming sequence (21), and the resulting deformations in echo planar images were unwarped using a field map. Nevertheless, tissue motion during swallowing or occlusion causes dynamic changes in the static magnetic field, which cannot be accounted for by shimming or field map unwarping. Instead, the use of motion parameters in the model as regressors of no interest reduced the move-

ment-correlated activation. Indeed, event-related experiments, such as the one described here, are less affected by motion artifacts (55), and, because the task occurs briefly, the motion can be separated from the BOLD response, which has a delay of 5–6 s (5). Nonetheless, these precautions offer no guarantee that brainstem activation is not a result of motion during swallowing and occlusion, especially because these actions are most prone to reveal motion artifacts in this region (55).

Brain stem neurons, in particular in the nucleus ambiguus organized to fire consecutively, produce a sequential excitation of esophageal muscles to provoke peristalsis (52, 58) lasting 10 or more seconds in conscious humans (20). This long-lasting excitation might induce a series of BOLD responses, which will overlap with ones from the proceeding swallow, confounding the signal. Nevertheless, an analysis in time using the hemodynamic response function model, as implemented in SPM8, showed activation in the brainstem timed with the actual swallowing task and not anywhere in between swallows. This temporally confined BOLD magnitude might be associated with the initial transport of oxygenated blood to the brainstem, which supplies enough oxygen to all sequentially organized cells responsible for peristalsis. Indeed, the amount of oxygen supplied greatly exceeds the one metabolized (6).

**Conclusions.** In conclusion, on a spatial resolution obtained here, cerebral representational areas of swallowing and occlusion showed a considerable overlap although the level of activation between conditions differed substantially. This finding gives rise to the idea that cerebral representations of both aspects of food intake are qualitatively widely overlapping but differ with respect to the quantity of neural resources involved. However, this increase of representational load is not associated with effort as controlled by peripheral physiology (SCR). Additionally, human brainstem fMRI activation for both swallowing and occlusion underlined results from previous animal studies and provided a new insight into subcortical processing of these tasks. In the brainstem, swallowing activated the sensory nucleus of the trigeminal nerve together with the solitary nucleus, whereas occlusion activated the trigeminal nerve (CN V), constituting a part of their individual CPGs.

## GRANTS

This study was supported by the Deutsche Forschungsgemeinschaft DFG LO 795/12-1.

## DISCLOSURES

No conflicts of interest, financial or otherwise, are declared by the authors.

## AUTHOR CONTRIBUTIONS

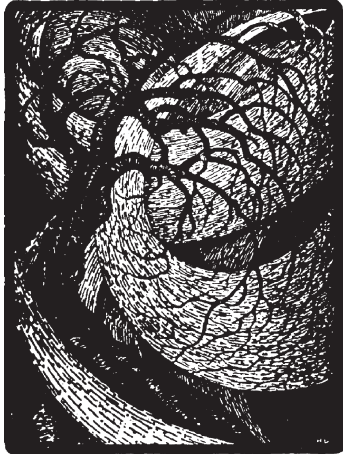
Author contributions: P.G.M. and M.L. performed experiments; P.G.M. analyzed data; P.G.M., O.v.B.u.H., and M.L. interpreted results of experiments; P.G.M. and M.L. prepared figures; P.G.M., O.v.B.u.H., and M.L. drafted manuscript; P.G.M., O.v.B.u.H., and M.L. edited and revised manuscript; P.G.M., O.v.B.u.H., and M.L. approved final version of manuscript; M.L. conception and design of research.

## REFERENCES

1. Amri M, Car A, Jean A. Medullary control of the pontine swallowing neurones in sheep. *Exp Brain Res* 55: 105–110, 1984.
2. Amri M, Lamkadem M, Car A. Effects of lingual nerve and chewing cortex stimulation upon activity of the swallowing neurons located in the region of the hypoglossal motor nucleus. *Brain Res* 548: 149–55, 1991.

3. Ball T, Breckel TPK, Mutschler I, Aertsen A, Schulze-Bonhage A, Hennig J, Speck O. Variability of fMRI-response patterns at different spatial observation scales. *Hum Brain Mapp* 1171: 1155–1171, 2011.
4. Benedek M, Kaernbach C. A continuous measure of phasic electrodermal activity. *J Neurosci Meth* 190: 80–91, 2010.
5. Birn RM, Bandettini P, Cox RW, Shaker R. Event-related fMRI of tasks involving brief motion. *Hum Brain Mapp* 7: 106–114, 1999.
6. Buxton RB. *Introduction to Functional Magnetic Resonance Imaging: Principles and Techniques*. Cambridge University: Cambridge, UK, 2002.
7. Chiao GZ, Larson CR, Yajima Y, Ko P, Kahrlas PJ. Neuronal activity in nucleus ambiguus during deglutition and vocalization in conscious monkeys. *Exp Brain Res* 100: 29–38, 1994.
8. Code CF, Heidel W. *Handbook of Physiology, Section 6, Alimentary Canal*. American Physiological Society: Washington, DC, 1968.
9. Cunningham R, Windischberger C, Deecke L, Moser E. The preparation and readiness for voluntary movement: a high-field event-related fMRI study of the Bereitschafts-BOLD response. *Neuroimage* 20: 404–412, 2003.
10. Doty R, Bosma J. An electromyographic analysis of reflex deglutition. *J Neurophysiol* 19: 44–60, 1956.
11. Dubner R, Sessle BJ, Storey AT. *The Neural Basis of Oral and Facial Function*. Plenum Press: New York, NY, 1978.
12. Eckert MA, Menon V, Walczak A, Ahlstrom J, Denslow S, Horwitz A, Dubno JR. At the heart of the ventral attention system: the right anterior insula. *Hum Brain Mapp* 30: 2530–2541, 2009.
13. Eickhoff SB, Stephan KE, Mohlberg H, Grefkes C, Fink GR, Amunts K, Zilles K. A new SPM toolbox for combining probabilistic cytoarchitectonic maps and functional imaging data. *Neuroimage* 25: 1325–1335, 2005.
14. Ertekin C, Aydogdu I. Neurophysiology of swallowing. *Clin Neurophysiol* 114: 2226–2244, 2003.
15. Ezure K, Oku Y, Tanaka I. Location and axonal projection of one type of swallowing interneurons in cat medulla. *Brain Res* 632: 216–224, 1993.
16. Foerster O. The motor cortex in man in the light of Hughlings Jackson's doctrines. *Brain* 59: 135–159, 1936.
17. Foki T, Geissler A, Gartus A, Pahs G, Deecke L, Beisteiner R. Cortical lateralization of bilateral symmetric chin movements and clinical relevance in tumor patients—a high field BOLD-fMRI study. *Neuroimage* 37: 26–39, 2007.
18. Gestreau C, Milano S, Bianchi a L, Grélot L. Activity of dorsal respiratory group inspiratory neurons during laryngeal-induced fictive coughing and swallowing in decerebrate cats. *Exp Brain Res* 108: 247–256, 1996.
19. Goyal R, Chaudhury A. Physiology of normal esophageal motility. *J Clin Gastroenterol* 42: 610–619, 2008.
20. Goyal R, Cobb B. Motility of the pharynx, esophagus, and esophageal sphincters. In: *Physiology of the Gastrointestinal Tract*, edited by Johnson LR. Raven Press: New York, NY, 1981, pp. 359–391.
21. Haacke EM, Brown RW, Thompson MR, Venkatesan R. *Magnetic Resonance Imaging: Physical Principles and Sequence Design*. Wiley-Liss: New York, NY, 1999.
22. Hamdy S, Aziz Q, Rothwell JC, Crone R, Hughes D, Tallis RC, Thompson DG. Explaining oropharyngeal dysphagia after unilateral hemispheric stroke. *Lancet* 350: 686–692, 1997.
23. Hamdy S, Rothwell JC, Brooks DJ, Bailey D, Aziz Q, Thompson DG. Identification of the cerebral loci processing human swallowing with  $H_2^{15}O$  PET activation. *J Neurophysiol* 81: 1917–1926, 1999.
24. Huang C, Hiraba H, Murray G, Sessel B. Topographical distribution and functional properties of cortically induced rhythmical jaw movements in the monkey (Macaca fascicularis). *J Neurophysiol* 61: 635–650, 1989.
25. Humbert IA, Fitzgerald ME, McLaren DG, Johnson S, Porcaro E, Kosmatka K, Hind J, Robbins J. Neurophysiology of swallowing: effects of age and bolus type. *Neuroimage* 44: 982–991, 2009.
26. Humbert IA, Robbins J. Normal swallowing and functional magnetic resonance imaging: a systematic review. *Dysphagia* 22: 266–275, 2007.
27. Jean A, Car A, Roman C. Comparison of activity in pontine versus medullary neurones during swallowing. *Exp Brain Res* 22: 211–220, 1975.
28. Jean A, Car A. Inputs to the swallowing medullary neurons from the peripheral afferent fibers and the swallowing cortical area. *Brain Res* 178: 567–572, 1979.
29. Jones B. *Normal and Abnormal Swallowing: Imaging in Diagnosis and Therapy*. Springer: Berlin, Germany, 1991, pp. 7–32.
30. Kern M, Birn R, Jaradeh S, Jesmanowicz A, Cox R, Hyde J, Shaker R. Swallow-related cerebral cortical activity maps are not specific to deglutition. *Am J Physiol Gastrointest Liver Physiol* 280: G531–G538, 2001.
31. Kessler J, Jean A. Identification of the medullary swallowing regions in the rat. *Exp Brain Res* 57: 256–263, 1985.
32. Kessler JP. Involvement of excitatory amino acids in the activity of swallowing-related neurons of the ventro-lateral medulla. *Brain Res* 603: 353–357, 1993.
33. Krüger G, Kastrup A, Glover GH. Neuroimaging at 1.5 T and 3.0 T: comparison of oxygenation-sensitive magnetic resonance imaging. *Magn Reson Med* 45: 595–604, 2001.
34. Lang IM. Brain stem control of the phases of swallowing. *Dysphagia* 24: 333–348, 2009.
35. Larson CR, Yajima Y, Ko P. Modification in activity of medullary respiratory-related neurons for vocalization and swallowing. *J Neurophysiol* 71: 2294–2304, 1994.
36. Lickteig R, Lotze M, Lucas C, Domin M, Kordass B. Changes in cortical activation in craniomandibular disorders during splint therapy—a single subject fMRI study. *Ann Anat* 194: 212–215, 2012.
37. Lotze M, Lucas C, Domin M, Kordass B. The cerebral representation of temporomandibular joint occlusion and its alternation by occlusal splints. *Hum Brain Mapp* 33: 2984–2993, 2011.
38. Lu WY, Bieger D. Vagovagal reflex motility patterns of the rat esophagus. *Am J Physiol* 274: R1425–R1435, 1998.
39. Malandraki GA, Sutton BP, Perlman AL, Karampinos DC, Conway C. Neural activation of swallowing and swallowing-related tasks in healthy young adults: an attempt to separate the components of deglutition. *Hum Brain Mapp* 30: 3209–3226, 2009.
- 39a. Martin RE, Kemppainen P, Masuda Y, Yao D, Murray GM, Sessle BJ. Features of cortically evoked swallowing in the awake primate (Macaca fascicularis). *J Neurophysiol* 82: 1529–1541, 1999.
40. Martin R, Barr A, MacIntosh B, Smith R, Stevens T, Taves D, Gati J, Menon R, Hachinski V. Cerebral cortical processing of swallowing in older adults. *Exp Brain Res* 176: 12–22, 2007.
41. Martin RE, MacIntosh BJ, Smith RC, Barr AM, Stevens TK, Gati JS, Menon RS. Cerebral areas processing swallowing and tongue movement are overlapping but distinct: a functional magnetic resonance imaging study. *J Neurophysiol* 92: 2428–2443, 2004.
42. Miller AJ. The neurobiology of swallowing and dysphagia. *Dev Disabil Res Rev* 14: 77–86, 2008.
43. Mochizuki G, Hoque T, Mraz R, Macintosh BJ, Graham SJ, Black SE, Staines WR, McIlroy WE. Challenging the brain: Exploring the link between effort and cortical activation. *Brain Res* 1301: 9–19, 2009.
44. Morquette P, Lavoie R, Phima MD, Lamoureux X, Verdier D, Kolta A. Generation of the masticatory central pattern and its modulation by sensory feedback. *Prog Neurobiol* 96: 340–355, 2012.
45. Mosier K, Bereznaya I. Parallel cortical networks for volitional control of swallowing in humans. *Exp Brain Res* 140: 280–289, 2001.
46. Neya T, Watanabe K, Yamasoto T. Localization of potentials in medullary reticular formation relevant to swallowing. *Rend Gastroenterol* 6: 107–110, 1974.
47. Oku Y, Tanaka I, Ezure K. Activity of bulbar respiratory neurons during fictive coughing and swallowing in the decerebrate cat. *J Physiol* 480: 309–324, 1994.
48. Ono T, Ishiwata Y, Inaba N, Kuroda T, Nakamura Y. Modulation of the inspiratory-related activity of hypoglossal premotor neurons during ingestion and rejection in the decerebrate cat. *J Neurophysiol* 80: 48–58, 1998.
49. Pameijer J, Glickman I, Roeber F. Intraoral occlusal telemetry. II. Registration of tooth contacts in chewing and swallowing. *J Prosthet Dent* 19: 151–159, 1968.
50. Penfield BYW. Somatic motor and sensory representation in the cerebral cortex of man as studied by electrical stimulation. *Brain* 60: 389–443, 1937.
51. Riecker A, Gastl R, Kühlein P, Kassubek J, Prosiegel M. Dysphagia due to unilateral infarction in the vascular territory of the anterior insula. *Dysphagia* 24: 114–118, 2009.
52. Roman C, Tieffenbach L. [Recording the unit activity of vagal motor fibers innervating the baboon esophagus]. *J Physiol (Paris)* 64: 479–506, 1972.

53. Rosen AM, Roussin AT, Di Lorenzo PM. Water as an independent taste modality. *Front Neurosci* 4: 175, 2010.
55. Soltysik DA, Hyde JS. Strategies for block-design fMRI experiments during task-related motion of structures of the oral cavity. *Neuroimage* 29: 1260–1271, 2006.
56. Suzuki M, Asada Y, Ito J, Hayashi K, Inoue H, Kitano H. Activation of cerebellum and basal ganglia on volitional swallowing detected by functional magnetic resonance imaging. *Dysphagia* 18: 71–77, 2003.
57. Teismann IK, Dziewas R, Steinstraeter O, Pantev C. Time-dependent hemispheric shift of the cortical control of volitional swallowing. *Hum Brain Mapp* 30: 92–100, 2009.
58. Tieffenbach L, Roman C. The role of extrinsic vagal innervation in the motility of the smooth-muscled portion of the esophagus: electromyographic study in the cat and the baboon. *J Physiol (Paris)* 64: 193–226, 1972.
59. Toogood JA, Barr AM, Stevens TK, Gati JS, Menon RS, Martin RE. Discrete functional contributions of cerebral cortical foci in voluntary swallowing: a functional magnetic resonance imaging (fMRI) “Go, No-Go” study. *Exp Brain Res* 161: 81–90, 2005.
60. Umezaki T, Matsuse T, Shin T. Medullary swallowing-related neurons in the anesthetized cat. *Neuroreport* 9: 1793–1798, 1998.
61. Wild W. *Funktionelle Prothetik*. Schwabe: Basel, Switzerland, 1950.
62. Yajima Y, Larson CR. Multifunctional properties of ambiguous neurons identified electrophysiologically during vocalization in the awake monkey. *J Neurophysiol* 70: 529–540, 1993.
63. Yao D, Yamamura K, Narita N, Martin RE, Murray GM, Sessle BJ. Neuronal activity patterns in primate primary motor cortex related to trained or semiautomatic jaw and tongue movements. *J Neurophysiol* 87: 2531–2541, 2002.
64. Yetkin FZ, Haughton VM, Cox RW, Hyde J, Birn RM, Wong EC, Prost R. Effect of motion outside the field of view on functional MR. *AJNR Am J Neuroradiol* 17: 1005–1009, 1996.
65. Zwaga HJ. Psychophysiological reactions to mental tasks: effort or stress? *Ergonomics* 16: 61–67, 1973.



# Sequential Evolution of Cortical Activity and Effective Connectivity of Swallowing Using fMRI

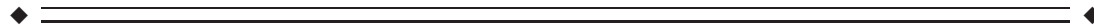
**Paul Glad Mihai,<sup>1\*</sup> Mareile Otto,<sup>2</sup> Thomas Platz,<sup>2</sup> Simon B. Eickhoff,<sup>3,4</sup> and Martin Lotze<sup>1</sup>**

<sup>1</sup>*Functional Imaging Unit, Department of Diagnostic Radiology and Neuroradiology, Ernst-Moritz-Arndt-Universität, Greifswald, Germany*

<sup>2</sup>*BDH-Klinik Greifswald, Neurorehabilitation Centre and Spinal Cord Injury Unit, Neuroscience Department, Ernst-Moritz-Arndt-Universität, Greifswald, Germany*

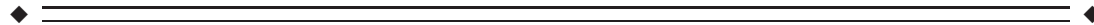
<sup>3</sup>*Institute for Clinical Neuroscience and Medical Psychology, Heinrich-Heine Universität Düsseldorf, Düsseldorf, Germany*

<sup>4</sup>*Institute of Neuroscience and Medicine (INM-1), Research Center Jülich, D-52425 Jülich, Germany*



**Abstract:** Swallowing consists of a hierarchical sequence of primary motor and somatosensory processes. The temporal interplay of different phases is complex and clinical disturbances frequent. Of interest was the temporal interaction of the swallowing network. Time resolution optimized functional magnetic resonance imaging was used to describe the temporal sequence of representation sites of swallowing and their functional connectivity. Sixteen young healthy volunteers were investigated who swallowed 2 ml of water 20 times per run with a repetition time for functional imaging of 514 ms. After applying the general linear model approach to identify activation magnitude in preselected regions of interest repeated measures analysis of variance (rmANOVA) was used to detect relevant effects on lateralization, time, and onset. Furthermore, dynamic causal modeling (DCM) was applied to uncover where the input enters the model and the way in which the cortical regions are connected. The temporal analysis revealed a successive activation starting at the premotor cortex, supplementary motor area (SMA), and bilateral thalamus, followed by the primary sensorimotor cortex, the posterior insula, and cerebellum and culminating with activation in the pons shortly before subsiding. The rmANOVA revealed that activation was lateralized initially to the left hemisphere and gradually moved to the right hemisphere over time. The group random effects DCM analysis resulted in a most likely model that consisted of inputs to SMA and M1S1, bidirectionally connected, and a one-way connection from M1S1 to the posterior insula. *Hum Brain Mapp* 35:5962–5973, 2014. © 2014 Wiley Periodicals, Inc.

**Key words:** swallowing; functional magnetic resonance imaging; dynamic causal modeling; high temporal resolution; event related



This article was published online on 17 July 2014. An error was subsequently identified. This notice is included in the online and print versions to indicate that both have been corrected on 25 July 2014. Contract grant sponsor: Deutsche Forschungsgemeinschaft (DFG); Contract grant number: LO 795-12; Contract grant sponsor: National Institute of Health Grants (to S.B.E.); Contract grant number: R01-MH074457-01A1; Contract grant sponsor: Deutsche Forschungsgemeinschaft [DFG (to S.B.E.)]; Contract grant numbers: EI 816/4-1, LA 3071/3-1; Contract grant sponsor: Helmholtz Initiative on Systems Biology (to S.B.E.); Contract grant sponsor: European EFT Program [Human Brain Project (to S.B.E.)].

\*Correspondence to: P. G. Mihai; Functional Imaging Unit, Department of Diagnostic Radiology and Neuroradiology, Ernst-Moritz-Arndt-Universität, 17475 Greifswald, Germany. E-mail: mihaip@uni-greifswald.de

Received for publication 22 January 2013; Revised 2 July 2014; Accepted 14 July 2014.

DOI: 10.1002/hbm.22597

Published online 17 July 2014 in Wiley Online Library (wileyonlinelibrary.com).

## INTRODUCTION

Swallowing consists of a combination of well-timed sensory and motor functions working together to safely and easily transport saliva or ingested material from the mouth to the stomach [Dodds, 1989]. It is divided into three phases: oral, pharyngeal, and esophageal. Both the pharyngeal and esophageal phases are involuntarily controlled [Dodds, 1989; Jean, 2001].

The functional representation of swallowing is widely investigated and the following representational sites have been described: bilateral inferior precentral and postcentral gyri [Malandraki et al., 2009; Toogood et al., 2005], bilateral anterior insula [Humbert et al., 2009; Humbert and Robbins, 2007; Mihai et al., 2013; Riecker et al., 2009], anterior cingulate cortex [Toogood et al., 2005], bilateral temporal pole, and supplementary motor area (SMA) [Hamdy et al., 1999; Mihai et al., 2013; Mosier and Bereznaya, 2001]. A study on monkeys [Arce et al., 2013] has shown that orofacial primary motor and somatosensory cortices are highly involved in the direction of tongue protrusion, which in turn is of great importance for proper bolus control during swallowing. Two reviews [Humbert and Robbins, 2007; Michou and Hamdy, 2009] and a meta-analysis [Sörös et al., 2009] describe that the SMA, the primary motor (M1) and sensory (S1) cortex, the anterior cingulate cortex, and insular cortex are consistently active during swallowing in human brain imaging studies. Additionally, lateralization is seen in the left hemisphere during the planning stage of swallowing and in the right hemisphere during execution of the task in young healthy volunteers [Malandraki et al., 2010]. Furlong et al. [2004] have shown in a magnetoencephalography (MEG) study that there is a temporal synchrony relating the sensory and motor cortices during volitional swallowing. Water infusion activates the caudolateral sensorimotor cortex which is said to prime the swallowing task and volitional swallowing and tongue movement provide a stronger activation in the superior sensorimotor cortex. Another MEG study [Dzięwas et al., 2003] shows a strong lateralization to the left during volitional swallowing with activation in the midlateral primary sensorimotor cortex and less left lateralization during reflexive swallowing. In a more time-resolved analysis, a lateralization corresponding to the early swallowing stage in the left hemisphere which gradually shifts to the right hemisphere during later stages has been recently reported [Teismann et al., 2009]. Nevertheless, the spatial resolution of MEG is limited and best identification of dipoles is only possible close to the scalp. Thus, time-dependent activation during swallowing among the consistently active regions in functional magnetic resonance imaging (fMRI) experiments is still open to questions on how they are connected and what their temporal progression is.

Dynamic causal modeling (DCM) models interactions between neuronal populations and is based on hemodynamic time series. It aims to estimate and make inferences

about the coupling among brain areas and how this coupling is influenced by experimental context [Friston et al., 2003]. In this study, DCM was used to make inferences about the coupling among regions during swallowing and where the direct influence enters the model.

The aim of this study was to investigate changes in activation over time during a water swallowing task in young healthy subjects. The swallowing task was cued visually by a color change, which indicated the 2-ml water infusion. Examining the statistical parametric maps of activated regions over time, consecutive activation patterns are expected: starting from the premotor and SMAs relating to the preparation of the task, continuing on to the somatosensory cortex, cerebellum, and posterior insula where conscious action of swallowing takes place and ending with activation in the brainstem, alongside cortical activation, in line with peristalsis [Goyal and Chaudhury, 2008]. Repeated measures analysis of variance (rmANOVA) was used to find significant effects on lateralization over time, time effect for each region, and onset effect between regions. With DCM, the effective connectivity between SMA, M1S1, and the posterior insula was investigated. It was postulated that the motor planning in the SMA receives the information over the on-screen color change, that is, the instructions to prepare the swallowing task, from the visual cortex (not covered in the scanning volume). Further, the sensory input from the liquid in S1 may also contribute to planning and executing the swallow. The information could then be passed on to the posterior insula, which mediates the task.

## METHODS

### Participants

Sixteen neurologically healthy volunteers [average age:  $24.9 \pm 3.5$  year (means  $\pm$  standard deviation); range: 20–33 years, 11 female] were analyzed in the study in return for monetary compensation. Informed, written consent was obtained from each participant. Subjects were asked for medication status, signs of chronic pain, sensory deficits, motor deficits, epilepsy, or problems with swallowing. No participant reported to have a history of these symptoms. Three female participants indicated use of an oral contraceptive, one of which also used iron supplements. Three of the sixteen subjects reported to be left handed.

All procedures were approved by the Ethics Committee of the Medical Faculty of the University of Greifswald (registration number BB 101/08).

### Procedure

Swallowing was recorded in three different runs: two functional and one MRI movie sequence. For each of the two functional runs (one using a slow repetition time (TR) of 2 s [slow echo planar image (EPI)], another using a fast

TR of 514 ms (fast EPI)), 20 swallows were recorded per run with a stimulus onset asynchrony (SOA) of 11 scans for slow EPI and 22 scans for fast EPI. For the MRI movie sequence, subjects had to swallow 10 times with a SOA of 6.1 s. The room temperature water (2 ml, injection velocity 2 ml/s) was delivered through a soft rubber tube (diameter: 1.5 mm), held between the subject's lips at midline, using a MR-safe contrast agent injector (Spectris Solaris; Medrad, Warrendale, PA). Water was used because it does not provide a high degree of swallowing difficulty compared to saliva. A thicker fluid reduces the swallowing difficulty further [Humbert et al., 2009], yet the choice of water was based on its universally reliable viscosity at room temperature ensuring reproducibility among and across experiments. Water delivery was marked by a cued color change (blue: rest, green: water injection) projected onto a translucent screen placed inside the scanner bore. The green light lasted for one scan for the slow TR measurement and two scans for the fast TR measurement. Subjects were instructed to swallow right after complete arrival of water (1 s after color change/water injection) and to avoid swallowing in between water delivery. According to a Go-No-Go swallowing experiment [Toogood et al., 2005] areas most significantly related to the No-Go task were restricted to the cuneus and precuneus, whereas precentral and postcentral gyri, together with the anterior cingulate cortex show a significantly greater activation related to the Go swallowing task. Hence, the influence of the instruction to avoid swallowing between water deliveries, which can be interpreted as a No-Go task, is not related to motor and somatosensory activation. Swallowing timing and task compliance was controlled using a pneumatic cushion attached to the neck of the subject. Thyroid cartilage movement exerts a pressure on the cushion during the swallowing task. The change in air pressure from the cushion is transformed by a pressure detector into an electrical signal measured by an electro-optical bio-signal recorder (Varioport-b; Becker meditec, Karlsruhe, Germany). The pressure was used as a reference to determine individual starting times for oral and pharyngeal stages of swallowing. Even though thyroid cartilage movement can reflect oropharyngeal movement in the absence of a pharyngeal swallow, subjects were clearly and repeatedly instructed to swallow once after each water delivery. It is highly unlikely that subjects would have raised the thyroid cartilage without a proceeding swallow, shortly after water delivery.

### Data Acquisition and Processing

MRI data acquisition was performed on a 3 T MRI scanner (Siemens Verio, Erlangen, Germany) using a 32-channel head coil. Two functional event-related imaging runs (one fast, one slow), an MRI movie sequence, and a T1-weighted high resolution whole head dataset were recorded in one experimental session. Field homogeneity

was optimized by a shimming sequence and a gradient echo sequence (34 phase and magnitude images, 7 slices,  $3 \times 3 \times 4 \text{ mm}^3$ , field of view (FoV) 192 mm, TR 488 ms, TE<sub>1</sub> 4.92 ms, TE<sub>2</sub> 7.38 ms,  $\alpha = 60^\circ$ ) was acquired to calculate a field map aiming at correcting geometric distortions in the EPI. Fast functional EPI (TR 514 ms, TE 30 ms,  $\alpha = 90^\circ$ , FoV 192 mm, voxel size  $3 \times 3 \times 4 \text{ mm}^3$ , distance factor 50%, base resolution  $64 \times 64$ , oblique orientation, 464 volumes, interleaved) consisted of seven slices in order to increase the temporal resolution of image acquisition for a more precise sampling of the blood oxygen level dependent (BOLD) signal. In addition, our experience in artifact reduction suggested the usage of slice orientation parallel to the central sulcus. This was a tradeoff between high temporal resolution and volume covered with the focus on the main sensorimotor areas. Unfortunately, areas such as the anterior cingulate cortex which has been shown to be consistently involved in swallowing [Humbert and Robbins, 2007; Michou and Hamdy, 2009; Sörös et al., 2009] could not be included. These slices encompass the brain areas involved in sensorimotor processing, posterior insula, and parts of the cerebellum and brainstem as shown in Figure 1a. Stereotaxic coordinates for the relevant anatomic regions encompassed by these slices are found in Table I. Slow functional EPI [Mihai et al., 2013] were the basis for the functional localizer of swallowing. The cinematographic (CINE) sequence (cardio vascular imaging sequence, TR 2.7 ms, TE 1.22 ms,  $\alpha = 50^\circ$ , FoV 270 mm, voxel size  $2.8 \times 2.8 \times 10 \text{ mm}$ , parallel acquisition using a *k*-space-based algorithm [GRAPPA] factor 2, distance factor 10%, base resolution  $96 \times 96$ , sagittal orientation, 1 slice, 200 volumes) was used to visualize the movement of water, tongue, and pharynx during 10 swallowing trials. The effective TR was 305 ms which resulted in a frame rate of 3.3 frames per second. In addition, a T1-weighted anatomical image was acquired (magnetization-prepared rapid gradient echo, TR 1690 ms, TE 2.52 ms,  $\alpha = 9^\circ$ , FoV 250 mm, voxel size  $1 \times 1 \times 1 \text{ mm}^3$ , parallel acquisition using a *k*-space-based algorithm [GRAPPA] factor 2, matrix  $256 \times 256$ , distance factor 50%, transversal orientation, 176 slices, ascending).

Color changes were triggered with fMRI scans, which in turn sent trigger signals to the pressure recorder. This ensured that all data acquisition modalities were synchronized, and allowed for exact timing of thyroid cartilage movement relative to light change.

The cinematographic imaging data were analyzed by a speech-language pathologist (MO) to distinguish the time points of oral and pharyngeal phases for each subject. The beginning of the oral and pharyngeal phases was marked relative to the thyroid cartilage movement by visual inspection of the CINE images. Individual average onset times of the oral and pharyngeal phases were thus obtained.

Preprocessing of fMRI data was done in SPM8 rev. 5236 (Wellcome Department of Imaging Neuroscience, London, UK) running on MATLAB R2011a (MathWorks, Natick,

♦ Cortical Activity and Effective Connectivity of Swallowing ♦

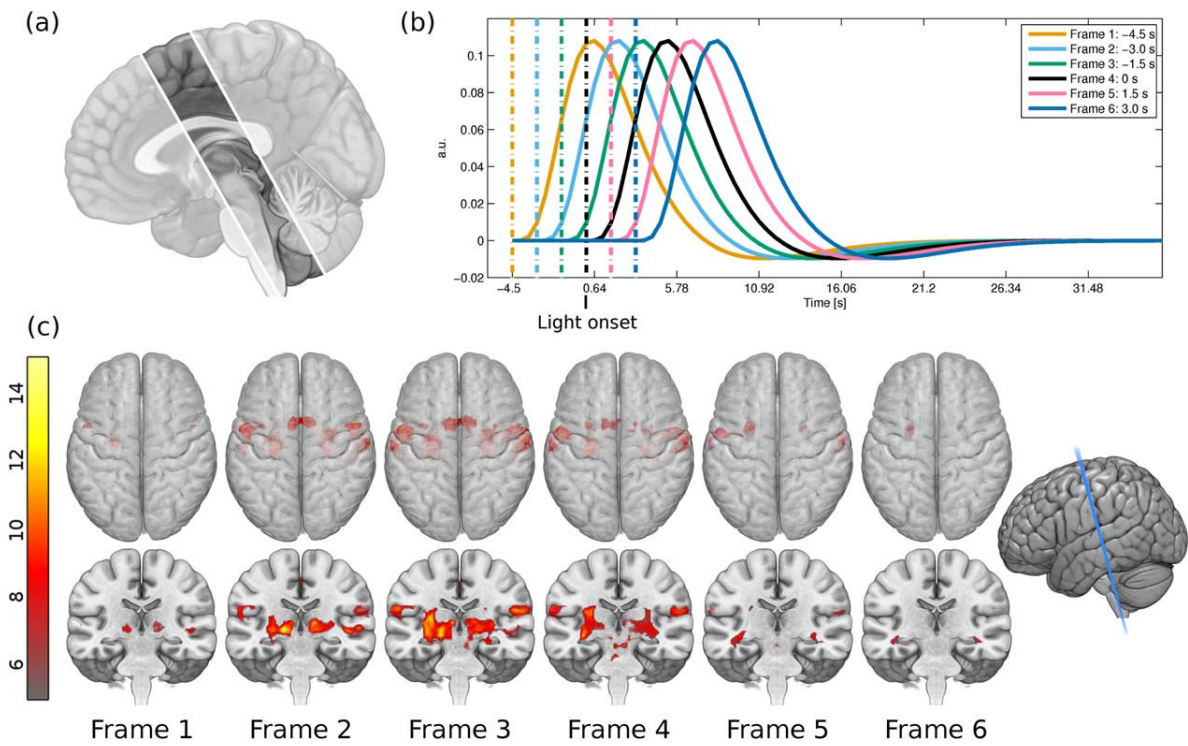


**Figure 1.**

(a) Only seven slices were recorded in the fast EPI measurement, which limited the scanned volume to slices encompassing the PMC, SMA, M1, S1, S2, posterior insula, cerebellum, and brain-stem. This image is a graphical representation of the brain covered by the seven slices; the faded parts were not included in the measurement. (b) A plot of the six different HRFs used in the GLM analysis, named Frame 1 through Frame 6 from left to right. Frame 4 represents the light onset. The interrupted lines represent the

onset times while the solid lines represent the corresponding HRFs. (c) Statistical parametric maps for the six HRFs used in the GLM analysis. The top row shows the axial view with the rendering made translucent, so that deeper activations can be seen. The bottom row shows a coronal cut, slightly oblique as depicted on the far right. The color bar depicts the *t*-score from gray (lowest) to bright yellow (highest). [Color figure can be viewed in the online issue, which is available at [wileyonlinelibrary.com](http://wileyonlinelibrary.com).]

MA). Every swallow causes head movement which is correlated with the stimulus. Movement parameters from a first realignment procedure were used to assess these

motion artifacts which were removed with the help of the ArtRepair Toolbox [Mazaika et al., 2009] by interpolating between the adjacent data points. Movement reduced data were processed as follows. Images were slice time corrected to the middle slice using SPM8's Fourier phase shift interpolation. Head motion was corrected with SPM8's Realign and Unwarp via a third degree b-spline interpolation using the first scan of the series as reference. Unwrapping of susceptibility by movement interaction was done with the help of a voxel displacement map calculated from the field map data. Each subject's T1 image was coregistered using the normalized mutual information from the last step to the mean EPI image. T1 images were segmented into gray and white matter maps using the modified International Consortium for Human Brain Mapping (ICBM) tissue probability maps in Montreal Neurological Institute (MNI) space provided by SPM8. EPI were normalized to the ICBM 152 nonlinear MNI template using a trilinear interpolation. A  $6 \times 6 \times 6 \text{ mm}^3$

**TABLE I. Stereotaxic coordinates of analyzed regions**

Region	MNI coordinates		
	x	y	z
M1S1 L	-56	-5	-24
M1S1 R	60	-5	23
SMA	2	9	52
Posterior Insula L	-34	-14	12
Posterior Insula R	37	-14	11
Cerebellum L	-14	-33	-23
Cerebellum R	17	-33	-22

Stereotaxic coordinates for central points where there is an overlap between slice coverage and anatomical regions. L: left, R: right.

full-width at half-maximum Gaussian kernel filter was used to increase the signal-to-noise ratio and reduce inter-subject differences.

Three methods were used to statistically analyze the fast functional data. The first used the general linear model (GLM) implemented in SPM8. rmANOVA was used to find significant interactions for region, side, and time. Lastly, effective connectivity of the regions involved in swallowing was examined.

### GLM Analysis

For the first method within subject, first-level analysis was performed using the GLM implemented in SPM8. Low frequency components were filtered with a high-pass filter having a cutoff of 128 s, or 0.008 Hz. SPM's canonical hemodynamic response function (HRF) was used as the model for the BOLD response. Motion parameters from the realignment procedure of the artifact repaired data were used as covariates in the design matrix. The autocorrelation inherent in the data was estimated by an autoregressive AR(1) model.

Hüslmann et al. [2003] used a self-paced task involving a random button press in a specific time interval to reveal a sequential activation in the anterior cingulate cortex through the SMA and premotor area to the primary motor (M1) and somatosensory (S1) cortex. Under assumption of the canonical HRF, the voxelwise calculation of maps prior and following the self-paced movement were analyzed. A partially comparable approach was used here. GLMs and contrasts of interest were calculated for swallowing versus baseline at six different onset times in steps of 1.5 s from -4.5 to 3.0 s with time 0 s being the light change from blue to green (Fig. 1b), that is, water injection time. The six onset times when convolved with the HRF cover an epoch that spans the expected BOLD responses initiated by swallowing. The choice of time windows was based on the analysis of the BOLD signal relative to the color change onset. Figure 2 shows a plot of the pressure cushion signal aligned with the BOLD response in M1S1 and compared with the theoretical HRF based on two different onsets. The onsets corresponded to the color change (interrupted blue vertical line) and to the approximate peak of the pressure signal from laryngeal movement (solid red, vertical line). The resulting HRFs (onset times convolved with canonical HRF) clearly showed that they are in agreement with the color change onset. The pressure signal onset results in a later HRF which is not mirrored in the measured signal. A GLM was calculated per time frame for each subject. These steps were chosen empirically in order to accommodate for significant changes between intervals. Smaller steps resulted in fewer changes from one frame to the next. Temporal derivatives were not included in the design matrix as they are only reliable for  $\pm 1$  s [Friston et al., 2007]. A random effects inference was done with a one sample *t*-test on the summary statistic per contrast of each time frame. Location of activation maxima for all

time points were recorded in a table with the help of anatomical masks obtained from the Anatomy Toolbox [Eickhoff et al., 2005] for the SMA, PMC, and M1S1. For the differentiation of the PMC and the SMA, which are cytoarchitectonically similar, a spatial differentiation was performed: the PMC was defined as the BA 6 lateral to the superior frontal sulcus of the MNI-template ( $-30 < x < 30$ ). Cerebellar maps, comprising Larsell's classification IV–VI (culmen and declive), insula, and pons were obtained from the WFU PickAtlas [Maldjian et al., 2003].

### Repeated Measures Analysis of Variance

A repeated measures analysis of variance (rmANOVA) was calculated for the beta-values averaged in a 6-mm sphere around the highest activated voxel within each regions of interest (ROI) used in the GLM analysis for the factors: region (PMC, SMA, M1S1, posterior insula, and cerebellum), side (left and right), and time (Frames 1, 2, 3, 4, 5, 6). The Greenhouse-Geisser correction was used for detecting significant main effects and interactions. Significant effects in rmANOVA were followed by the following post hoc *t*-tests, based on our hypotheses and the results from previous studies:

1. Lateralization effect over time for three time frames: Frame 2, Frame 3, and Frame 6 (three comparisons per region;  $p_{corr} = 0.016$ );
2. Time effect for each region (averaged for side; six comparisons;  $p_{corr} = 0.008$ );
3. Onset effect between regions (averaged for side; five comparisons;  $p_{corr} = 0.01$ ).

### Dynamic Causal Modeling

The second method dealt with effective connectivity and used DCM [Friston et al., 2003] as implemented in SPM8 (DCM10 for SPM8). DCM models interactions at the cortical level using hemodynamic time series. It aims to estimate and make inferences about coupling among brain regions and how this coupling is influenced by changes in experimental contexts.

DCM's purpose in this experiment was two-fold. First, what was the role of the input, especially as there are two possible cues to plan and execute swallowing—visual and somatosensory? Second, based on these cues, what is the directionality of the connections during motor planning, motor execution, and mediation? Models were based on simplicity and focused on three seeds. These included the SMA, used in planning and execution stages of complex motor movements such as swallowing [Hamdy et al., 1999; Mosier and Bereznaya, 2001]. The primary sensorimotor cortex (M1S1) plays an important role on muscle control and sensory feedback during swallowing [Malandraki et al., 2009]. M1 and S1 were grouped together as M1S1 due to low spatial resolution and smoothing, smearing activation in such a small volume. Lastly, the insula was included

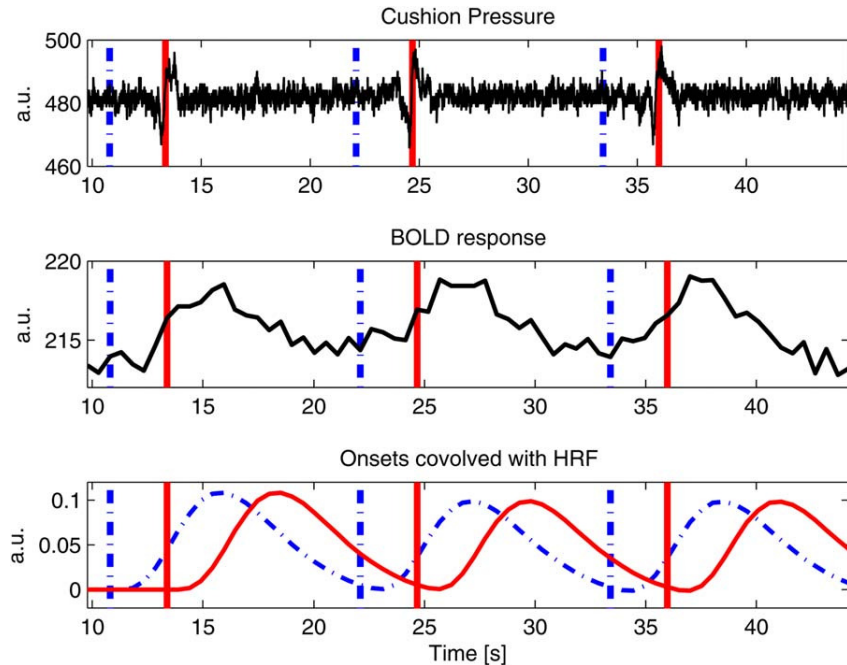


**Figure 2.**

A plot illustrating the pressure cushion signal, BOLD response from the highest activated voxel in M1S1 for a representative subject and onsets convolved with the HRF, plotted against time. All three plots are synchronized in time. Vertical lines indicate onset times for color change (interrupted line) and thyroid carti-

lage movement (solid line). The HRF aligned with color change (interrupted line) properly corresponds with the BOLD response, as opposed to the HRF aligned with thyroid cartilage movement (solid line). [Color figure can be viewed in the online issue, which is available at [wileyonlinelibrary.com](http://wileyonlinelibrary.com).]

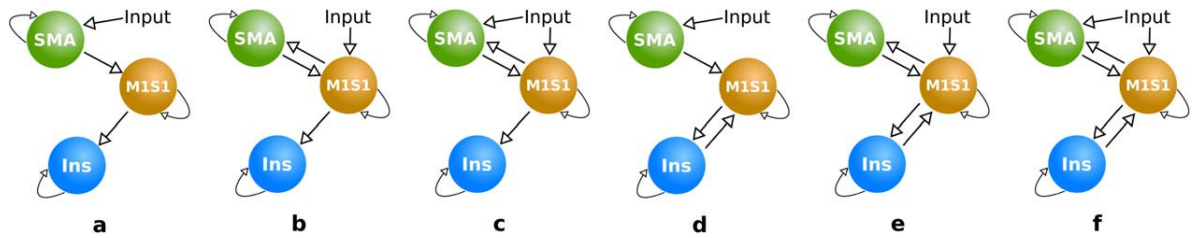
which has connections to primary and supplementary motor cortices and is key in mediation of oropharyngeal swallowing [Daniels and Foundas, 1997]. The limitation to three regions was introduced to reduce the complexity of the models and to gather information on which input is used as a cue to swallow, where it enters the model and how these three regions interact given this input. Furthermore, the seven slices limited the full coverage of the regions. Left and right hemispheres were analyzed separately, save for the SMA due to its central location and short pathways between hemispheres.

Seed regions for DCM computation were made using a combination of functional ROI and the Anatomy Toolbox for SPM8 [Eickhoff et al., 2005] as well as the WFU PickAtlas [Maldjian et al., 2003]. The functional ROIs were extracted from the EPI data recorded with a TR of 2 s (slow EPI). This data had 34 slices and thus a larger volume providing better coverage. The slow EPI experiment also showed activation for the three seed ROI in the DCM analysis [Mihai et al., 2013]. The functional ROI was masked by the probabilistic ROIs from the Anatomy Toolbox which included masks for the SMA (combined left and right hemisphere due to the short connections between the hemispheres, BA 6), M1S1 (left and right hemisphere, BA 4a, 4p, 3a, 3s, 1, 2). The insula (left and

right hemisphere) was provided by the WFU PickAtlas [Maldjian et al., 2003]. A representative time course from voxel data in terms of the first eigenvariate in all supra-threshold voxels ( $P < 0.05$  FWE corrected) in the fast EPI data was extracted using the combined ROIs for each subject.

### Model Selection and Comparison

Figure 3 shows the models. For model (a), the stimulus information enters the SMA which is connected directionally to M1S1. The idea here is that color change marking the time of water infusion through the visual cortex induces a preparatory activation in the SMA. Model (b) connects both SMA and M1S1 bidirectionally while the input enters M1S1. Here, the water entering the mouth stimulates S1, which sends the signal to the SMA, inducing swallowing action through M1. Model (c) is based on (b) with the exception that the input reaches both the SMA as a visual input and M1S1 as a sensory input. All models have a one-way connection from M1S1 to the posterior insula. The unidirectional connection from M1S1 to the anterior insula was chosen because it has been suggested that the function of the posterior insula lays predominantly in monitoring body states and integrating

**Figure 3.**

Description of the models used to test the effective connectivity of the regions. Model (a) receives the input at the SMA, which is connected unidirectionally to M1S1. Model (b) receives the input at M1S1; both regions are connected bidirectionally. Model (c) has inputs going to both the SMA and M1S1; both regions are con-

nected bidirectionally. All models have a one-way connection from M1S1 to the posterior insula. Models (d) through (f) are similar to models (a) through (c), with the exception of a bidirectional connection between M1S1 and insula. [Color figure can be viewed in the online issue, which is available at [wileyonlinelibrary.com](http://wileyonlinelibrary.com).]

somatosensory input to this state [Damasio, 1996]. Therefore, the direction of the model should be unidirectional from the sensorimotor system to the posterior insula. However, to test the influence of the bidirectional connection between M1S1 and posterior insula, three additional models [Fig. 3 models (d), (e), and (f)] were added. These were based on the first three, with an affixed connection from anterior insula to M1S1.

The six models were specified, estimated, and compared at the group level.

To identify the most likely generative model for the observed data among the six different models, a random-effects Bayesian Model Selection (BMS) procedure was employed [Stephan et al., 2009] where all models were tested against each other. This Bayesian method treats the model as a random variable and estimates the parameter of a Dirichlet distribution, which describes the probabilities for all models being considered and allows computing the exceedance probability of one model being more likely than any other model tested.

## RESULTS

All results reported here are based on the fast EPI data (TR = 514 ms).

### Task Performance

The swallowing task was verified with the help of the pneumatic cushion measurements. All subjects swallowed 20 times except for two, each omitting one swallow. This was accounted for in the analysis. The mean ( $\pm$  standard deviation) time difference across subjects from color change to pressure cushion signal was  $2.8 \pm 0.6$  s.

### GLM Analysis

The evolution of BOLD activity over time as calculated by the GLM analysis is depicted in Figure 1c. At the first

time frame, cortical activation was exhibited in the left posterior SMA and premotor cortex (PMC) in the somatotopic height of lip and tongue and subcortical bilateral thalamus. In Frame 2, the bilateral anterior and posterior SMA and PMC were activated, primary motor (M1) activation was detected, and the bilateral thalamus was active. In Frame 3, activation magnitude was highest for all areas described including bilateral primary and secondary somatosensory cortex (S1 and S2) but also bilateral posterior insula. Activation difference was minimal in the BOLD magnitude of the following time frame (Frame 4; light change/water injection time), compared to the current one, with the exception of the brainstem activation. The next time frame only showed residual cortical activation in the left SMA and left M1/S1. The last frame (Frame 6) showed no significant activation magnitude. Activation maxima for all time points using anatomical maps of the PMC, SMA, M1S1, posterior insula, cerebellum, and brainstem can be found in Table II.

No significant (FWE,  $P < 0.05$ ) activation was found for the individual average onset times of the oral and pharyngeal phases as calculated from the cinematographic images. The clarification of this result is given in Discussion Section.

### Repeated Measures Analysis of Variance

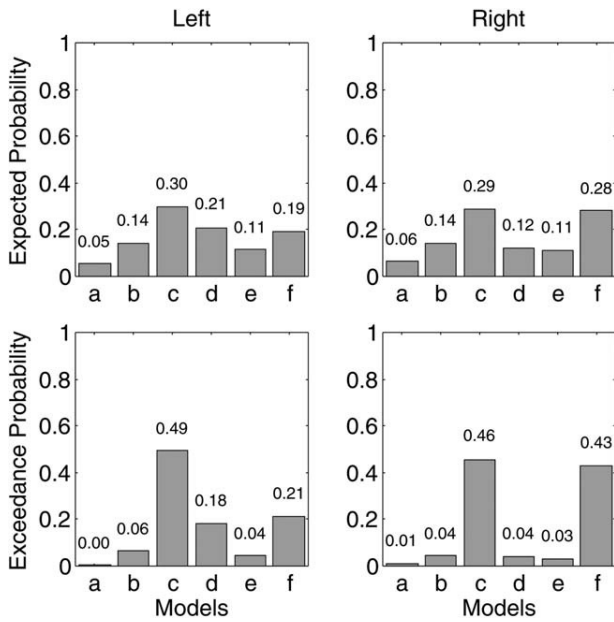
Repeated measures ANOVA (rmANOVA) revealed a significant main effect for region (PMC, SMA, M1S1, posterior insula, cerebellum;  $F(4, 60) = 81.92$ ;  $P < 0.001$ ), time (six time frames;  $F(5, 75) = 8.17$ ;  $P < 0.01$ ) and a significant interaction for region  $\times$  time ( $F(20, 300) = 15.93$ ;  $P < 0.001$ ), side  $\times$  time ( $F(5, 75) = 37.40$ ;  $P < 0.01$ ) and region  $\times$  side  $\times$  time ( $F(20, 300) = 4.30$ ;  $P < 0.01$ ). Post hoc *t*-tests showed a significant lateralization effect over time for M1S1 starting with a left lateralization in Frame 2 ( $t(15) = 2.80$ ;  $P = 0.011$ ) and ending with a right lateralization in Frame 6 ( $t(15) = -2.94$ ;  $P = 0.010$ ). For the posterior insula, a right lateralization at Frame 3 was observed ( $t(15) = -2.75$ ;  $P = 0.015$ ) but in other areas no significant lateralization within time frames was

♦ Cortical Activity and Effective Connectivity of Swallowing ♦

**TABLE II. Coordinates of highest activation in GLM analysis for all six time frames**

Time frames Macroanatomical location	1			2			3			4			5			6		
	T	MNI coordinates	T	MNI coordinates	T	MNI coordinates	T	MNI coordinates	T	MNI coordinates	T	MNI coordinates	T	MNI coordinates	T	MNI coordinates	T	MNI coordinates
x	y	z	x	y	z	x	y	z	x	y	z	x	y	z	x	y	z	
L PMC	8.61	-56	2	32	16.09	-56	2	32	14.19	-56	-2	30	14.95	-56	-2	30	10.09	-56
R PMC	7.62	52	4	42	11.57	52	4	42	10.23	58	-2	28	8.97	58	-2	28	6.72	58
L SMA	—	—	—	—	8.82	-8	4	46	9.26	8	6	48	7.81	8	12	54	—	—
R SMA	—	—	—	—	10.47	4	8	48	8.77	-8	4	46	6.91	-8	4	46	—	—
L M1SI	—	—	—	—	9.19	-54	-2	28	15.02	-54	-2	28	15.92	-54	2	28	10.61	-54
R M1SI	—	—	—	—	9.51	54	-4	20	12.16	58	-4	24	10.41	58	-4	24	7.93	62
L Insula	—	—	—	—	8.14	-36	-14	2	12.68	-32	-24	6	10.44	-32	-26	4	—	—
R Insula	—	—	—	—	8.96	42	-22	-2	9.96	32	-22	6	7.93	32	-28	8	—	—
L Cerebellum	—	—	—	—	—	—	—	—	—	—	—	—	7.80	-18	-38	-26	—	—
R Cerebellum	—	—	—	—	8.07	20	-38	-24	8.57	20	-38	-22	7.56	20	-36	-28	—	—
L Pons	—	—	—	—	—	—	—	—	—	—	—	—	9.50	-4	-30	-26	—	—
R Pons	—	—	—	—	—	—	—	—	—	—	—	—	—	—	—	—	—	—

Statistical parametric mapping coordinates (Montreal Neurological Institute,  $x, y, z$  [mm]) and  $t$ -values ( $T$ ) of the highest activated voxel for the six different HRFs used in the GLM analysis. All results are plotted for  $P < 0.05$ , family-wise error corrected. L, left; R, right; PMC, premotor cortex; SMA, supplementary motor area; M1SI, primary sensory-motor cortex; Cerebellum, cerebellar hemisphere Larsell IV–VI.

**Figure 4.**

Expected and exceedance probabilities for the models tested in the DCM analysis. The left column depicts the results for left hemisphere while the right column depicts the results for the right hemisphere.

present. As the side effect was not significant as a main factor, all activation magnitudes were averaged out per region and time frame for both hemispheres. When testing over time (moving *t*-tests to the prior time frame), there was a relevant increase in PMC and M1S1 from Frame 1 up to Frame 3 (Frame 1 to 6: PMC:  $t(15) = -4.59$ ;  $P < 0.001$ , M1S1:  $t(15) = -9.62$ ;  $P < 0.001$ ; Frame 2 to 3: PMC:  $t(15) = -7.55$ ;  $P < 0.001$ ; M1S1:  $t(15) = -5.45$ ;  $P < 0.001$ ), then a plateau (M1S1 and PMC between Frames 3 and 4) and then a significant decrease (Frame 4 to 5: M1:  $t(15) = 4.23$ ;  $P < 0.001$ ; Frame 5 to 6 s: PMC:  $t(15) = 6.61$ ;  $P < 0.001$ ; M1:  $t(15) = 9.21$ ;  $P < 0.001$ ). In SMA, the increase seemed to be earlier (Frame 1 to 6:  $t(15) = -7.06$ ;  $P < 0.001$ ) and was already reversed at Frame 3 to 4 ( $t(15) = 2.86$ ;  $P < 0.012$ ). The increase in the posterior insula was early (Frame 1 to 2;  $t(15) = -3.59$ ;  $P < 0.003$ ) and was reversed already at Frame 3 to 4 ( $t(15) = 3.79$ ;  $P < 0.002$ ). No relevant changes were seen for the cerebellar hemisphere over time. Between the regions, there were highest BOLD-magnitudes for the PMC and M1S1 compared to SMA during the whole period between Frames 3 and 6 ( $t > 5.6$ ;  $P < 0.001$ ). The posterior insula showed lower BOLD magnitude during Frames 1 and 4 ( $t \approx -4.2$ ;  $P < 0.001$ ) followed by a comparable activation magnitude as the SMA.

### Dynamic Causal Modeling

In Figure 4, the expected probability (top row) and exceedance probabilities (bottom row) of the six models

tested are presented. In the left hemisphere, the winning model as computed with random effects BMS is (c) with an expected and exceedance probability of 0.30 and 0.49, respectively. In the right hemisphere, model (c) is also the winner (expected probability of 0.29, exceedance probability of 0.46) with model (f) following closely (expected probability of 0.28, exceedance probability of 0.43). Both models (c) and (f) have inputs to the SMA and M1S1 which are bidirectionally connected. The difference between the two lies in the connection to the anterior insula. Model (c) has a unidirectional connection from M1S1 to the posterior insula, while model (f) has a bidirectional connection between the two.

### DISCUSSION

Cortical, cerebellar, and subcortical areas contribute to deglutition. In an attempt to discover the effective connectivity and timing between the most common activated regions during swallowing in fMRI, GLM analysis over six different time points during the task and DCM were examined in young healthy adults. In the general linear modeling analysis in time, consecutive activations were seen during swallowing starting at the PMC, SMA, and bilateral thalamus, continuing on to M1S1, insula, and cerebellum and reaching the brainstem shortly before subsiding. A rmANOVA revealed a significant activation over time in M1S1 starting in the left hemisphere and moving to the right hemisphere. The BMS of the six DCM models resulted in the most likely model having an input to both the SMA and M1S1, which were bidirectionally connected, and a one-way connection from M1S1 to the insula.

### GLM Analysis

Using the GLM as implemented in SPM, statistical *t*-maps were calculated for six time points covering the whole swallowing response including the oral and pharyngeal phases. The results show a gradual increase of activation over time starting in the PMC, SMA, and bilateral thalamus, and continuing on to M1S1, posterior insula, and cerebellum. Activation in PMC and SMA were preceding movement execution and were the first sites being active for swallowing. The visual cue (color change from blue to green) was the first indicator of the task and raised awareness to prepare the swallow. Water infusion, the second cue, has been shown to activate the caudolateral sensorimotor cortex [Furlong et al., 2004]. The second frame shows starting activation in M1S1 suggesting a response to water infusion. Subcortical activation in the thalamus might have been due to a somatosensory feedback of the water pressure stimulating the tongue before the swallowing process is started. The actual execution of movement and the concomitant somatosensory processing during swallowing was expressed in the activation of M1S1, posterior insula, and cerebellum. Tongue and lips performing

the coordinated movement are guided by the sensory feedback to push the water toward the oropharynx. The activation of the pons might be indicative of the pharyngeal phase of swallowing, where the water enters the pharynx to be pushed toward the esophagus. The activation observed in the pons is consistent with the one reported in a previous study [Mihai et al., 2013] where the sensory nucleus of the trigeminal nerve and the solitary nucleus are found to be involved in the swallowing network. This study employed a lower spatial resolution and also cut out the ventral part of the brainstem when limited to only seven slices. This resulted in only one significant highest activation (coordinates:  $-4, -30, -26$ ), the most likely candidate being the solitary nucleus.

### Repeated Measures Analysis of Variance

The repeated measures ANOVA revealed a lateralization over time in M1S1 gradually moving from the left hemisphere (starting at Frame 1) to the right hemisphere (ending at Frame 6). Earlier stages, including the preparatory phase, were lateralized to the left and later stages were lateralized to the right hemisphere. Our findings are, therefore, consistent with the MEG findings of Teismann et al. [2009], where left hemispheric activation is found for the first 600 ms, followed by a bihemispheric activation in the next 200 ms and ending in a right hemispheric activation during the last 200 ms. The posterior insula showed a significant lateralization only at Frame 3. This may be due to its early increase and early reversal, as calculated in the region  $\times$  time interaction and its comparably low activation. The SMA over time started earlier and decreased earlier corresponding to its function of readying the swallowing action. It does not explain, however, why the PMC mimics the M1S1 activation over time with a relevant increase in the early frames (Frames 1–3), a plateau (Frames 3 and 4) and a significant decrease in the latter frames. Both these regions also show a significantly higher between region activation when compared to the SMA. M1S1 activation is a reflection of the sensory-motor interaction during swallowing. The sensory aspect of the water being injected into the mouth, furthered by the swallowing action, results in a strong activation of these areas over time. The observed shift in brain activation from left to right may be associated with different specializations of cortical areas. Thus, the left hemisphere could be better specialized in the control of the preparatory phases of swallowing, while the right hemisphere may play a larger role in the involuntary phases of swallowing. This is corroborated with studies on dysphagic patients after a right hemispheric stroke. The pharyngeal phase is delayed more severely and there is a higher incidence of laryngeal penetration and aspiration in patients with right hemispheric stroke and dysphagia [Robbins, 1993]. Daniels and Founas [1997] have shown that dysphunction and dysmotility in the pharyngeal swallowing stage were the result of

right hemispheric damage. Using MEG, Dziewas et al. [2003] showed a strong lateralization to the left during volitional swallowing with activation in the midlateral primary sensorimotor cortex and less left lateralization during reflexive swallowing. Teismann et al. [2009] hypothesized that right hemispheric activation, which they have shown to occur later than left hemispheric activation, corresponds to the pharyngeal stage whereas the left hemispheric lateralization was attributed to the preparatory phase of swallowing.

### DCM Analysis

The results of the DCM analysis revealed that models (c) and (f) (Fig. 3) explained the data well. Here, the SMA and M1S1 are connected bidirectionally with inputs going to both regions. The difference in models lies in the connection between M1S1 and posterior insula, with model (c) having a unidirectional connection, while model (f) a bidirectional connection. The more likely model, however, involves a unidirectional input from M1S1 to the insula [model (c)]. In the right hemisphere, models (c) and (f) have comparable exceedance probabilities, suggesting a stronger involvement of the posterior insula on M1S1 as compared to the left hemisphere. It could be argued that the posterior insula plays a greater role in the modulation of swallowing in the right hemisphere, suggesting finer involvement in later swallowing stages. The SMA most likely receives the input from the visual cortex. Due to the need for high temporal resolution, the number of slices has been reduced, omitting the visual cortex. Thus, a model involving this cortical area could not be tested. The best model also had an input to M1S1 as the primary somatosensory cortex receives information as soon as the water enters the oral cavity. The assumption that both the visual and sensory inputs play a role in this experiment is furthered by the bidirectional connection between the SMA and M1S1. The somatosensory cortex, after sensing the water entering the mouth passes this information to the SMA to prepare the motor action of swallowing. Shortly before this happens, the subject is alerted through the light change that water will soon enter the oral cavity and is thus readying the swallow. The integration of both of these cues then leads to the swallowing action performed by the motor cortex.

The DCM analysis showed that the most likely starting candidate would either be the SMA or M1S1. It cannot be discounted that both SMA and M1S1 simultaneously act as starting candidates. However, the methods outlined in this article were unable to provide a definite answer to this proposition. It can only be speculated that the visual feedback would most likely reach the cortical pathways first, as there is a reaction-time lag between color change and button-press, which results in a water injection delay relative to color change. As the infusion period is a constant for all water delivery instances, the only uncertainty factor

remains the human reaction to push the button. Nonetheless, this interruption was always in the subsecond range.

### Limitations

A possible interaction of handedness and lateralization of sensorimotor representation during swallowing has been discussed before [Daniels, 2000; Dziewas et al., 2003; Hamdy et al., 1997; Kern et al., 2001; Martin et al., 2001; Mosier et al., 1999; Teismann et al., 2009]. This study did not confine the sample on right handers but used a representative one. This might have had a decreasing effect on lateralization of representation maps; yet excluding left-handed participants would have decreased the explanatory power of the study.

The study has some limitations for both the GLM and the DCM-analysis. For the GLM analysis, no significant results were found for the individual average start times of the oral and pharyngeal phases as computed from the cinematographic images. An experienced swallowing therapist, well versed in the evaluation of cinematographic data of swallowing, differentiated the onsets of these two phases. The temporal onset of the cinematographic and fMRI data was related via the pneumatic cushion which recorded thyroid cartilage movement during swallowing. Results showed no suprathreshold voxels active for the averaged onsets. However, there was a clear indication of a consecutive progression during swallowing which included these two phases when examining the activation over time. Average times from the cinematographic sequence were used for the functional calculation and there is no guarantee that the subjects performed similarly during the functional run. The cinematographic sequence used to pinpoint individual time points relating to the oral and pharyngeal phase had a temporal resolution of 305 ms (around 3.3 frames per second) comparable to pulsed fluoroscopy sequences used in low dose diagnostics (3.75 frames per second) [Stueve, 2006]. The temporal resolution affords a rough estimate of the sought out time-points which provides sufficient precision for the use as onsets in the design matrix of the GLM. The data are fitted using the canonical HRF which is fixed. Miezin et al. [2000] have shown that there is a strong amplitude reduction when using intertrial intervals of 5 s compared to longer ones. If swallow latency from the oral to the pharyngeal stage is thought to be in the range of 1 s [Ramsey, 1955; Reimers-Neils, 1994], it can be assumed that BOLD amplitudes from the pharyngeal stage are so low that they might fuse with the amplitudes of the oral stage. Hence, measured BOLD signal might contain information from both stages which may be indistinguishable with current methods. A resolution to this problem would be to differentiate the phases experimentally by instructing subjects at the first signal to move the bolus toward the pharynx, lift it, and wait for the signal to push the bolus into it. The first signal would correspond to the oral phase and the second to the pharyngeal phase. Due to the nature of the BOLD

response and the way it is modeled in SPM, the timing information extracted through the GLM analysis provides limited insight and may be confusing. The activation starts at -4.5 s before light change, and thus before water injection, which is not a true reflection of the actual events. Instead, it is a result of the HRF model and its fit to the measured BOLD signal. The useful information provided by this approach is the relative sequential evolution of the cortical and subcortical activation related to the task, and not the absolute timing. In short, onset times which are thought to correspond to the oral and pharyngeal phases as calculated from the cinematographic images with the help of the thyroid cartilage movement as a reference point, do not seem to correspond to the actual time points for the swallowing stages in question of the functional images. This is furthered by the fact that BOLD responses do not correspond to thyroid cartilage movements as seen in Figure 2.

To truly differentiate the visual from the sensory input, the visual cortex should also be included in the measurement and DCM models. However, high temporal resolution at the cost of spatial coverage was a priority in this experiment. With higher field strengths and faster sequences, this may be possible in the future. Additionally, the PMC, basal ganglia, cerebellum, and pons were left out of the models to reduce complexity. The main focus of this study was the activation over time during swallowing. DCM, although not suited for timing calculations, provided a means of determining where the input enters the model and nature of directionality of the connections between regions. These results help interpret the GLM analysis.

## CONCLUSIONS

The GLM results of this study reveal a consecutive activation during swallowing of 2 ml of water starting at the PMC, SMA, and bilateral thalamus, continuing on to M1S1, posterior insula, and cerebellum and reaching the brainstem shortly before it subsides. This sequence reflects the preparation and execution stages of swallowing, including the involuntarily controlled pharyngeal phase. An rmANOVA revealed a significant activation over time in M1S1 starting in the left hemisphere and moving on to the right hemisphere. In a DCM model comparison, the model with the highest likelihood is one encompassing the SMA, M1S1, and posterior insula with two different inputs: one to the SMA and the other to M1S1. SMA and M1S1 are connected bidirectionally while M1S1 has a simple connection going to the posterior insula.

## REFERENCES

- Arce FI, Lee JC, Ross CF, Sessle BJ, Hatsopoulos NG (2013): Directional information from neuronal ensembles in the primate orofacial sensorimotor cortex. *Journal of Neurophysiology* 110: 1357–1369. doi:10.1152/jn.00144.2013.

◆ Cortical Activity and Effective Connectivity of Swallowing ◆

---

- Damasio AR (1996): The somatic marker hypothesis and the possible functions of the prefrontal cortex. *Philos Trans R Soc London B Biol Sci* 351:1413–1420.
- Daniels SK (2000): Swallowing apraxia: A disorder of the praxis system? *Dysphagia* 16:159–166.
- Daniels SK, Foundas AL (1997): The role of the insular cortex in dysphagia. *Dysphagia* 12:146–156.
- Dodds W (1989): The physiology of swallowing. *Dysphagia* 17: 171–178.
- Dziewas R, Sörös P, Ishii R, Chau W, Henningsen H, Ringelstein E., Knecht S, Pantev C (2003): Neuroimaging evidence for cortical involvement in the preparation and in the act of swallowing. *Neuroimage* 20:135–144.
- Eickhoff SB, Stephan KE, Mohlberg H, Grefkes C, Fink GR, Amunts K, Zilles K (2005): A new SPM toolbox for combining probabilistic cytoarchitectonic maps and functional imaging data. *Neuroimage* 25:1325–1335.
- Friston KJ, Harrison L, Penny W (2003): Dynamic causal modeling. *Neuroimage* 19:1273–1302.
- Friston KJ, Ashburner JT, Kiebel SJ, Nichols TE, Penny WD (Eds.). (2007): Statistical Parametric Mapping: The Analysis of Functional Brain Images. Functional neuroimaging: Technical (First edition., p. 656). London: Academic Press.
- Furlong PL, Hobson AR, Aziz Q, Barnes GR, Singh KD, Hillebrand A, Thompson DG, Hamdy S (2004): Dissociating the spatio-temporal characteristics of cortical neuronal activity associated with human volitional swallowing in the healthy adult brain. *Neuroimage* 22:1447–1455.
- Goyal R, Chaudhury A (2008): Physiology of normal esophageal motility. *J Clin Gastroenterol* 42:610–619.
- Hamdy S, Aziz Q, Rothwell JC, Crone R, Hughes D, Tallis RC, Thompson DG (1997): Explaining oropharyngeal dysphagia after unilateral hemispheric stroke. *Lancet* 350:686–692.
- Hamdy S, Rothwell JC, Brooks DJ, Bailey D, Aziz Q, Thompson DG (1999): Identification of the cerebral loci processing human swallowing with  $H_2^{15}O$  PET activation. *J Neurophysiol* 81:1917–1926.
- Hülsmann E, Erb M, Grodd W (2003): From will to action: Sequential cerebellar contributions to voluntary movement. *Neuroimage* 20:1485–1492.
- Humbert IA, Robbins J (2007): Normal swallowing and functional magnetic resonance imaging: A systematic review. *Dysphagia* 22:266–275.
- Humbert IA, Fitzgerald ME, McLaren DG, Johnson S, Porcaro E, Kosmatka K, Hind J, Robbins J (2009): Neurophysiology of swallowing: Effects of age and bolus type. *Neuroimage* 44:982–991.
- Jean A (2001): Brain stem control of swallowing: Neuronal network and cellular mechanisms. *Physiol Rev* 81:929–969.
- Kern MK, Jaradeh S, Arndorfer RC, Shaker R (2001): Cerebral cortical representation of reflexive and volitional swallowing in humans. *Am J Physiol Gastrointest Liver Physiol* 280:G354–G360.
- Malandraki GA, Sutton BP, Perlman AL, Karampinos DC, Conway C (2009): Neural activation of swallowing and swallowing-related tasks in healthy young adults: An attempt to separate the components of deglutition. *Hum Brain Mapp* 30:3209–3226.
- Malandraki G, Sutton B, Perlman A, Karampinos D (2010): Age-related differences in laterality of cortical activations in swallowing. *Dysphagia* 25:238–249.
- Maldjian JA, Laurienti PJ, Kraft RA, Burdette JH (2003): An automated method for neuroanatomic and cytoarchitectonic atlas-based interrogation of fMRI data sets. *Neuroimage* 19:1233–1239.
- Martin RE, Goodyear BG, Gati JS, Menon RS (2001): Cerebral cortical representation of automatic and volitional swallowing in humans. *J Neurophysiol* 85:938–950.
- Mazaika PK, Whitfield-Gabrieli S, Reiss A, Glover G (2009): Artifact Repair for fMRI Data from High Motion Clinical Subjects. Poster presented at the Human Brain Mapping Conference in San Francisco, CA, USA.
- Michou E, Hamdy S (2009): Cortical input in control of swallowing. *Curr Opin Otolaryngol Head Neck Surg* 17:166–171.
- Miezin FM, MacCott L, Ollinger JM, Petersen SE, Buckner RL (2000): Characterizing the hemodynamic response: effects of presentation rate, sampling procedure, and the possibility of ordering brain activity based on relative timing. *NeuroImage* 11(6 Pt 1):735–759. doi:10.1006/nimg.2000.0568.
- Mihai PG, von Bohlen Und Halbach O, Lotze M (2013): Differentiation of cerebral representation of occlusion and swallowing with fMRI. *Am J Physiol Gastrointest Liver Physiol* 304:847–854.
- Mosier K, Bereznaya I (2001): Parallel cortical networks for volitional control of swallowing in humans. *Exp Brain Res* 140:280–289.
- Mosier KM, Liu WC, Maldjian JA, Shah R, Modi B (1999): Lateralization of cortical function in swallowing: A functional MR imaging study. *AJR Am J Neuroradiol* 20:1520–1526.
- Ramsey GH, Watson JS, Gramiak R, Weinberg SA (1955): Cineroentgenographic analysis of the mechanism of swallowing. *Radiology* 64(4):498–518.
- Reimers-Neils L (1994): Viscosity effects on EMG activity in normal swallow. *Dysphagia* 10:101–106.
- Riecker A, Gastl R, Kühnlein P, Kassubek J, Prosiegel M (2009): Dysphagia due to unilateral infarction in the vascular territory of the anterior insula. *Dysphagia* 24:114–118.
- Robbins J (1993): Swallowing after unilateral stroke of the cerebral cortex. *Arch Phys Med Rehabil* 74:1295–1300.
- Sörös P, Inamoto Y, Martin RE (2009): Functional brain imaging of swallowing: An activation likelihood estimation meta-analysis. *Hum Brain Mapp* 30:2426–2439.
- Stephan KE, Penny WD, Daunizeau J, Moran RJ, Friston KJ (2009): Bayesian model selection for group studies. *Neuroimage* 46: 1004–1017.
- Stueve D (2006): Management of pediatric radiation dose using Philips fluoroscopy systems DoseWise: Perfect image, perfect sense. *Pediatr Radiol* 36(Suppl 2):216–220.
- Teismann IK, Dziewas R, Steinstraeter O, Pantev C (2009): Time-dependent hemispheric shift of the cortical control of volitional swallowing. *Hum Brain Mapp* 30:92–100.
- Toogood JA, Barr AM, Stevens TK, Gati JS, Menon RS, Martin RE (2005): Discrete functional contributions of cerebral cortical foci in voluntary swallowing: A fMRI “Go, No-Go” study. *Exp Brain Res* 161:81–90.



## Research report

## Neural representation of swallowing is retained with age. A functional neuroimaging study validated by classical and Bayesian inference

Anne-Sophie Windel<sup>1</sup>, Paul Glad Mihai<sup>\*,1</sup>, Martin Lotze

Functional Imaging Unit, Department of Diagnostic Radiology and Neuroradiology, University Medicine, University of Greifswald, Germany

## HIGHLIGHTS

- We studied cortical activation of swallowing in healthy young adults and healthy seniors using fMRI.
- Differences in the swallowing network between seniors vs. young participants were found in BA10 only using Bayesian inference.
- Seniors showed increased swallowing latency and higher skin conductance response (SCR).
- fMRI-activation in seniors was positively associated with SCR in areas processing sensorimotor performance, arousal and emotional perception.

## ARTICLE INFO

## Article history:

Received 8 January 2015

Received in revised form 27 February 2015

Accepted 4 March 2015

Available online 13 March 2015

## Keywords:

Age

Swallowing

fMRI

Bayes

BA 10

SCR

## ABSTRACT

We investigated the neural representation of swallowing in two age groups for a total of 51 healthy participants (seniors: average age 64 years; young adults: average age 24 years) using high spatial resolution functional magnetic resonance imaging (fMRI). Two statistical comparisons (classical and Bayesian inference) revealed no significant differences between subject groups, apart from higher cortical activation for the seniors in the frontal pole 1 of Brodmann's Area 10 using Bayesian inference. Seniors vs. young participants showed longer reaction times and higher skin conductance response (SCR) during swallowing. We found a positive association of SCR and fMRI-activation only among seniors in areas processing sensorimotor performance, arousal and emotional perception. The results indicate that the highly automated swallowing network retains its functionality with age. However, seniors with higher SCR during swallowing appear to also engage areas involved in attention control and emotional regulation, possibly suggesting increased attention and emotional demands during task performance.

© 2015 Elsevier B.V. All rights reserved.

## 1. Introduction

Swallowing is a complex sensorimotor event that has been investigated via several imaging methods such as functional magnetic resonance imaging (fMRI), magnetoencephalography (MEG), positron emission tomography (PET), transcranial magnetic stimulation (TMS) and electroencephalography (EEG). However, little research has been dedicated to healthy older subjects [26,33,34,36,58] despite the fact that swallowing difficulties are more prevalent among seniors. Age is a major risk factor for the most common neurogenic causes of dysphagia such as stroke [22],

Morbus Parkinson and dementia [55] leading to as much as 38% of older people affected by dysphagia [53]. Even without the presence of disease, the swallowing process changes with age (presbyphagia) [27] and studying such changes is of utmost importance [27,33]. Compared to young healthy participants, studies of older people have shown age-related changes in the swallowing process such as delayed initiation of swallowing, prolonged oral phase [9,26,52,54] declining laryngo-pharyngeal sensitivity [3], reduced lingual and pharyngeal pressure [18,27] accompanied by increased rates of laryngeal penetration [15]. Moreover, a good understanding of the neural control of swallowing in elderly allows a comparison of same age dysphagic patients. This may lead to a better understanding of cortical reorganization after dysphagia, enabling possible increased therapeutic efficacy.

Previous fMRI studies investigating the neural representation of swallowing in older populations reported inconsistent results. Martin and colleagues described increased neural representation for seniors in the lateral pericentral, perisylvian and anterior

\* Corresponding author at: Functional Imaging Unit, Department of Diagnostic Radiology and Neuroradiology, Ernst-Moritz-Arndt-Universität, Walther-Rathenau Str. 46, 17475 Greifswald, Germany. Tel.: +49 3834 86 6944; fax: +49 3834 86 6898.

E-mail address: [paulglad.mihai@uni-greifswald.de](mailto:paulglad.mihai@uni-greifswald.de) (P.G. Mihai).

<sup>1</sup> These authors contributed equally to this work.

cingulate cortex [36]. Humbert et al. [26] described similar findings with increased blood oxygenation level dependent (BOLD)-magnitude in seniors compared to young healthy volunteers in primary and secondary motor areas such as the right pre- and post-central gyri, bilateral frontal lobe, bilateral parietal regions and right superior temporal gyrus. They also reported increased lateralization only in young participants to the left hemisphere in the primary sensorimotor cortex (MS1) and supplementary motor area (SMA). Using MEG Teismann and colleagues found elevated bilateral amplitudes over the pre- and post-central gyrus in seniors, which was interpreted as increased demand in neural processing with decreasing sensorimotor functionality [58].

Contrary to the studies stated above, Malandraki and colleagues used fMRI and found reduced cortical activity in seniors compared to young adults in the somatosensory cortex, and no significant differences in primary motor or other brain areas [34]. In another fMRI-study, the same group reported more symmetrical activation and less lateralization to the dominant hemisphere in seniors during swallowing of water [33], and reported no other significant differences between the senior and younger group.

Common to all above mentioned studies is the suggestion that older people need compensatory mechanisms in the execution of swallowing. In a study measuring performance of complex motor tasks in older subjects, Loibl et al. [31] found that those participants who show early increased recruitment in simple motor tasks decompensate in motor performance with increasing motor complexity. In swallowing, however, it is unclear whether increased neural activation in seniors is an indicator of higher arousal and attentional demand specific to swallowing or less overall efficiency [26].

In general, a missing between group effect and inconsistent findings in age-related swallowing studies might be the result of underpowered study designs (group sizes 9–11 subjects). Based on different paradigms, the recommendation for random effects statistics is at least 20 participants; more optimal would be about 27 participants [60]. Also, different methodological approaches might also account for discrepant results. Teismann et al. [58] used MEG where swallowing took place in an upright position whereas in the case of the fMRI studies participants had to swallow in a supine position. Humbert et al. [26] restricted the analysis to preselected cortical regions and did not correct for multiple comparisons. Martin and colleagues analyzed neural activity on a voxel-by-voxel basis with a fixed-effects model [36]. Malandraki et al. [33] used Z statistics by employing cluster significance thresholding with an analysis focused on Regions of Interests (ROI). Additionally, different amounts of water have been used ranging from 3 to 5 ml per swallow or even with a continuous water delivery of 8–12 ml/min in the MEG-study by Teismann et al. [58]. Also, different interstimulus intervals have been used between the swallows (between 11 and 40 s). Furthermore, age ranges differ among studies from 60 to 85 (mean ages vary between 64.8 and 74.2 years) making it potentially difficult to compare results properly.

In order to complement the previous studies, we aimed to characterize the neural representation of swallowing in healthy seniors compared to healthy young participants with a large sample size (24 young and 27 senior volunteers), high resolution functional imaging methods, and motor performance during imaging. Furthermore, we wanted to quantify physiological parameters in order to examine possible changes with age in task performance and arousal. Swallowing performance and latency was measured using a pneumatic control of the larynx movement. To monitor arousal during swallowing while the subject was in the scanner, we measured skin conductance responses (SCR; [30,41]) as has been done in an earlier swallowing study [40]. SCRs have been used as a psychophysiological measurement of arousal and

controllability [44,64] and are described as a useful measure of distress and effort in recent studies [41,56,57] with increased BOLD-effects in motor areas during increased task challenge [41,66]. A higher SCR has also been associated with task-related changes in arousal [25,64]. Since seniors report more swallowing difficulties and swallowing disorders, we aimed to evaluate if swallowing difficulties are also associated with increased arousal. In order to detect neural representation differences between seniors and young healthy participants, we applied two different robust statistical methods in data evaluation, both of which are based on the general linear model (GLM) – classical and Bayesian inference – to exclude statistical processing dependent effects and ensure high statistical validity of our results. The classical approach is more conservative while Bayesian inference is more specific and avoids the multiple comparison problem [19]. By using multiple regression analysis, we looked for associations between BOLD-magnitude during swallowing, age, changes in arousal measured by SCR, and changes in performance measured by swallowing latency.

We hypothesized that seniors show an overall greater bilateral cortical activation in primary and secondary motor areas, Brodmann Area 44/45 and cerebellum compared to young participants as reported in previous studies. Secondly, we expected a more specific representation and higher sensitivity of activation related to swallowing using Bayesian inference. Additionally, we assumed increased activation in elderly accompanied by prolonged swallowing latency and an increased skin conductance response.

## 2. Methods

### 2.1. Participants

Data from 24 young healthy volunteers (average age  $\pm$  standard deviation:  $24.2 \pm 3.1$  years, age range 20–33 years, 16 female) and 27 old healthy volunteers (average age  $\pm$  standard deviation:  $64.8 \pm 6.5$  years, age range 55–75 years, 22 female) were analyzed in return for monetary compensation. The data from 21 of the 24 participants from the young subject group has been reported previously using unified segmentation, normalization, and the classical statistical approach [40]. Since unified segmentation is inferior to the New Segment and DARTEL normalization [2], we felt obliged to report the improved results here. However, in this study we focused on the comparison of cortical activation in both groups with respect to the difference of age and arousal. Senior participants were recruited through posting flyers in fitness centers, libraries, sports and church groups, and through referral from a general practitioner. Young participants were recruited through flyers and personal contacts. Participants were screened with a questionnaire for medication status, signs of chronic pain, chronic medical conditions, sensory, motor, swallowing, speech or otolaryngologic deficits, epilepsy, and history of stroke or other diseases provoking problems with swallowing. Additionally, they were asked about swallowing problems in the past. No participant reported having a history of these symptoms. Three young participants reported using oral birth control, one of which indicated the use of iron supplements. Of the old participants, ten mentioned use of medication to regulate blood pressure, one takes a pain reliever regularly, one uses anti-diabetic medication, and another uses medication to treat anxiety. Three young subjects reported to be left handed. Senior participants were all right handed as confirmed by the Edinburgh Handedness Inventory [45]. Procedures were approved by the Ethics Committee of the Medical Faculty of the University of Greifswald (registration number BB 101/08).

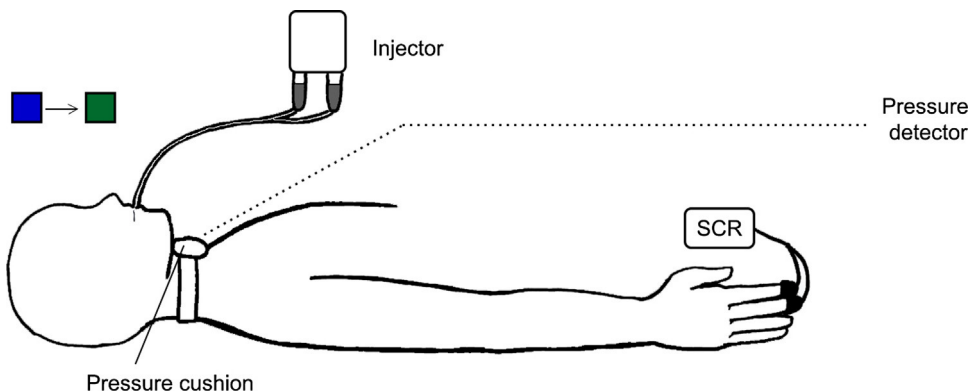


**Fig. 1.** Experimental setup. Two milliliters of water was delivered through a thin tube connected to a contrast agent injector. The delivery was marked by a change in ambient color projected into the scanner bore (blue to green). Thyroid cartilage movement was monitored using a pneumatic cushion secured with a hook-and-loop fastener band around the subject's neck. Skin conductance (SCR) responses were measured from the distal phalanges of the index fingers. (For interpretation of the references to color in this figure legend, the reader is referred to the web version of the article.)

## 2.2. Procedure

A functional imaging run was used to record brain responses related to swallowing water. Twenty swallows were recorded with a fixed stimulus onset asynchrony of 6 scans (12 s). The inter-stimulus interval was 11 s (end of water injection to beginning of next water injection). The room temperature water (2 ml, injection velocity 2 ml/s) was delivered through a soft rubber tube (diameter = 1.5 mm), held between the subject's lips at midline, using a MR-safe contrast agent injector (Spectris Solaris; Medrad, Warrendale, PA, USA). The volume of water was chosen experimentally. Higher volumes lead to partial swallows of the liquid, resulting in multiple swallows per trial. For a robust event related analysis a single swallow per trial was indispensable. Water was used because it does not provide a high degree of swallowing difficulty and has a reliable viscosity at room temperature ensuring reproducibility across experiments. Water delivery was indicated by a queued color change (blue: rest, green: water injection) projected onto a translucent screen placed inside the scanner bore. Subjects were clearly and repeatedly instructed to swallow as soon as they felt all of the water reach the mouth and to avoid swallowing in between water delivery. To control swallowing timing and task compliance, thyroid cartilage movement was measured using a pneumatic cushion placed around the participant's neck. During swallowing thyroid cartilage movement exerted pressure on the pneumatic cushion. The pressure was transformed to an electrical signal measured by an electro-optical biosignal recorder (Varioport-b; Becker Meditec, Karlsruhe, Germany). Time between water injection and measured thyroid cartilage movement indicates approximate swallow duration. A similar procedure has been used in the studies conducted by Malandraki et al. [34,33]. The experimental setup is depicted in Fig. 1.

In a healthy, task-compliant subject, the elevation of the thyroid cartilage indicates the engagement of the pharyngeal swallowing phase. If the time between water delivery to thyroid cartilage movement is longer, the oral phase is also longer. If the sensory and motor aspect is reduced, the subject might need additional time to perform the volitional part of swallowing. Therefore, time spent in oral phase may reflect the difficulty of the task. In this sense, the latency period measured by pneumatic control of the larynx (as detailed in [34,33,40]) may provide an approximation of the swallowing difficulty. Fig. 2 shows a characteristic pneumatic cushion response. The first trigger point marks both the color change of water from blue to green and the water injection time. At the second trigger point the color changes back to blue. The marked displacement of the pressure curve is the time of thyroid cartilage movement.

In order to measure autonomic responses of arousal during swallowing, skin conductance responses (SCR; [30,44]) were recorded by placing two Ag/AgCl electrodes on the distal phalanges of the index and middle finger of the dominant hand as recently done in a previous study [40]. Skin conductance as a measure of distress and effort has been described in two recent studies ([41,56,57]), which report an increased BOLD-effect in motor areas during more challenging tasks [41,66]. SCR-data were recorded using BrainAmp Analyzer 2.0 (Brain Products, Gilching, Germany).

## 2.3. Physiological data processing

Laryngeal movement data was recorded and transformed using an electro-optical biosignal recorder (Varioport-b). The time between the visual color cue and peak thyroid cartilage movement after each swallow was singled out using MATLAB R2011a (MathWorks, Natick, MA, USA). Extracted data of swallowing latency was compared in young and old participants using a student's *t*-test.

SCRs were preprocessed using BrainAmp Analyzer 2.0 (Brain Products, Gilching, Germany). Data were artifact corrected, down-sampled to 100 Hz, low-pass filtered with a cutoff frequency of 40 Hz, and exported to a MATLAB-compatible file. SCRs were analyzed using the Ledalab toolkit [5] in MATLAB through a deconvolution approach. The signal was separated into tonic and phasic activity. The scoring method was the average phasic driver within the response window, providing the most accurate representation of phasic activity given in  $\mu$ s. Mean SCRs were computed for each subject. A student's *t*-test assessed the difference in SCR between young and old participants. In addition, a linear correlation was calculated between age of participant, swallowing latency and mean SCR.

## 2.4. MRI data acquisition

MRI data were acquired on a 3 T MRI scanner (Siemens Verio, Erlangen, Germany) using a 32-channel head coil. Functional and structural images were recorded. Field homogeneity was optimized by a shimming sequence and a gradient echo sequence (34 phase and magnitude images, 34 slices,  $2 \text{ mm} \times 2 \text{ mm} \times 2 \text{ mm}$ , field of view [FoV] 192 mm, repetition time (TR) 488 ms, echo time (TE)<sub>1</sub> 4.92 ms, TE<sub>2</sub> 7.38 ms, flip angle ( $\alpha$ ) 60°) was acquired to calculate a field map aiming at correcting geometric distortions in the echo planar images (EPI). Functional EPI images (TR 2 s, TE 22 ms, FoV 192 mm, slice spacing 2.5 mm, matrix 96 × 96,  $\alpha=90^\circ$ , voxel size  $2 \text{ mm} \times 2 \text{ mm} \times 2.5 \text{ mm}$ ) were sliced in an oblique direction in order to ensure coverage of brain areas involved in

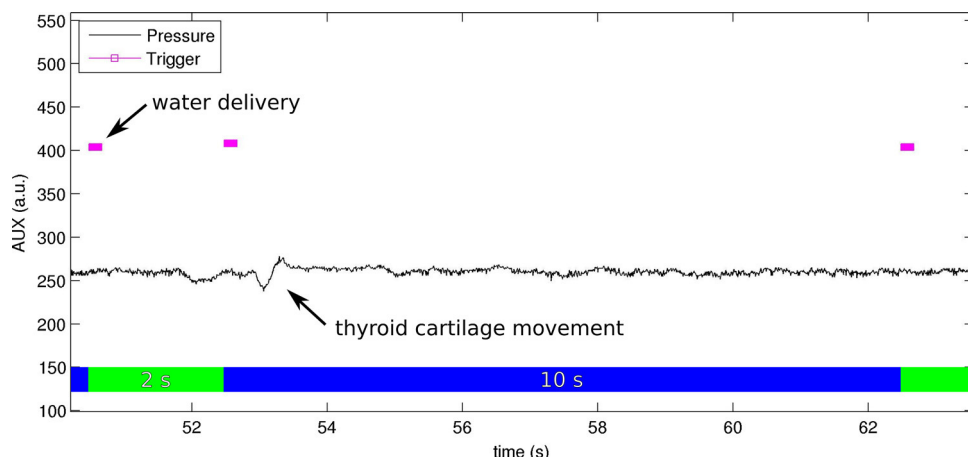


**Fig. 2.** Thyroid cartilage movement Single subject measurement of a representative air pressure change as a direct result of thyroid cartilage movement during swallowing. The first trigger point marks the color change from blue to green and the water injection time. At the second trigger point the color reverts back to blue. The pressure signal shows a displacement approximately 2.5 s after water delivery marking the time of thyroid cartilage movement.

sensorimotor processing, cerebellum and brainstem. A structural T1-weighted anatomical image was measured for each subject (magnetization-prepared rapid gradient echo, TR 1690 ms, TE 2.52 ms,  $\alpha = 9^\circ$ , FoV 250 mm, voxel size 1 mm  $\times$  1 mm  $\times$  1 mm, parallel acquisition using a k-space based algorithm [GRAPPA] factor 2, matrix 256  $\times$  256, distance factor 50%, transversal orientation, 176 slices, ascending). To ensure synchronization of all data acquisition modalities (fMRI, thyroid cartilage movement and SCR) trigger signals attuned to fMRI scans were recorded for the color change onset.

## 2.5. Preprocessing of MRI data

Preprocessing of fMRI data was done in SPM8 rev. 5236 (Wellcome Department of Imaging Neuroscience, London, UK) running on MATLAB R2011a. To reduce the influence of head motion related artifacts, a threshold of 2 mm translational motion was chosen. None of the subjects exceeded this threshold. Head motion was corrected with SPM8's Realign and Unwarp via a third degree b-spline interpolation using the first scan of the series as reference. Unwarping of susceptibility by movement interaction was done with the help of a voxel displacement map calculated from the field map data. Each subject's structural T1 image was coregistered using normalized mutual information from the last step to the mean EPI image. T1 images were segmented into gray and white matter, bias corrected and spatially normalized using the New Segment function of SPM8. A template normalized image was created with the help of the DARTEL toolbox [2] and the segmented gray and white matter images from all 51 subjects, using Linear Elastic Energy regularization. This image was then normalized to Montreal Neurological Institute (MNI) space using DARTEL's Normalize to MNI Space function with the flow fields of the previous step. The same procedure was used to normalize the functional and structural images of every participant. The normalized T1 images were averaged to acquire a structural image representative of the group. Normalized functional images were smoothed using SPM8's smoothing function with a Gaussian kernel of 6 mm  $\times$  6 mm  $\times$  6 mm full-width at half-maximum to increase the signal to noise ratio and reduce inter-subject differences. A 6 mm<sup>3</sup> smoothing isovoxel was used as it provides a signal-to-noise ratio increase without significant smearing across adjacent brain regions [4]. Furthermore, the same smoothing kernel was used in our two previous studies [39,40] facilitating comparisons across studies.

## 2.6. Statistical analysis of fMRI data

Two different statistical analysis methods were employed in analyzing the functional swallowing data sets. Both were based on the general linear model (GLM) as implemented in SPM8. The first method uses the classical statistical approach – the default way of analyzing functional data in SPM8. The second method uses Bayesian inference.

The justification to use two statistical analysis methods is that the classical approach is more conservative but less sensitive while Bayesian inference is more specific. The classical approach is more conservative due to the severe correction for multiple comparisons, which renders the inference relatively insensitive. Bayesian inference is generally much more specific than classical inference and avoids the multiple comparison problem altogether [19]. For details on the difference between classical and Bayesian inference please refer to the supplementary material.

## 2.7. Classical inference

Smoothed data were entered into the GLM. Low frequency components were filtered with a high-pass filter having a cutoff of 128 s. BOLD responses were modeled using SPM's canonical basis set: the hemodynamic response function (HRF) and its temporal derivative (1st order). Onsets were modeled for each swallow and chosen to correspond to the water injection time (queued by color change) based on results from previous work [39,40]. In short, the BOLD responses were in alignment with the color change and not with the thyroid cartilage movement [39]. This stems from the complicated nature of the swallow, which consists of a multitude of actions, and is not solely characterized by a movement of thyroid cartilage. Swallows which did not correspond to the standard onsets, as reflected in the thyroid cartilage movement data, were modeled with the canonical HRF and included as regressors of no interest in the design matrix. Every swallow causes head movement which is moderately correlated with the stimulus [26]. Even though head motion and susceptibility-distortion-by-movement-interaction was corrected using the Realign and Unwarp step [1], we chose a more conservative approach to ensure the smallest impact of head motion on the data. Thus, motion parameters from the realignment procedure were used as regressors of no interest in the design matrix. The autocorrelation inherent in the data was estimated by an autoregressive AR(1) model. An explicit mask provided by SPM8 (brainmask.nii) was used to exclude inference on

voxels outside the brain. Model parameters were estimated using Restricted Maximum Likelihood.

Contrasts (swallowing > baseline) were computed for each subject for the swallow onset. To make inferences about the population a random effects two-sample *t*-test was calculated: the first sample measured swallowing activation in young subjects; the second measured swallowing activation in senior subjects. In addition, SCRs were used as covariates in a regression analysis for old and young subjects separately. We also applied swallowing latency as a covariate. All contrasts were computed using a family-wise error-corrected (FWE,  $p < 0.05$ ) threshold. Activation maxima (MNI coordinates, *t*-value, cluster size) for the *old SCR* and *young SCR* contrasts were extracted using masks created with the Anatomy Toolbox [16].

### 2.8. Bayesian inference

Non-smoothed data were entered into the GLM [47] using unweighted Graph Laplacian as signal priors and block type partitioning into slices. The autocorrelation inherent in the data was estimated by an autoregressive AR(3) model. Low frequency components were filtered with a high-pass filter having a cutoff of 128 s. BOLD responses were modeled using SPM's canonical basis set as described in the classical approach. The same onsets, regressors of no interest, and brain mask were used as in the classical approach. Approximate posteriors were computed using variational Bayes, which delivers a factorized, minimum Kulback–Liebler divergence approximation to the true posterior density [47].

Posterior probability maps (PPMs) were computed for each subject for the swallow onset. Probabilistic empirical Bayes was used to calculate the conditional distribution for the parameter estimates across subjects at each voxel, by employing the contrasts from the first level. Activation maxima (MNI coordinates, *t*-value, cluster size) for the *old SCR* and *young SCR* contrasts were extracted using masks created with the Anatomy Toolbox [16] as well as with WFU Pick Atlas [35].

## 3. Results

### 3.1. Statistical parametric maps – classical inference

During swallowing senior participants showed activation in the bilateral primary motor and somatosensory cortex (MS1), secondary somatosensory cortex (parietal operculum, S2), pre-motor cortex (PMC), supplementary motor area (SMA), Broca's area and Broca's analogon, pars opercularis, insula, thalamus, caudate nucleus, pallidum, putamen, pons in the region of the trigeminal nerve and the nucleus tractus solitarius (NTS), cerebellar hemisphere I–VIIa and vermis, bilateral hippocampus and in the right amygdala, anterior cingulate cortex (ACC), visual cortex, inferior parietal cortex, intraparietal sulcus, superior parietal lobules, middle and inferior temporal gyrus and auditory cortex.

Activation occurred in comparable regions for younger participants with additional activation in the left medial cingulate cortex (MCC) and right posterior cingulate cortex.

When comparing neural representation maps during swallowing between both groups using a two-sample *t*-test, no significant differences were found (FWE,  $p < 0.05$ ). This holds true even when applying an uncorrected approach ( $p < 0.001$ , uncorr. for multiple comparisons) or by using small volume corrections. This strengthens the interpretation that a true lack of difference exists in activation patterns between young and old swallowers.

### 3.2. Posterior probability maps – Bayesian inference

Regarding the analysis of the senior participants' data with Bayesian statistics, we found in addition to the above stated areas activation in the ACC and bilaterally in the cerebellar hemisphere I–IX, i.e. additional activation in lobules VIII and IX and in the vermis lobules VIII–X. In the representational maps of the group of young participants, additional bilateral activation in the cerebellum lobules VIII and IX was found. When comparing both subject groups with a two-sample *t*-test, seniors showed increased bilateral activation in BA10 corresponding to the frontal pole 1 (Fp1) [6]. In the young cohort no such activation was found.

### 3.3. Correlation analyses – SPMs – classical inference

The correlation of BOLD-magnitude with age (*Swallowing activation over young subjects* and *Swallowing activation over senior subjects*) did not show any significant results.

Furthermore, no significant activations were found when testing an association between BOLD-magnitude during swallowing and SCR in young subjects. This also holds true for an association between BOLD-magnitude and swallowing latency across groups.

However, correlation analysis of BOLD-magnitude during swallowing and SCR in seniors resulted in significant voxels for the left SMA, left superior temporal gyrus and right Broca's analogon (BA45) (see Table 1).

### 3.4. Correlation analyses – PPMs – Bayesian inference

Correlating the BOLD-magnitude with age did not show any significant results. Also, no association between BOLD-magnitude and swallowing performance, in form of swallowing latency, was found. Moreover, there were no significant associations between BOLD-magnitude during swallowing and SCR in young subjects. However, SCR and BOLD-magnitude during swallowing in seniors were positively associated in bilateral MS1, left S2, bilateral SMA, ACC and MCC, left BA44 and BA45, left hippocampus, left insula and in the dorsolateral pons in the region of the ascending reticular activating system (AAS) (see Table 1, Fig. 4).

### 3.5. Behavioral data

Senior participants needed additional time to swallow than younger participants ( $t(39)=4.69$ ,  $p < 0.001$ ). For the seniors the average time between the visual cue and the thyroid cartilage movement was  $3.42 \pm 0.53$  s compared to  $2.60 \pm 0.40$  s in the younger group. Both values contain the water delivery latency of 1 s.

### 3.6. Skin conductance response

SCRs were larger in seniors (averaged to  $0.148 \pm 0.126$   $\mu$ S) than in younger participants ( $0.073 \pm 0.068$   $\mu$ S;  $t(47)=2.46$ ,  $p < 0.05$ ). At the beginning of each scan SCRs showed a drastic tonic change with phasic peaks correlated with onset light changes. Within the run, tonic and phasic activity diminished as part of the subject's adjustment to the scanner's noise and the swallowing task (as depicted in Fig. 3). The systematic decrease of SCR with an increasing number of stimuli of the same mode, such as swallowing, has already been described earlier [30]. High initial arousal activity through scanner noise and concentration on task may subside over time [40].

### 3.7. Correlation analysis of SCR, performance and age

Since the age range from 55 to 75 years for the seniors was wide, we performed a linear correlation analysis of age and SCR,

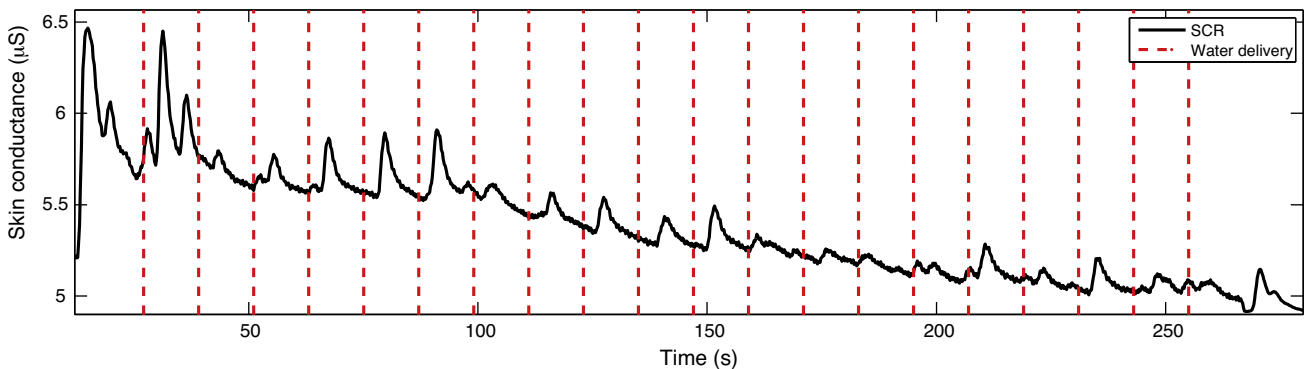


**Fig. 3.** Skin conductance response. SCR curve of a single subject from the elderly group during swallowing. The vertical lines indicate water delivery followed immediately by a swallow. The high initial values arise from the sudden onset of scanner noise initiating a startle response, which subsides as the experiment continues, and the subject adjusts to the noise and task. After each water delivery there is a clear SCR. This response is overwhelmingly underrepresented in the young patient group. For a comparison refer to [40].

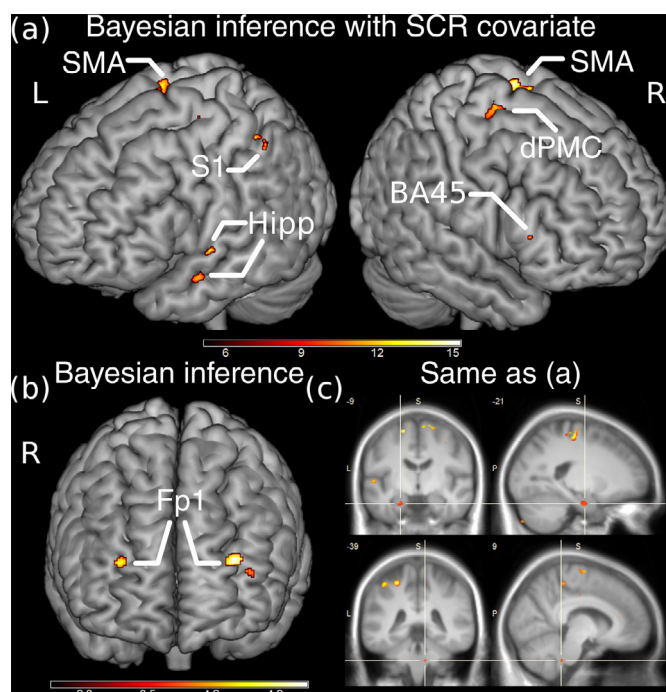


**Fig. 4.** Cortical activation during swallowing. BOLD-magnitude during swallowing correlated positively with skin conductance responses. (a) Posterior probability maps (PPM) calculated using Bayesian inference ( $p > 95\%$ ) displayed on a 3-dimensional rendered brain. Activation is shown in primary somatosensory cortex (S1), bilateral supplementary motor area (SMA), dorsolateral premotor cortex (dPMC), left Brodmann Area (BA) 45, and Hippocampus (Hipp). Although the hippocampal activation should be below the cortical surface, the rendering was chosen to depict it on the surface. (b) PPM for the contrast swallowing: old vs. young showing with 95% probability that the activation in the bilateral Fp1 of BA 10 is greater than the prior standard deviation. (c) Same PPM as in (a) overlaid on top of the mean normalized T1 image from the 51 participants showing the coronal (left) and sagittal (right) sections. The top images display the activation in the pons possibly corresponding to the ascending reticular activation system (AAS). The bottom images display activation in the hippocampus.

age and swallowing latency, and SCR and swallowing latency in the older cohort. The regression analysis between age and SCR in seniors revealed no significant associations ( $r^2 = 0.09$ ; n.s.). Non-significant correlations were also found for age and swallowing latency ( $r^2 = 0.02$ ; n.s.) and SCR and swallowing latency ( $r^2 = 0.0002$ ; n.s.) in seniors.

Testing for SCR and swallowing latency across groups (young and old), resulted in no significant correlation ( $r^2 = 0.015$ ; n.s.).

#### 4. Discussion

To investigate possible differences between fMRI-representation of swallowing, we applied two different statistical approaches to a significant group sample of senior and young participants. In addition, we controlled performance and SCR which is associated with arousal [30,44]. We sought to differentiate patterns of activation in relation to these factors. A classical statistical approach revealed no differences in neural activation maps during swallowing between groups even when applying an uncorrected approach. Bayesian inference was more sensitive, identifying additional bilateral activation in Fp1 of BA 10 as part of working memory [6,21] when using a two sampled *t*-test of elderly vs. young adults. Within the young group, no associations of BOLD-magnitude and SCR or BOLD-magnitude and swallowing latency was found. Swallowing latency was delayed in seniors but not associated with BOLD-magnitude. Arousal as measured by SCR seemed to be a relevant factor in the recruitment of cortical areas associated with planning and integrating sensorimotor tasks as well as emotional processing during task performance in some seniors when examining the positive association of SCR with BOLD-magnitude in our study.

##### 4.1. General considerations on cortical activation during swallowing

We found activation in several cortical and subcortical areas in both young and senior subjects in line with findings of other functional imaging studies on swallowing [17,23,26,34,36,37,40,43,58]. We also found additional activation bilaterally in the cerebellum which has been described before [32,34,42,56,57]. Furthermore, there were activations in the pons as described recently [40]. In order to prevent spontaneous swallows to influence the experimental results, they were accounted for as regressors of no interest in the design matrix. This ensures a robust analysis without the influence of unwanted activations.

##### 4.2. Group comparisons: increased prefrontal activation

Our data support previous findings between neural swallowing representation of seniors and young subjects [33]. In line with this study and contrary to other swallowing studies with a small sample size [26,34,36], there were no differences in the comparison of activation in the swallowing network across groups, when applying classical inference even with an uncorrected approach and a more liberal activation threshold. Different experimental and methodological designs described in detail within the

**Table 1**

Coordinates of highest activation for seniors correlated with SCR.

Area (Brodmann's Area)	<i>k</i>	<i>T</i>	<i>x</i>	<i>y</i>	<i>z</i>
<i>SPM (frequentist inference)</i>					
L SMA (BA 6)	5	7.20	-42	-10	53
L Superior temporal gyrus	7	6.94	-53	-5	-1
R Broca's analogon (BA45 pars triangularis)	10	7.34	45	16	27
<i>PPM (Bayesian inference)</i>					
L M1 (BA 4)	228	<i>P</i>			
		13.94	-17	-28	63
		13.21	-26	-34	56
		13.05	-20	-24	57
		10	11.93	-35	56
		9	10.87	-35	53
R M1 (BA 4)	1	11.75	20	-27	69
	11	11.59	9	-36	56
	6	11.58	24	-24	53
	3	11.40	33	-33	57
	1	10.58	20	-25	56
	1	10.33	23	-33	62
	6	10.28	37	-15	51
	5	10.26	2	-30	62
L S1 (BA 1,2,3)	209	14.95	-26	-37	56
		14.42	-41	-37	54
	16	11.37	-33	-33	44
	5	10.31	-38	-25	53
R S1 (BA 1,2,3)	8	11.30	33	-33	59
	5	11.01	11	-37	56
	11	10.99	23	-33	60
L S2	8	12.81	-51	-4	0
L + R SMA	23	15.25	18	-25	72
	56	14.84	-8	-18	72
		12.62	-11	-10	71
	25	14.22	-18	-9	63
	237	14.05	15	-12	71
		13.23	5	-10	69
		11.26	25	-13	68
	70	13.99	24	-22	56
	85	13.30	-20	-22	59
	6	12.97	-14	-27	62
	3	12.24	-21	-27	62
	11	12.02	-6	-25	56
	20	11.72	36	-12	50
	12	11.27	-6	-15	62
	4	10.43	31	-19	54
	1	9.51	-24	-24	51
L Broca pars opercularis (BA 44/45)	9	12.57	-48	9	23
R Broca pars opercularis (BA 44/45)	3	10.63	-47	23	11
	2	11.24	52	27	12
ACC	4	11.35	11	36	17
MCC	7	11.40	9	-37	54
	4	10.40	8	8	41
L Hippocampus	121	14.27	-53	-3	-1
	48	11.97	-51	-19	5
	56	11.68	-53	0	-16
	10	11.02	-50	-25	9
	1	9.75	-24	-10	-27
	1	9.74	-62	3	-13
L Insula	2	10.81	-50	-3	0
Pons	8	10.21	9	-37	-40

Top row shows statistical parametric mapping (SPM) coordinates. All results are  $p < 0.05$ , family-wise error corrected. Posterior probability mapping (PPM) coordinates with posterior expectation of 95% confidence (*P*). MN1: Montreal Neurological Institute, *t*-value (*T*), and number of activated voxels in the cluster (*k*) of the highest activated voxel for cortical activation in seniors correlated with SCR. L: left; R: right; BA: Brodmann's Area; M1: primary motor cortex; S1: primary somatosensory cortex; S2: secondary somatosensory cortex; SMA: supplementary motor area; ACC: anterior cingulate cortex; MCC: medial cingulate cortex.

introduction (use of quantity of water, age range, statistical analysis methods) might account for the inconsistent results. Also, the inclusion of the motion parameters as regressors of no interest may remove some of the expected variance in the data. This is due to the task correlated movement. Here we needed to balance

loss of sensitivity and task specificity (arising from task correlated movement) with expected true activations. We chose the more conservative approach, i.e. removal of susceptibility-distortion-by-movement-interaction through the realign and unwarp step [1] in the pre-processing pipeline, and inclusion of the estimated motion parameters as regressors of no interest. This choice might also be responsible for a lack of neural activation difference between seniors and young participants, as the inclusion of the motion parameters reduces the degrees of freedom.

Bayesian inference was more sensitive and found additional activated areas not seen using the classical frequentist approach. We found activation in BA 10, particularly Fp1, comparing old and young participants, a finding echoing increase of activation in seniors independent on the task performed [24,28,38,51,65]. As part of the prefrontal lobe, BA 10 is associated with attention and working memory retrieval [21]. Specifically, Fp1 may be an important substrate for organized behavior, planning of actions and managing multiple goals based on both episodic and short-term memory information [6]. It suggests that older participants utilized additional attention in swallowing performance as seen in other motor tasks [24,28].

#### 4.3. Swallowing latency

In line with other studies, seniors showed prolonged swallowing latency. In seniors, a later onset of pharyngeal activity has been described [9,52,61] and has been associated with age-related decline of muscle tissue [7]. In addition, recent functional imaging studies on swallowing reported age-related increase in swallowing latency [34]. At the same time, a prolonged swallowing latency does not seem to impede swallowing representation on the cortical level. This delay most likely implies a longer time spent in the transport phase, hence a longer time to trigger a pharyngeal swallow. Older participants may have applied more effort and concentration in the oral transport phase in order to reduce the chance of choking. This is reflected in the measured SCR. Moreover, the Fp1 activation suggests higher concentration on the task.

#### 4.4. Higher skin conductance response in elderly

In our study, SCR was significantly larger in the senior group reflecting higher arousal and possibly illustrating an increased attentional demand to perform the task of swallowing. A linear association between SCR and the intensity of negative emotional stimuli has been described in a recent study [20], suggesting that seniors with higher SCR experienced more negative emotions during the swallowing task. It matches unsystematic statements of some seniors in our study mentioning anxiousness of choking while lying in the scanner, whereas young participants did not express any such concern. Also, Croft et al. [13] reported in their study on autonomic responses to public speaking anxiety a relation between skin conductance response and experience of anxiety. In our case, it might also be reasonable and understandable that some older participants felt more anxious about lying in a supine position given the fact that laryngeal penetration while swallowing can occur more frequently in the healthy older population than in younger ones [8]. Swallowing in a supine position is rather unnatural and more difficult than in an upright position. Taking this into account, when interpreting differences in swallowing latency, motor planning, and attention, one has to be careful in giving too much importance to a longer swallowing latency and increased activation in motor planning. Thus anxiety and increased task requirements might primarily explain group differences.

#### 4.5. Higher arousal due to higher motor planning, emotional perception and attentional demand of swallowing

Although SCRs were significantly higher for seniors, they were not significantly associated with age. However, activation magnitude during swallowing of the older cohort was positively associated with SCR, suggesting an individual and not an age-related interpretation of our results. This finding resulted in the following conclusions. Firstly, association of premotor and sensorimotor areas with higher SCR may suggest additional recruitment of cortical areas for planning, preparation, and performance of the complex motor task of swallowing; it may be linked to attentional arousal [25,50]. This is consistent with other studies describing an increased BOLD-effect in motor areas with increased task challenge [41,66]. Secondly, supplementary activation in the pons, insula, ACC, MCC and hippocampus may indicate higher arousal and higher attention due to a seemingly more exertive task, emotional processing, and additional task memorization compared to other seniors with no increased SCR scores. Pons activation has been described as important in the excitation process of electrodermal activity [50]. This is also supported by studies in patients with pons and ACC lesions that show selective loss of SCR [50,62]. In our case, the localization of the activated region in the pons seemed to be in line with the ascending reticular activating system (ARAS) that has been described to be important for general arousal [14]. Concerning ACC activation, it has also been described as an integrative area of cognitive processes and autonomic arousal represented by higher electrodermal activity with an association of cognitive demand in tasks demanding attention [12,48]. Cognitive processes such as recalling task instructions might also explain the hippocampal activation of elderly with higher SCR since the hippocampus is crucial for memorizing function [59]. Furthermore, activation of insula and co-activation with the dorsal ACC has been described as characteristic for visceral arousal combined with attentional engagement as well as perception and awareness of emotions [11,12] such as anxiety [46]. Taking all these findings together, the recruitment of ACC, MCC, insula, and hippocampus, as seen in our study, may imply that those seniors with higher SCR demonstrated more attentional arousal accompanied by an emotional valence of swallowing, and a repeated recall of task instructions. Additionally, they may have found the swallowing task more demanding and exertive to fulfill, integrate and coordinate.

#### 4.6. Study limitations

Since our studied seniors were relatively healthy and showed a high level of social and athletic activity, there might be a healthy-bias effect in our study. In future studies it is advisable to include the status of physical activity for each subject to better interpret the results. Moreover, it might be possible that the participants' performance was better than that of the general age matched population not included in the study due to disease and disability. The age range of the senior group was chosen to facilitate comparison between groups in a future study of dysphagic patients after stroke. The expected age of dysphagia patients is 59 years [49] with an expected range of 55–75 years. Furthermore, after the age of 75 people tend to become increasingly frail [63]. Also, it may be difficult to compare our relatively younger sample of elderly with those in previously published studies on swallowing. Because our senior group was comparably younger, it is possible that age effects occur later, e.g. upwards of 70 years. Hence, a more heterogeneous and older sample of participants should be recruited in the future. Secondly, it would be advisable to standardize the water bolus volume for all fMRI experiments, since different quantities of water have been used in previous studies by different research groups, making it more difficult to compare findings. In addition

to the screening questionnaire, an objective sensory and motor test of tongue movement and swallowing performance should also be administered to each participant prior to the experiment. This ensures that participants swallow normally at baseline. Additionally, as stated above, some senior participants expressed fear and extra effort needed to swallow. It is important to better distinguish the source of arousal for seniors with higher skin conductance responses. In future studies, a more objective questionnaire or a visual analog scale regarding perceived attentional demand and emotion should be implemented. This may further explain the neural representation of arousal and may differentiate the emotional perception during swallowing in elderly.

In this experiment the inter-trial intervals did not differ in length so as to prevent an anticipatory effect. The subjects were queued by a color change (from blue to green) which also represents the water delivery time. In this sense, the subjects anticipated the next swallow and a randomization of the trials was unnecessary. Further, activation in each subject group (young and old) was described extensively in the Results section. This widespread activation in expected regions (somatosensory, motor, insula, cerebellum, etc.) found in the literature (and detailed in the introduction) underlines the robustness of the experiment. Likewise, both groups performed the same experiment, and any effect due to expected water delivery would be accounted for in the comparison between groups.

In general, one must exercise caution when analyzing brainstem responses using fMRI. Cardiac or respiratory effects are strongest in subcortical regions, particularly the brainstem; however, they are correlated with the position of blood vessels on the surface of the medulla and the pons outside the brain tissue or on the boundaries of the cerebrospinal fluid [10]. Since our data does not exhibit activations in such regions, we can assume that brainstem BOLD-effects are task related. Furthermore, the location of brainstem activations reported here seem anatomically consistent with results on deglutition from microelectrode recordings [29]. Nonetheless, in future brainstem studies, it is highly advisable to measure and include cardiac and respiratory responses as effects of no interest in the design matrix.

## 5. Conclusion

In summary, only the Bayesian approach found a functional activation difference in old vs. young participants in a swallowing task. This activation was limited to the bilateral Frontal pole 1 of BA 10, and can be interpreted as an increased task-dependent attention in the older group. Furthermore, these results seem to show that neuronal processing of swallowing remains intact as people age. They also stress the importance and validity of Bayesian inference compared to the classical-frequentist approach. Additionally, we found a prolonged swallowing latency as well as a significantly higher skin conductance in seniors compared to young participants. Seniors with a higher measure of skin conductance showed cortical activation in areas associated with sensorimotor performance, arousal and emotion, possibly suggesting increased attention and emotional demands during the task.

## Conflict of interest

All authors confirm that they have no financial, actual or potential conflicts of interest that could inappropriately influence or bias this work.

## Acknowledgements

This study was supported by the Deutsche Forschungsgemeinschaft (DFG, LO 795-12). The authors would like to thank Ulrike

Horn for lending her artistic talent toward an illustration included in this manuscript, and Gretchen Adele Ferber for the valuable feedback regarding the language aspect.

## Appendix A. Supplementary data

Supplementary data associated with this article can be found, in the online version, at <http://dx.doi.org/10.1016/j.bbr.2015.03.009>.

## References

- [1] Andersson JL, Hutton C, Ashburner J, Turner R, Friston K. Modeling geometric deformations in EPI time series. *Neuroimage* 2001;13(5):903–19, <http://dx.doi.org/10.1006/nimg.2001.0746>.
- [2] Ashburner J. A fast diffeomorphic image registration algorithm. *Neuroimage* 2007;38:95–113, <http://dx.doi.org/10.1016/j.neuroimage.2007.07.007>.
- [3] Aviv JE. Effects of aging on sensitivity of the pharyngeal and supraglottic areas in. *Am J Med* 1997;103:745–63.
- [4] Ball T, Breckel TPK, Mutschler I, Aertsen A, Schulze-Bonhage A, Hennig J, et al. Variability of fMRI-response patterns at different spatial observation scales. *Hum Brain Mapp* 2012;33:1155–71.
- [5] Benedek M, Kaernbach C. A continuous measure of phasic electrodermal activity. *J Neurosci Methods* 2010;190:80–91, <http://dx.doi.org/10.1016/j.jneumeth.2010.04.028>.
- [6] Bludau S, Eickhoff SB, Mohlberg H, Caspers S, Laird AR, Fox PT, et al. Cytoarchitecture, probability maps and functions of the human frontal pole. *Neuroimage* 2014;93(Pt 2):260–75, <http://dx.doi.org/10.1016/j.neuroimage.2013.05.052>.
- [7] Brooks SV, Faulkner JA. Skeletal muscle weakness in old age: underlying mechanisms. *Med Sci Sports Exerc* 1994;26:432–9.
- [8] Butler SG, Stuart A, Leng X, Wilhelm E, Rees C, Williamson J, et al. The relationship of aspiration status with tongue and handgrip strength in healthy older adults. *J Gerontol A Biol Sci Med Sci* 2011;66:452–8, <http://dx.doi.org/10.1093/gerona/gllq234>.
- [9] Cook IJ, Weltman MD, Wallace K, Shaw DW, McKay E, Smart RC, et al. Influence of aging on oral-pharyngeal bolus transit and clearance during swallowing: scintigraphic study. *Am J Physiol* 1994;266:G972–7.
- [10] Corfield DR, Murphy K, Josephs O, Fink GR, Frackowiak RS, Guz A, et al. Cortical and subcortical control of tongue movement in humans: a functional neuroimaging study using fMRI. *J Appl Physiol* 1999 (Bethesda, Md.: 1985).
- [11] Craig ADB. How do you feel – now? The anterior insula and human awareness. *Nat Rev Neurosci* 2009;10:59–70, <http://dx.doi.org/10.1038/nrn2555>.
- [12] Critchley HD. Neural mechanisms of autonomic, affective, and cognitive integration. *J Comp Neurol* 2005;154–66, <http://dx.doi.org/10.1002/cne.20749>.
- [13] Croft RJ, Gonsalvez CJ, Gander J, Lechem L, Barry RJ. Differential relations between heart rate and skin conductance, and public speaking anxiety. *J Behav Ther Exp Psychiatry* 2004;35:259–71.
- [14] Dänälä L, Pascu ML. Clinical Management and Evolving Novel Therapeutic Strategies for Patients with Brain Tumors. InTech 2013, <http://dx.doi.org/10.5772/45956>.
- [15] Daniels SK, Corey DM, Hadskey LD, Legendre C, Priestly DH, Rosenbek JC, et al. Mechanism of sequential swallowing during straw drinking in healthy young and older adults. *J Speech Lang Hear Res* 2004;47:33–45.
- [16] Eickhoff SB, Stephan KE, Mohlberg H, Grefkes C, Fink GR, Amunts K, et al. A new SPM toolbox for combining probabilistic cytoarchitectonic maps and functional imaging data. *Neuroimage* 2005;25:1325–35, <http://dx.doi.org/10.1016/j.neuroimage.2004.12.034>.
- [17] Ertekin C, Aydogdu I. Neurophysiology of swallowing. *Clin Neurophysiol* 2003;114:2226–44, [http://dx.doi.org/10.1016/S1388-2457\(03\)00237-2](http://dx.doi.org/10.1016/S1388-2457(03)00237-2).
- [18] Feng X, Todd T, Lintzenich CR, Ding J, Carr JJ, Ge Y, et al. Aging-related geniohyoid muscle atrophy is related to aspiration status in healthy older adults. *J Gerontol A Biol Sci Med Sci* 2013;68:853–60, <http://dx.doi.org/10.1093/gerona/gls225>.
- [19] Friston KJ, Penny W. Posterior probability maps and SPMs. *Neuroimage* 2003;19:1240–9, [http://dx.doi.org/10.1016/S1053-8119\(03\)00144-7](http://dx.doi.org/10.1016/S1053-8119(03)00144-7).
- [20] Fusar-Poli P, Landi P, O'Connor C. Neurophysiological response to emotional faces with increasing intensity of fear: a skin conductance response study. *J Clin Neurosci* 2009;16:981–2, <http://dx.doi.org/10.1016/j.jocn.2008.09.022>.
- [21] Gilbert SJ, Spengler S, Simons JS, Steele JD, Lawrie SM, Frith CD, et al. Functional specialization within rostral prefrontal cortex (area 10): a meta-analysis. *J Cogn Neurosci* 2006;18:932–48, <http://dx.doi.org/10.1162/jocn.2006.18.6.932>.
- [22] Hamdy S, Aziz Q, Thompson DG, Rothwell JC. Physiology and pathophysiology of the swallowing area of human motor cortex. *Neural Plast* 2001;8:91–7, <http://dx.doi.org/10.1155/NP.2001.91>.
- [23] Hamdy S, Rothwell JC, Aziz Q, Thompson DG. Organization and reorganization of human swallowing motor cortex: implications for recovery after stroke. *Clin Sci (Lond)* 2000;99:151–7.
- [24] Heuninckx S, Wenderoth N, Debaere F, Peeters R, Swinnen SP. Neural basis of aging: the penetration of cognition into action control. *J Neurosci* 2005;25:6787–96, <http://dx.doi.org/10.1523/JNEUROSCI.1263-05.2005>.
- [25] Howells FM, Stein DJ, Russell VA. Perceived mental effort correlates with changes in tonic arousal during attentional tasks. *Behav Brain Funct* 2010;6:39, <http://dx.doi.org/10.1186/1744-9081-6-39>.
- [26] Humbert IA, Fitzgerald ME, McLaren DG, Johnson S, Kosmatka K, Hind J, et al. Neurophysiology of swallowing: effects of age and bolus type. *Neuroimage* 2009;44:982–91, <http://dx.doi.org/10.1016/j.neuroimage.2008.10.012>.
- [27] Humbert IA, Robbins J. Dysphagia in the elderly. *Phys Med Rehabil Clin N Am* 2008;19(November (4)), <http://dx.doi.org/10.1016/j.pmr.2008.06.002>, 853–x.
- [28] Hutchinson S. Age-related differences in movement representation. *Neuroimage* 2002;17:1720–8, <http://dx.doi.org/10.1006/nimg.2002.1309>.
- [29] Jean A. Brain stem control of swallowing: neuronal network and cellular mechanisms. *Physiol Rev* 2001;81:929–69.
- [30] Lim C, Seto-Poon M, Clouston P, Morris JG. Sudomotor nerve conduction velocity and central processing time of the skin conductance response. *Clin Neurophysiol* 2003;114:2172–80, [http://dx.doi.org/10.1016/S1388-2457\(03\)00204-9](http://dx.doi.org/10.1016/S1388-2457(03)00204-9).
- [31] Loibl M, Beutling W, Kaza E, Lotze M. Non-effective increase of fMRI-activation for motor performance in elder individuals. *Behav Brain Res* 2011;223:280–6, <http://dx.doi.org/10.1016/j.bbr.2011.04.040>.
- [32] Lowell SY, Poletto CJ, Knorr-Chung BR, Reynolds RC, Simonyan K, Ludlow CL. Sensory stimulation activates both motor and sensory components of the swallowing system. *Neuroimage* 2008;42:285–95, <http://dx.doi.org/10.1016/j.neuroimage.2008.04.234>.
- [33] Malandraki GA, Perlman AL, Karampinos DC, Sutton BP. Reduced somatosensory activations in swallowing with age. *Hum Brain Mapp* 2011;32:730–43, <http://dx.doi.org/10.1002/hbm.21062>.
- [34] Malandraki GA, Sutton BP, Perlman AL, Karampinos DC. Age-related differences in laterality of cortical activations in swallowing. *Dysphagia* 2010;25:238–49, <http://dx.doi.org/10.1007/s00455-009-9250-z>.
- [35] Maldjian JA, Laurienti PJ, Kraft RA, Burdette JH. An automated method for neuroanatomic and cytoarchitectonic atlas-based interrogation of fMRI data sets. *Neuroimage* 2003;19:1233–9.
- [36] Martin R, Barr A, MacIntosh B, Smith R, Stevens T, Taves D, et al. Cerebral cortical processing of swallowing in older adults. *Exp Brain Res* 2007;176:12–22, <http://dx.doi.org/10.1007/s00221-006-0592-6>.
- [37] Martin RE, Goodyear BG, Gati JS, Menon RS. Cerebral cortical representation of automatic and volitional swallowing in humans. *J Neurophysiol* 2001;85:938–50.
- [38] Mattay VS, Fera F, Tessitore A, Hariri AR, Das S, Callicott JH, et al. Neurophysiological correlates of age-related changes in human motor function. *Neurology* 2002;58:630–5, <http://dx.doi.org/10.1212/WNL.58.4.630>.
- [39] Mihai PG, Otto M, Platz T, Eickhoff SB, Lotze M. Sequential evolution of cortical activity and effective connectivity of swallowing using fMRI. *Hum Brain Mapp* 2014;35:5962–73, <http://dx.doi.org/10.1002/hbm.22597>.
- [40] Mihai PG, von Bohlen Und Halbach O, Lotze M. Differentiation of cerebral representation of occlusion and swallowing with fMRI. *Am J Physiol Gastrointest Liver Physiol* 2013;304:847–54, <http://dx.doi.org/10.1152/ajplgi.00456.2012>.
- [41] Mochizuki G, Hoque T, Mraz R, Macintosh BJ, Graham SJ, Black SE, et al. Challenging the brain: exploring the link between effort and cortical activation. *Brain Res* 2009;1301:9–19, <http://dx.doi.org/10.1016/j.brainres.2009.09.005>.
- [42] Mosier K, Bereznaya I. Parallel cortical networks for volitional control of swallowing in humans. *Exp Brain Res* 2001;140:280–9, <http://dx.doi.org/10.1007/s002210100813>.
- [43] Mosier K, Patel R, Liu WC, Kalnin A, Maldjian J, Baredes S. Cortical representation of swallowing in normal adults: functional implications. *Laryngoscope* 1999;109:1417–23, <http://dx.doi.org/10.1097/00005537-199909000-00011>.
- [44] Nikula R. Psychological correlates of nonspecific skin conductance responses. *Psychophysiology* 1991;28:86–90.
- [45] Oldfield RC. The assessment and analysis of handedness: the Edinburgh inventory. *Neuropsychologia* 1971;9:97–113, [http://dx.doi.org/10.1016/0028-3932\(71\)90067-4](http://dx.doi.org/10.1016/0028-3932(71)90067-4).
- [46] Paulus MP, Stein MB. An insular view of anxiety. *Biol Psychiatry* 2006, <http://dx.doi.org/10.1016/j.biopsych.2006.03.042>.
- [47] Penny WD, Trujillo-Barreto NJ, Friston KJ. Bayesian fMRI time series analysis with spatial priors. *Neuroimage* 2005;24:350–62, <http://dx.doi.org/10.1016/j.neuroimage.2004.08.034>.
- [48] Phan KL, Wager T, Taylor SF, Liberzon I. Functional neuroanatomy of emotion: a meta-analysis of emotion activation studies in PET and fMRI. *Neuroimage* 2002;16:331–48, <http://dx.doi.org/10.1006/nimg.2002.1087>.
- [49] Prosiegel M, Heintze M, Wagner-Sonntag E, Hannig C, Wuttge-Hannig A, Yassouridis A. Deglutition disorders in neurological patients. A prospective study of diagnosis, pattern of impairment, therapy and outcome. *Nervenarzt* 2002;73:364–70.
- [50] Raine A, Reynolds GP, Sheard C. Neuroanatomical correlates of skin conductance orienting in normal humans: a magnetic resonance imaging study. *Psychophysiology* 1991;28:548–58.
- [51] Riecker A, Gröschel K, Ackermann H, Steinbrink C, Witte O, Kastrup A. Functional significance of age-related differences in motor activation patterns. *Neuroimage* 2006;32:1345–54, <http://dx.doi.org/10.1016/j.neuroimage.2006.05.021>.

- [52] Robbins J, Hamilton JW, Lof GL, Kempster GB. Oropharyngeal swallowing in normal adults of different ages. *Gastroenterology* 1992;103:823–9. S0016508592003846 [pii].
- [53] Roy N, Stemple J, Merrill RM, Thomas L. Dysphagia in the elderly: preliminary evidence of prevalence, risk factors, and socioemotional effects. *Ann Otol Rhinol Laryngol* 2007;116:858–65, doi:Article.
- [54] Shaw DW, Cook JJ, Gabi M, Holloway RH, Simula ME, Panagopoulos V, et al. Influence of normal aging on oral-pharyngeal and upper esophageal sphincter function during swallowing. *Am J Physiol* 1995;268:G389–96.
- [55] Sura L, Madhavan A, Carnaby G, Crary Ma. Dysphagia in the elderly: management and nutritional considerations. *Clin Interv Aging* 2012;7:287–98, <http://dx.doi.org/10.2147/CIA.S23404>.
- [56] Suzuki M, Asada Y, Ito J, Hayashi K, Inoue H, Kitano H. Activation of cerebellum and basal ganglia on volitional swallowing detected by functional magnetic resonance imaging. *Dysphagia* 2003;18:71–7, <http://dx.doi.org/10.1007/s00455-002-0088-x>.
- [57] Suzuki S, Kumano H, Sakano Y. Effects of effort and distress coping processes on psychophysiological and psychological stress responses. *Int J Psychophysiol* 2003;47:117–28.
- [58] Teismann IK, Steinstraeter O, Schwindt W, Ringelstein EB, Pantev C, Dziewas R. Age-related changes in cortical swallowing processing. *Neurobiol Aging* 2010;31:1044–50, <http://dx.doi.org/10.1016/j.neurobiolaging.2008.07.001>.
- [59] Teyler TJ, DiScenna P. The role of hippocampus in memory: a hypothesis. *Neurosci Biobehav Rev* 1985;9:377–89, [http://dx.doi.org/10.1016/0149-7634\(85\)90016-8](http://dx.doi.org/10.1016/0149-7634(85)90016-8).
- [60] Thirion B, Pinel P, Mériaux S, Roche A, Dehaene S, Poline JB. Analysis of a large fMRI cohort: Statistical and methodological issues for group analyses. *Neuroimage* 2007;35:105–20, <http://dx.doi.org/10.1016/j.neuroimage.2006.11.054>.
- [61] Tracy J, Logemann J, Kahrilas P. Preliminary observations on the effects of age on oropharyngeal deglutition. *Dysphagia* 1989;9.
- [62] Tranel D, Damasio H. Neuroanatomical correlates of electrodermal skin conductance responses. *Psychophysiology* 1994;31:427–38, <http://dx.doi.org/10.1111/j.1469-8986.1994.tb01046.x>.
- [63] Torpy J, Lynn C, Glass R. Frailty in older adults. *JAMA* 2006;296(18):8724, <http://dx.doi.org/10.1001/jama.296.18.2280>.
- [64] VaezMousavi SM, Barry RJ, Rushby JA, Clarke AR. Arousal and activation effects on physiological and behavioral responding during a continuous performance task. *Acta Neurobiol Exp (Wars)* 2007;67:461–70.
- [65] Ward NS, Frackowiak RSJ. Age-related changes in the neural correlates of motor performance. *Brain* 2003;126:873–88.
- [66] Wexler BE, Fulbright RK, Lacadie CM, Skudlarski P, Kelz MB, Constable RT, et al. An fMRI study of the human cortical motor system response to increasing functional demands. *Magn Reson Imaging* 1997;15:385–96, [http://dx.doi.org/10.1016/S0730-725X\(96\)00232-9](http://dx.doi.org/10.1016/S0730-725X(96)00232-9).